CHALMERS

Creating cell microenvironments *in vitro*

PATRIC WALLIN

Division of Biological Physics
Department of Applied Physics
Chalmers University of Technology
Gothenburg, Sweden, 2012

Thesis for the degree of Licentiate of Engineering

Creating cell microenvironments *in vitro*

Patric Wallin

CHALMERS

Division of Biological Physics
Department of Applied Physics
Chalmers University of Technology
Gothenburg, Sweden, 2012

Creating cell microenvironments *in vitro*

Patric Wallin

Division of Biological Physics
Department of Applied Physics
Chalmers University of Technology
SE-412 96 Gothenburg
Sweden
Telephone + 46 (0)31-722 6116
Email wallinp@chalmers.se

Cover illustration:
Photo collage of three images combined in Photoshop CS5
"Microfluidics - from ideas to applications"

Printed by:
Chalmers Reproservice
Gothenburg, Sweden, 2012

Creating cell microenvironments *in vitro*

Patric Wallin

Division of Biological Physics
Department of Applied Physics
Chalmers University of Technology
Gothenburg, Sweden, 2012

Abstract

Stem cells have a great potential to bring about advancements in fields like developmental biology, drug discovery, cancer biology and tissue engineering. In order to be able to use stem cells to their full potential, it is important to have control over their behavior. In vivo cellular fate processes are controlled by the microenvironment around them and the many different factors in it. Cells communicate with their surrounding environment and shape it actively via cell-cell, cell-matrix and cell-liquid interactions. These interactions often happen on the cellular and subcellular length scale in defined time dependent sequences. Consequently, it is important to have systems that can provide different molecular cues with a high spatial and temporal resolution, in order to mimic cell microenvironments in vitro and study cells under controlled conditions.

This thesis focuses on cell-matrix and cell-liquid interactions and different ways to create cell niches in cell culture systems. The focus is on designing and characterizing microfluidic cell culture platforms and, in particular, systems that are capable of forming molecular gradients. Flow-based and diffusion-based microfluidic gradient generators were combined with substrates coated with biofunctionalized gold nano dots, chemical active molecules, or electrospun microfibers. Thus, it was possible to provide cells with topographical cues and a defined surface chemistry, as well as soluble molecular cues in a gradient manner, simultaneously. COMSOL Multiphysics simulations were used to assist the design process and characterization of the microfluidic systems, and also to study cell receptor binding interactions in great detail. The developed toolbox of COMSOL modeling, a liquid handling system, a variety of microfluidic networks, surface modification techniques and molecular gradients allows the formation of multifactorial microenvironments to now study induction of cellular fate process of different cell types in vitro.

Keywords

Microfluidics, mammalian cell culture, cell microenvironments, chemotractant gradients, surface functionalization, cell differentiation, cell migration, liquid handling, lipid bilayers, *in vitro* screening assay

This thesis is based on the work contained in the following papers:

Paper I

A method to integrate patterned electrospun fibers with microfluidic systems to generate complex microenvironments for cell culture applications

Patric Wallin, Carl Zandén, Björn Carlberg, Johan Liu and Julie Gold

Biomicrofluidics 6, 024131 (2012)

My contribution: I had the initial idea for the study. I planned the experiments together with the co-authors and performed most of the experiments, but did not produce the electrospun fiber samples. I wrote the main part of the manuscript.

Paper II

Simulation of Chemotractant Gradients in Microfluidic Channels to Study Cell Migration Mechanism in silico

Patric Wallin, Elin Bernson and Julie Gold

Comsol User meeting Milano, (2012)

My contribution: I had the idea for the study. I performed nearly all the simulations and analyzed the data. I wrote the manuscript.

Publications not included in the thesis

Kinetics of ligand binding to membrane receptors from equilibrium fluctuation analysis of single binding events

Anders Gunnarsson, Linda Dexlin, Patric Wallin, Sofia Svedhem, Peter Jönsson, Christer Wingren and Fredrik Höök

Journal of the American Chemical Society 133, 14852-5 (2011)

Continuous lipid bilayers derived from cell membranes for spatial molecular manipulation

Lisa Simonsson, Anders Gunnarsson, Patric Wallin, Peter Jönsson and Fredrik Höök

Journal of the American Chemical Society 133, 14027-32 (2011)

Lipid-membrane water-permeability measurements on single vescile level using hydrodynamic focusing

Gabriel Ohlsson, Seyed R. Tabaei, Patric Wallin, Göran Petersson, Johan Andersson, Fredrik Höök and Jonas O. Tegenfeldt

In manuscript

Table of contents

Table of boxes

Preface

There are a few things, a few personal remarks that I want to say at the beginning of this book, because it is different from many other Licentiate theses. It is difficult to pinpoint why exactly I choose to write it in a different way – it just felt right this way. I wanted to tell the whole story of the first two and half years of my PhD studies and did not want to reduce it to the parts that worked and got published. Did I succeed to make a story worthwhile reading – I do not know, you as a reader are the only one able to judge, but I really hope you will enjoy it and keep reading beyond this preface and acknowledgement.

There is one point that I want to stress that is at the heart of all the work that I did and the reason why I do what I do – and that is curiosity. I think there is always something interesting, extraordinary and fascinating around us, we just have to look for it. I believe that it is important that we do not take anything for granted, that we try to attack a challenge from different directions and that we not limit ourselves by rationality, but use our imagination to find new solutions.

When I started my PhD studies, I thought it was exciting I really liked what I was doing and I actually still do. I really enjoy planning experiments and testing new ideas. I like to talk about my research both to people I am working with, but also to others. I even realized that it is important to write up things and find it ok now – I think I even like it. I love to supervise and guide people, see how they develop, to inspire them, give them a feeling that they belong to something bigger, something wonderful. I also enjoy teaching, to explain something very complex in a way that people will understand, to see how they follow the lecture - to see how their eyes light up when they start to understand something they did not know before. I think it is fascinating how some people are able to talk to an audience, capture their attention, take them into a world they might not even know existed before and give them an amazing time. Like the ability to give a one hour talk where people afterwards think that it only took a couple of minutes. I really would like to learn and master that skill. Those things might not be the ones that are highest on the list of being a successful PhD student, but they are very rewarding for me. I enjoyed talking at the Science Slam at the Gothenburg science festival, I learned a lot from the other people presenting there and I hope I will get the chance to participate again at some point in the future.

I am driven by curiosity and by the wish to understand why things work in the way they do. I need to see the relation and connections between different parts, and I need to see a goal that I find worthwhile pursuing. This goal might be very far away, the research I am doing only a very small part of the puzzle and it does not need to have a direct application, but there must be a larger aim. At the beginning of my PhD I really struggled to define a scientific question and formulate it in a proper way. However, looking back to my application for the position, I think it was actually not that bad:

"It is incredible with which speed and precision cells can respond to a wide variety of stimuli, cell-cell and cell-surface interactions."

It is very vague and a rather large area, and it was not even formulated as a real goal, but it served well as one at the beginning. I lost this initial idea or question a little bit during the first year of my PhD studies trying to figure out if I was more a "method-de-

velopment-guy" or a "cell-biology-guy" – I still do not know, but it probably does not matter so much. I think it might even be limiting to define you as one of the two. It took me a while to figure that out, but now I think that I will need both skills, if I want to succeed with my original aim. I will need the ability to design a system ("method-development-guy") that is capable of studying cellular fate processes in microenvironments ("cell-biology-guy"). The original question has developed over time and is now more refined than before:

"Using microfluidic systems in combination with different materials to generate combinatorial multifactor gradients to create defined microenvironments *in vitro*."

It still is a large area, but there are certain questions which I have formulated in more detail to have something to work with on a day to day basis. It was not always easy to pursue with my work, but I never lost my curiosity and the dream to see something that nobody else had seen before. Things will change, but I believe as long as you are curious and passionate about what you are doing, everything will work out at the end.

I want to thank Julie, my supervisor and mentor, for all the things she has done for me. I know it was not always easy, but she did a fantastic job. I remember when I started my PhD studies my project was not very defined, but Julie took me with her to the kick-off meeting for the two EU projects I would be working on and I was able to get an idea what they were about. On the flight back, we discussed what I could work on and how it would fit into those projects. I am very grateful for all the opportunities Julie gave to define my own questions, work on things I thought were interesting and most of all the chance she gave me to develop as a person. Thank you Julie.

I also want to thank Fredrik my co-supervisor and examiner for giving me the opportunity to work at the division of Biological Physics, the interesting discussions about how life started and that he asked me to teach at a workshop for architecture students in Stockholm.

Another person who made a big contribution to this work is Elin Bernson and I am very happy that we have the chance to work together. It was great to have such an enthusiastic master thesis student to supervise and work with. And it is even better to have her as a colleague now.

There are a lot of people that I have been working with and will continue working with in the future and I am very happy to have the chance to do so. I want to thank: All the people at the machine shop at Physics and Chemistry, all partners in the European projects and the Vinnova project, Samuele at SuSoS, Michael at Q-Sense, Carl, Björn and Johan from Bionanosystems, Laurent, Hossein and Francesco from Biological Physics, and Nina E, Georg and their students at the Center for Brain Repair and Rehabilitation.

All students I had the pleasure to teach, it was not always easy, but it was rewarding most of the time and their questions made me think, made me improve the way I prepare my lectures and present them. We also did some very interesting research together in the Tissue Engineering course.

I also want to thank all my colleagues at the division of Biological Physics for the great discussions about science and other things in life , all my other colleagues that I have met at courses, summer schools, meetings and all the other occasions. In particular the people at Surface Chemistry, who I really enjoy playing innebandy with every Wednesday. Furthermore, I would like to thank the people at technical service, administration, and everybody else how takes care of all the things around the research and are always of great help.

Finally, I want to thank my wonderful wife Maria for all her support, being there for me when I need her and everything else. You are wonderful. I am looking so much forward to our child and being the three of us in October.

Chapter 1

Introduction

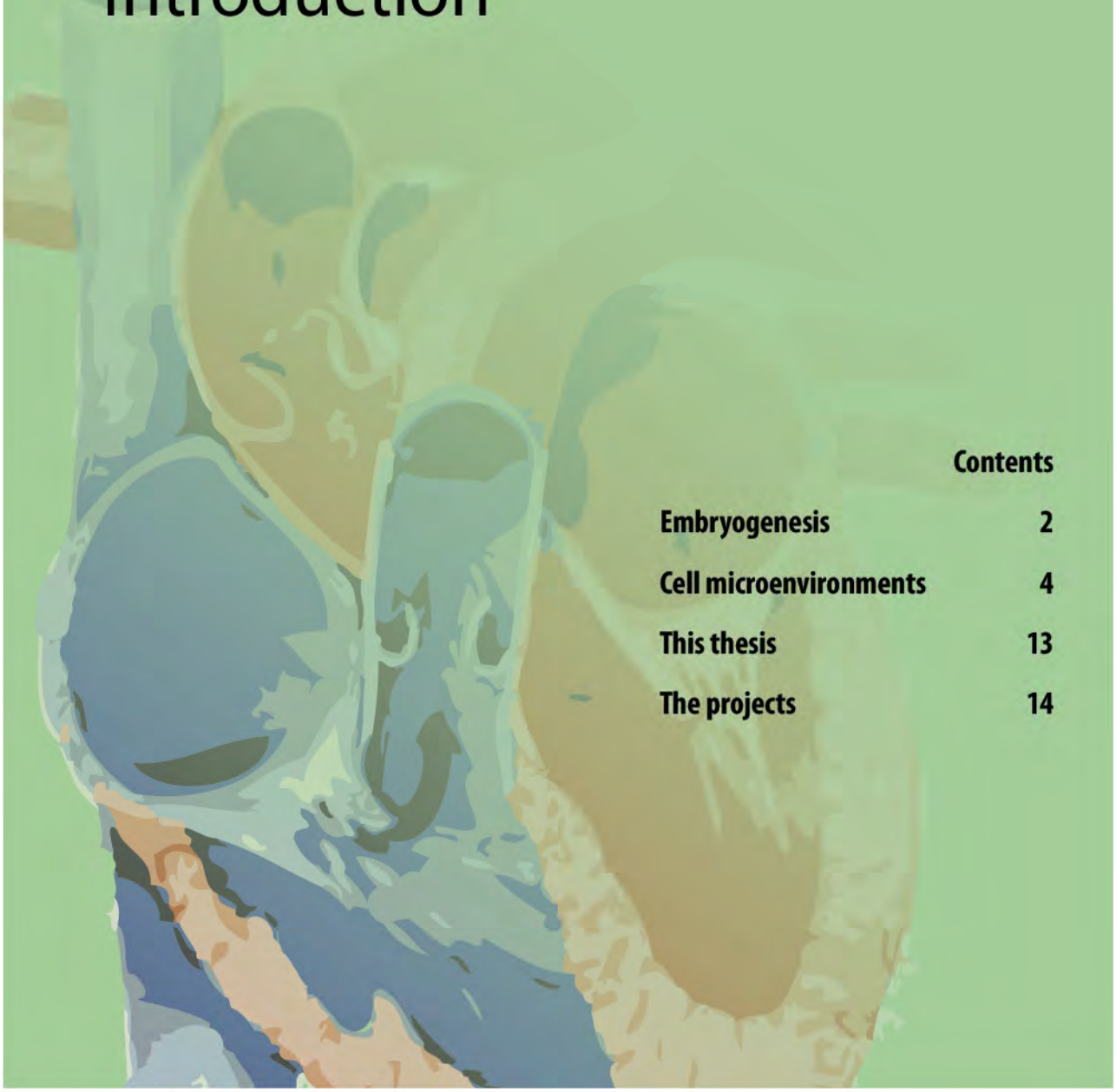

Contents

Embryogenesis

Often when we talk about science, we talk about very complicated experiments, but we easily forget that some of the most interesting questions are very simple and that everybody, kids, teens and adults, can ask questions that carry us to the border of human knowledge. I think it is rather fascinating how most of us are born with two arms and two legs, 5 fingers on each hand and all the other small details. There are a lot of differences as well, some are female, some are male, some are taller, some are smaller,..., but all those variations take place within the boundaries that define us as humans.

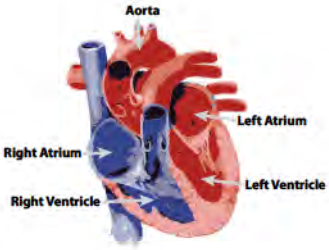

One particular striking example of similarity is the position and form of our heart. It is normally situated slightly to the left side in the thorax and has four chambers. Deoxygenated blood passes through the right atrium into the right ventricle, gets pumped through the lungs, where it gets oxygenated, enters back into the heart via the left atrium to the left ventricle and finally gets distributed through the whole body from the aorta. This is true for 99.992% [1] of all humans, but there are a few people who have a condition called "Dextrocardia situs inversus"; their heart is positioned slightly to the right in the thorax and mirrored, thus blood enters through the left atrium and gets pumped out from the right ventricle [2]. What I think is amazing is the fact that there are not more people with this condition; there is no clear disadvantage of having your heart on the right side [1], but still the position is defined and not random. This means there must be strong directional cues already very early on during development [3–5]. The heart starts beating around 22 days after fertilization and the four chambers and their function can easily be visualized by ultrasound in week 16.

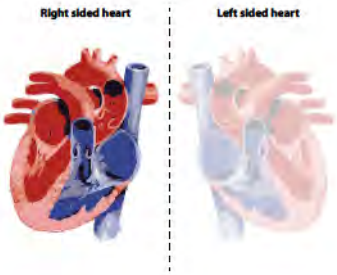

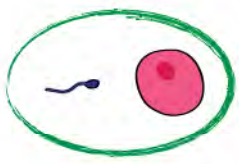

Each one of us consists of 50 to 75 trillion cells [6] and those cells can be classified into more than 210 different cell types [6], each having a particular task and position within the body – resulting in a tremendous complexity, but still it all starts with an egg (ovum) and a sperm in the right environment of the uterus. Some basic, but very interesting, questions that arise then are: how does the zygote (fertilized egg) give rise to all the cells in our body and develop into all the different cells types, even though each cell has the same genetic information, the same DNA? There are five fates a cell can pursue (see "BOX 1.1" on page 3); how does a cell know what to become or do? How does a cell know where in the growing embryo it is located? Why is the heart situated slightly to the left and how are the cells controlled to achieve this? Fortunately a lot of research has been done to answer those questions in the field of developmental biology and, although we still do not understand all details, we have a fairly good idea about the main processes [7].

Cellular fate processes

BOX 1.1

There are five basic cell fates: quiescence, self-renewal, migration, differentiation and apoptosis. Each fate is associated with the expression of a different subset of genes and consequently, specific cell morphological and phenotypic features.

Self-renewal is the symmetric division of cells. The cell is going through the whole mitotic cycle; it is doubling its genetic information and eventually divides in two similar cells. This self-replication is likely to be the process that distinguishes biological life most from other things. [6], [8]

Cell differentiation is the phenotypic change of a cell towards a more specialized type and is achieved by an alternation of the gene expression pattern. A cell can either differentiate through asymmetric division, similar to self-renewal, but instead of two similar cells the two daughter cells have different gene expression patterns. Or it can differentiate in the response to external stimuli received through cell receptors. [6], [8]

Cell migration is the movement of a cell. The movement can be directional along a gradient that is sensed by the cell or it can be random. Cell migration is needed for cells to move from one part of the body to another, for example during wound healing. Cell migration is described in more detail in chapter 4. [6]

Quiescence is the resting state of a cell. In this state, the cell is neither preparing nor undergoing cell division. However, cells in the quiescence state are still performing their tasks and a large number of final differentiated cells are in this state. For example Muscle cells that allow us to move our arms, are finally differentiated and cannot self-renewal. On the other hand, there are cells that are only temporally quiescence. These cells are normally not finally differentiated, but are progenitor cells that wait in a special niche environment until they get reactivated. [6], [8]

Apoptosis is controlled cell death, in contrast to necrosis, which is the uncontrolled death of cells due to trauma or toxins. During apoptosis cells undergo a preprogrammed sequence of events and eventually disintegrate; the remains are encapsulated and degraded. The effect on the surrounding tissue is minimized. Apoptosis plays an important role in many processes and is for example responsible for the formation of fingers on the hand during early development. [6], [8]

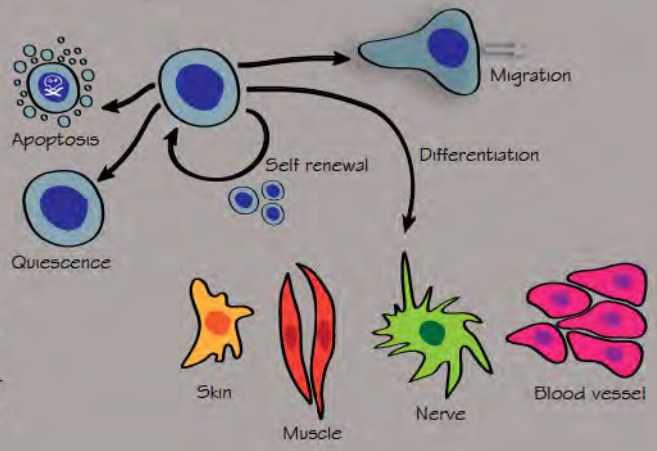

Figure 1.1
Schematic of the 5 different cell fates: migration, differentiation, self renewal, quiescence, and apoptosis

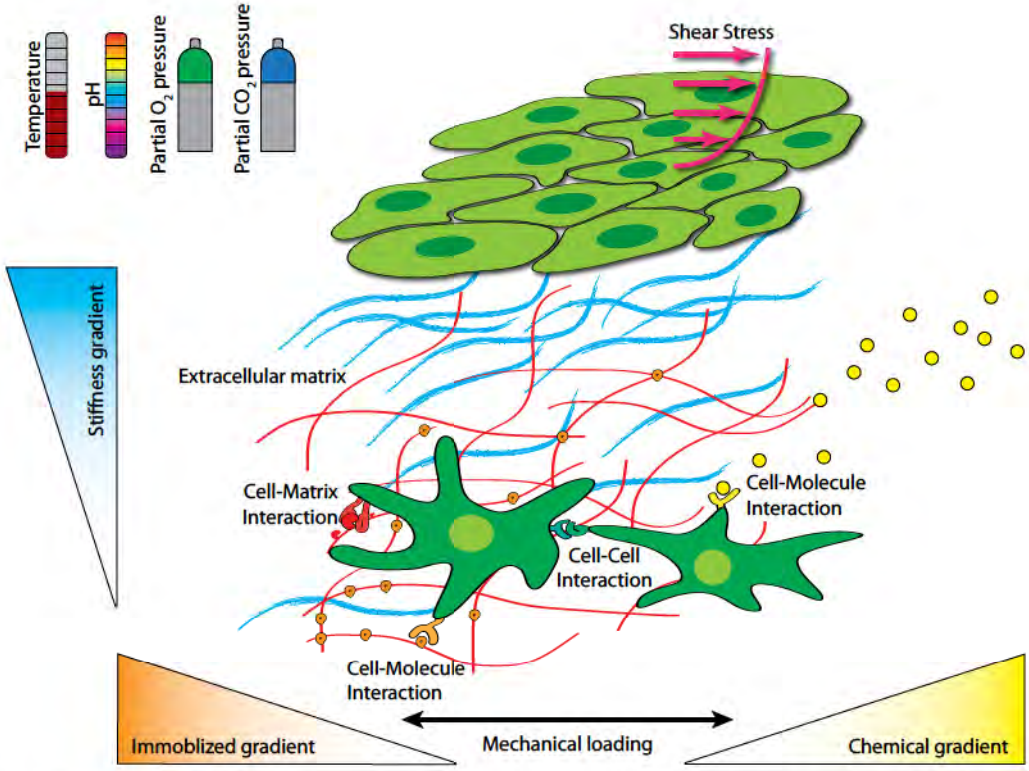

Figure 1.2
Schematic of cell microenvironments and its defining properties, including cell-cell, cell-liquid and cell-matrix interactions, as well as physiochemical conditions

Cell microenvironments

It was found that one very important factor that influences cellular fate processes is the context in which the cell is present, the environment that surrounds the cell; this is often referred to as the cell microenvironment [9–11] or stem cell niche [12–14]. Cells are sensing and interacting with their surrounding by cell-cell contacts ("BOX 1.2" on page 5), cell-matrix interactions ("BOX 1.3" on page 6), soluble factors ("BOX 1.4" on page 9) and specific physiochemical cues ("BOX 1.5" on page 10), all those properties are tightly controlled and location specific. Each cell is not only controlled by their microenvironment, but at the same time they are changing and modifying it. Figure 1.2 shows a schematic of a complex, multifactorial cell microenvironment, defined by several basic parameters: surface topology, surface chemistry, matrix stiffness, mechanical stress, shear stress, molecular liquid composition, and physiochemical are presented to the cells in the form of a gradient, rather than in an on/off like manner and I will come back to this fact later.

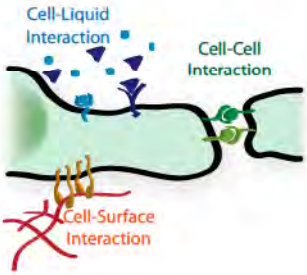

Cell-Cell interactions

BOX 1.2

In vivo, cells are surrounded by other cells and normally form direct contacts with each other through different cell junctions. This kind of direct communication via cell-cell contacts is referred to as juxtacrine signaling. One large superfamily of cell-cell junctions are called cadherins (calcium depended adhesion), which can be further classified into classical, desmosomal, protocadherins and unconventional. [6] For each of these four groups many different variants of transmembrane proteins have been identified and it is cell type and location specific which proteins are expressed by a cell. Endothelial cells, for example, form pre-dominantly VE-cadherins (vascular endothelial or CD144) between themselves, but are attached to the underlying cell layer of pericytes mainly through N-cadherins [15]. This means there is a high degree of spatial organization and an individual cell can respond differently on its borders in response to the surrounding.

Another important type of junction between cells is called tight junctions. This type of junction brings cells in very close contact to each other to form a nearly impermeable barrier between them. For endothelial cells who are forming the inner lining of blood vessels and are situated at the interface between the blood and the surrounding vessel, this is a very important mechanism, because it ensures that blood cannot pass the layer of closely coupled endothelial cells. [16] For endothelial cells these tight junctions are mainly formed by the transmembrane protein claudin-5 [15].

There are many more ways of how cells make contact which each other and are able to communicate. One particular important pathway, especially for cell fate and stem cell differentiation, is the notch signaling pathway. It is a key pathway in pattern formation and the spatial organization during embryogenesis found nearly all tissues and throughout the animal kingdom [17], [18]. It plays an important role in early orientation and is partially responsible for why the heart sits slightly on the left side in the body. Notch signaling can be either restrictive, it hinders two cells from pursuing the same fate, or it can be endorsing, it induces neighboring cells to follow the same fate. In this way, it is possible to control populations and limit the amount of cells of a specific type, and to form boundaries.

There have been many different approaches to study cell-cell interactions *in vitro* and various platforms have been used. With the development of microfluidic cell culture systems, people have been able to precisely place individual cells close to each other to study their interactions. Jean-Philippe Frimat et al., for example designed a system to place two cells, either of different or similar type, next to each other and study how they behave and communicate. Each chip contained 200 traps that could be studied simultaneously and they reached up to 70% successful co-culture pairs. [19] Another approach is to mimic a cell by selective functionalization of a lipid bilayer and placing a real cell on top. This allows very controlled conditions and detailed studies of temporal and spatial organization [20], [21]. The approach is descried in more detail in "Supported lipid bilayers" on page 23.

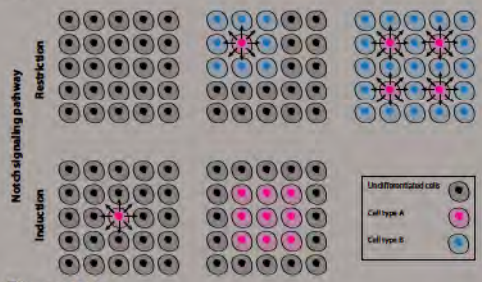

Figure 1.3
Notch signaling pathway showing restriction and induction

Cell-Matrix interactions

BOX 1.3

Cells in native tissue are normally situated in extra cellular matrix (ECM) with which they interact and attach to. It gives cells a structure to attach to and grow on, and it is essential for tissue formation. The ECM is providing cells with a specific topology, as well as chemical composition, both are important cues for cells and are regulators in cellular fate processes. The ECM consists of many proteins like collagen, elastin and laminin, and also different glycosaminoglycans including heparan sulfate and hyaluronic acid. Collagen gives the ECM its structure by forming long fibers and it stiffens the matrix to allow cells to exert forces on the ECM. Elastin on the other hand provides elasticity to the ECM and lets it stretch and relax depending on outer forces or the cells them self. Laminin, in contrast to elastin and collagen, forms interconnected meshes instead of long fibers and adds tensile strength to the ECM. The glycosaminoglycans have various functions, for example to keep the ECM and cells hydrated, regulate cell attachment, and functions as a depot for other molecules like growth factors and hormones that can be released in response to certain events and thus quickly change microenvironments, amongst others. [6], [22], [23]

The ECM composition, the amount and organization of its different components, is specific for each tissue and provides cells with informational cues on where in the body they are located and induces the progression of cellular fate processes [24], [25]. This is achieved by various, highly conserved molecular motifs within the ECM proteins and glycosaminoglycans. Cells interact with these motifs via special receptors, in particular integrin receptors, a family with more than 20 known receptors [22], [26], [27]. Integrin receptors are heterodimers with two distinct subunits called ALPHA and BETA subunit, these can be combined in different ways to bind to specific motifs, for example $ALPHA_5$ $BETA_1$ binds to fibronectin [28], $ALPHA_6$ $BETA_1$ to laminin [29] and $ALPHA_V$ $BETA_3$, as well as $ALPHA_{IIa}$ $BETA_3$ to RGD (amino acid sequence Arginine-Glycine-Aspartic) [30], [31]. The receptor binding triggers a whole cascade of internal signaling pathways that enables a cell to response to the external stimuli by changing or maintaining its current cell fate. This signal transduction is a multicomponent system where different integrin receptors bind to their motifs and other molecules bind to their receptors resulting in an integration of the signal to response to a specific condition. For example, cells are unable to respond to endothelial growth factors (EGF) and platelet derived growth factors (PDGF) if they are not attached to the ECM via integrin receptors. [32], [33]

Integrin receptors can assemble into different forms of multi-protein complexes that link many integrin receptors together and connect them with the intracellular cytoskeleton [34]. The complexes differ in size and attachment strength and are depending on the cell fate, a highly migratory cell will form different attachment complexes compared to a cell that does not move [35]. The first adhesive assemblies are called nascent adhesions [36], they link the dendritic actin network, a highly branched actin network found in lamellipodia [37], [38], to integrin receptors and are very small. Nascent adhesions are highly transient and either mature or disappear quickly. If they mature they form focal complexes which are larger and depend on myosin II [39]; they are highly transient as well. Both nascent adhesions and focal complexes are predominantly present in migratory cells and their fast turnover rate allows cells to quickly move. If the attachment matures further, cells are slowing down and eventually will stop. During maturation of focal complexes more and more integrin receptors

are linked to the actin filaments to increase the strength of the attachment, this can be observed as focal complex elongation along actin filaments [40]. These fully mature cell attachments are called focal adhesions; they are linked to large actomyosin and actin bundles to strongly anchor the whole cell within the ECM [41]. The link between integrin receptors and the cytoskeleton is achieved with different linker proteins, mainly talin [42], [43], ALPHA-actinin [44] and vinculin [44], [45] and cell signaling is governed by paxillin [46], zyxin [47], tensin [48], tyrosine kinase FAK and SRC [49], amongst others.

It is very challenging to mimic both the exact structural and chemical properties of the ECM *in vitro*. This is one of the reasons why decellularization of native tissues and re-seeding with stem cells is such a promising approach for tissue engineering, because it solves the technical challenging task of designing a very complex structure de novo [50–52].If the aim is rather to study cell behavior in controlled microenvironments instead of generating whole tissues, there are different ways to mimic ECM properties. These approaches can be either focused on the topography of a substrate [53], the chemistry [54] or both [55]. The aim can be either to mimic native ECM properties as closely as possible or to test different artificial features and observe and characterize for example cell morphology and gene expression patterns.

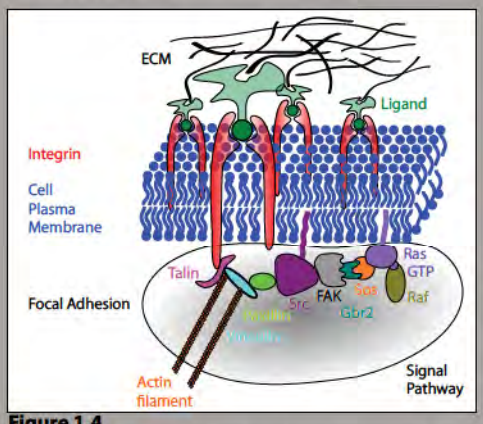

Figure 1.4
Schematic of a focal adhesion showing some of the involved proteins and receptors

For the fabrication of substrates with specific nano- and micro-structure electrospinning and microfabrication amongst other offers many ways to control *in vitro* surface topology. Electrospinning is an interesting technique, because it allows the batch production of substrates that structurally mimic fibrous components in the ECM [56]. The ability to easily produce large amounts and coat large substrates is a big advantage of electrospinning in comparison to other microfabrication techniques. The advantages of lithographic based techniques, on the other hand, are the high degree of control and the ability to pattern topographical features in the nanometer regime [53].

To mimic the chemical properties of the ECM *in vitro* there are two main ways, either surfaces are coated with a complex mixture derived from solubilized native ECM or specific molecules are used. Complex mixtures have the advantage that they mimic the *in vivo* situation more closely, but compositions might change from batch to batch and isolation of a particular signaling pathway is difficult [23], [54]. When using engineering principles for molecular functionalization there are basically three main ways to influence surface chemistry: the bulk chemical composition of the substrate material, covalently bonding of a molecule to the surface (chemisorption) or physical adsorption caused by van der Waals forces (physisorption). Stephan Dertinger et al. generated surface adsorbed gradients of laminin by poly-L-lysine (PLL) pre-coating and competitive adsorption of laminin and bovine serum albumin (BSA) [57]. Rico Gunawan et al.

produced surface immobilized laminin gradients as well, but used covalently coupling of laminin to a previously formed self-assembled monolayer of carboxylic acid-terminated alkanethiols on a gold substrate [58]. Marco Arnold et al. took this approach even further and used gold nano dots spaced in a hexagonal pattern with inter particle distances in the nanometer regime. They functionalized these substrate with cyclic RGD peptides, a highly conserved amino acid sequence (Arginine-Glycine-Aspartic) found in many ECM proteins. Thus, they were able to have very good spatial control in the distance between individual cyclic RGD integrin binding sites. [59] This approach is described in more detail in chapter 4.

One thing that is important to note that surface chemistry can be influenced by surface topology, especially at and below the nanometer length scale. This might be on purpose, like with the gold nano dots. However, the chemistry might change unintentionally during the processing needed to achieve the right topology. Nonetheless, careful experimental design allows the separation of the two in *in vitro* culture systems. This opens the possibility to discriminate between them, look at their effects on cellular fate processes individually and fine tune properties. [27], [60]

Another parameter that is defined by the ECM composition and structure in native tissue is the stiffness of the surrounding matrix which varies greatly between different tissues and even within the same tissue. Brain tissue has an elasticity between 0.2-1 kPa, muscle tissue around 10 kPa and pre-calcified bone of 30-40 kPa. It has been shown that by merely adjusting the substrate stiffness mesenchymal stem cells can be differentiated into these three tissues *in vitro*, illustrating the importance of substrate stiffness for cellular fate [61], [62]. The most common way to adjust the stiffness of a cell culture growth substrate is to use polymers with different cross-linking densities, often in the form of hydrogels. The advantage of using polymers is that the chemical properties are not dramatically changed and the effect of stiffness can be investigated independently from chemical composition.

An additional function of the ECM is the transduction of mechanical stresses. In some tissues cells residing in the ECM are exposed to different forms of mechanical stress, which will influence their behavior. Cells can be subjected to mechanical loading normal to their surface and the loading can be either in the form of compression or tension resulting in normal stress. Compression forces are normally found in e.g. bone and cartilage tissue, whereas tension forces can be seen in e.g. muscle tissue. If the force does not act normal to the cell surface, but instead parallel the cell will experience shear stress. One specific example of shear stress is caused by liquid flow above cells which plays a key role in development of tight endothelial layers. In most cases cells encounter a combination of normal and shear stress, which can be either statically or changing with time.

All four parameters - substrate topology, chemistry, stiffness and mechanical stress - are important to consider both for *in vitro* model systems and also in the design of scaffold materials for tissue engineering. The aim is to match native properties as closely as possible to get a more reliable *in vitro* model or improve host integration of the implanted scaffold.

Cell-Liquid interactions

BOX 1.4

Cells are not limited to direct communication via cell-cell contacts, but can also signal each other over longer distances by using molecules. This kind of intercellular communication can be further divided into three parts depending on the distances.

1) Autocrine signaling is the process when a cell is both the source and the target of a signal, but in contrast to intracrine signaling the molecule passes through the plasma membrane and binds to a receptor on the outside of the cell membrane. [6]

2) Paracrine signaling is limited to the close proximity around a cell. The distance between a source and target cell, which can be of the same or different type, can differ between a few micrometers up to several hundred micrometers. The distance is greatly influenced by the half-life time of the molecule, the extra cellular matrix surrounding the cells ("BOX 1.3" on page 6) and the size and composition of the molecule. [6]

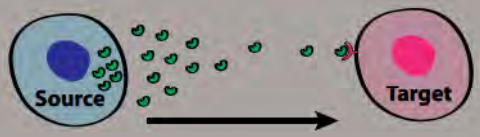

3) Endocrine signaling enables cells to communicate over much larger distances and throughout the whole body. In endocrine signaling, the source cell is located in a gland and releases molecules into the bloodstream, which are received by the target cell. The response in this case is rather slow, because the molecules have to travel through the whole blood circulation system. [6]

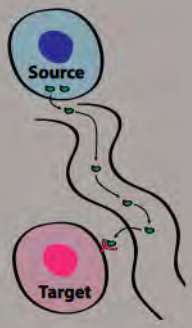

Although, microfluidic cell culture systems have been used in many areas, one of the main areas is still to study cell-liquid interactions. As described in detail in chapter 3 and 4, microfluidics offer unique possibilities to control liquid environments and to form molecular gradients. Elisa Cimetta et al. for example used a microfluidic gradient generator to study effects of Wnt3a on cell fate [63]. The Wnt signaling pathway plays a very important role in embryogenesis and cancer [64]. During embryogenesis, this paracrine signal is present in a gradient manner and in this way helps in the spatial organization of cells; thus, it is also part of the mechanism that ensures that our heart sits slightly to the left [65]. My work is not focused on Wnt, but on other paracrine signaling pathways (see chapter 4) and how to mimic gradient conditions with the help of microfluidic chips.

Physiochemical conditions

BOX 1.5

The temperature in humans is regulated and kept at 37°C and long term deviations will have severe health effects. However, short term elevated temperatures in the form of fever are common and normally not dangerous. The pH is also tightly controlled and kept between 7.35 and 7.45, several buffer system are helping to maintain this pH. One particular example is the bicarbonate buffer system, where CO_2 and H_2O react to form HCO_3^- and H^+, therefore coupling the pH directly to the CO_2 concentration. Furthermore, the amount of circulating CO_2 is actively regulated by respiration and thus the chemical equilibrium of the reaction can be shifted to maintain a stable pH.

Whereas temperature, pH and CO_2 are normally stable and only under special circumstances change, partial oxygen pressure differs between arterial blood vessels with oxygenated blood and a high partial pressure and venous blood vessels with a low partial oxygen pressure. Depending on the tissue, the distance from the nearest blood vessel, the blood oxygen level, and the partial oxygen pressure experienced by a cell can vary dramatically. This variation is often not considered in *in vitro* systems, but might have severe effects on cell behavior [66]. There are, however, systems that allow the control of oxygen levels in cell culture incubators [67]. Maciej Skolimowski et al. developed a microfluidic systems that allows them to create gradients of dissolved oxygen in media to study cell responses [68].

In most experiments, the aim is to keep physicochemical conditions similar to the ones found *in vivo* and keep them constant, but there are studies that investigate their influence in more detail. For example, Susan McKiernan et al. looked at the influence of several physicochemical parameters (temperature and salt concentration) on blastocyst development of hamster 2-cell embryos [69]. The variation of physicochemical conditions is also of interest for tissue models, where there is a large variation in those parameters either throughout the tissue (spatial) or time dependent (temporal) in the. During cancer for example, oxygen levels in the tumor decrease with disease progression (hypoxia) [70] and pH levels are lower than in healthy tissue [71]. The ability to mimic those disease conditions *in vitro* is interesting to gain a better understanding of the effects and implications and eventually to develop new treatments.

Tissue Engineering

BOX 1.6

Tissue engineering and regenerative medicine describe a field in medicine that aims at restoring, maintaining and enhancing tissue functions [85]. In order to achieve these goals tissue engineering combines the expertise from many different fields and competences in basic cell biology, stem cell biology, physiology, medicine, surgery, material science, transport processes and legislation are needed to succeed. Tissue engineered products can be divided in three categories: hybrid products of biological and synthetic materials, products that induce a specific tissue response and cells that have been manipulated or expanded *in vitro*. [8]

The overall dream of tissue engineering is the ability to grow whole tissues *in vitro* that can be produced on demand, specific for each patient and thereby solve the problem of the mismatch between demand and availability of transplant organs. To achieve this goal detailed knowledge about cellular fate processes and the way tissues are formed is needed and systems to control all necessary parameters *in vitro* are necessary. They fall into categories: competent cells that can come either from the patient or another individual, scaffolds that cells can attach too and that mimic the extracellular matrix, chemical compounds like growth factors and hormones to steer cells in certain directions, and a bioreactor to maintain the cells and supply them with nutrition and oxygen. [85]

Even though the microfluidic systems presented in this thesis cannot directly be used to produce tissue engineered products, they offer a great tool to study and screen cells under defined conditions. The ability to change the microenvironment around a cell in a controlled manner is very important and the knowledge generated can be used to improve tissue engineering approaches. [86]

The knowledge about the significance of cell microenvironments and their composition *in vivo* is one important part to understand cell behaviour and cues in cellular fate processes. It helps us to answer some of the questions, like how does the cell know what to do and it also forms the foundation to mimic those conditions *in vitro*. The possibility to generate cell microenvironments *in vitro* that are similar to the ones *in vivo* is a crucial step for many application areas. The ability to manipulate all or some of the microenvironment parameters is needed to advance in many cell biology and biotechnology areas. For example, in tissue engineering and regenerative medicine ("BOX 1.6" on page 11), one controls microenvironments in order to create a well-defined stem cell niche *in vitro*, which provides key regulators for stem cell survival, self-renewal and differentiation. [10], [12], [72–75] The importance of defined microenvironments is, however, not limited to stem cells, but extends to cancer research [76–79], drug screening [80], [81] and immunological studies [82], [83] amongst others.

The problem is that we are still limited in our capability to form well defined microenvironments. Many studies have been carried out to look at how isolated factors influence cellular fate, but it has become more and more clear that often the interplay between several factors is essential for a cellular response [10], [75], [82], [84]. Therefore, new ideas are needed to generate multifactorial microenvironments *in vitro* that can mimic several properties of an *in vivo* situation at the same time. This will ultimately lead to better *in vitro* model systems that can predict for example the response of the body to a certain drug. They will also help to understand stem cell behavior in more detail, which subsequently will hopefully lead to better tissue engineered products. From embryonic development (embryogenesis), we know that stem cells are capable of forming functional tissues and it is only a matter of putting them into the right conditions. The cell itself is the only real tissue engineer [10].

Microfluidics and microfabrications can be used to achieve a better control of microenvironments. The goal for *in vitro* cell culture system is normally to recapitulate *in vivo* conditions as closely as possible and design an *in vitro* model that is of high biological relevance. On the other hand, the system needs to be simple enough to vary certain parameters individually to verify an initial hypothesis and to get reproducible and statistically significant data in a reasonable amount of time. Microfluidic devices have the potential to address both goals simultaneously: the high control of fluid properties can improve model accuracy and the physical dimensions help to develop systems that allow higher throughput with large reliability. A more detailed introduction and description of microfluidics is given in chapter 3 "BOX 3.1" on page 65.

This thesis

In the work that I have performed during the last two and a half years, I have been focusing on controlling the liquid composition around cells, the modification of the cell culture substrates and especially on the combination of both. At the beginning, the focus was more on the cell culture substrates and using lipid bilayers to stimulate cells. This work never really reached its final goal for several reasons as described in chapter 2 and I went away from this approach to move more towards microfluidic systems. In order to work with microfluidics, I needed a liquid handling system and in the beginning, I worked a lot on technical issues, because nobody at Biological Physics had used microfluidics for cell culture applications previously. Thus, it took some time to set up everything, test different protocols and approaches. I learned a lot from all the mistakes that I did on the way and was finally able to perform real cell experiments. This way is described in chapter 3. It was not always easy, but I think it was very interesting and I was always having the goal in mind to build a setup that is capable to form defined liquid microenvironments around cells to study how they influence cell behavior.

Chapter 4 is focusing on two cell studies; the first one still focused more on the technical development of a model test system and the second one more towards a particular cell fate. In the first study [87], which was published in June 2012 (paper 1), we describe a new method to integrate electrospun fibers with microfluidic networks. The developed platform is capable to form gradients of soluble cues that are either in the same direction as the patterned aligned electrospun fibers or perpendicular. In this way, it is possible to study the interplay between cell contact guidance by the fibers and chemotactic influence by the gradient. The second study is currently ongoing and is focused on endothelial cell migration. The main question in this study is, if cell migration speed is influenced by cell adhesion ligand density on the surface and if there is an optimal spacing for cell migration. Cell migration is stimulated by a gradient of vascular endothelial growth factor (VEGF) which is formed by a diffusion based gradient generator, different from the gradient generator used in the first study. Additionally, the interactions of VEGF with the cell receptor have been investigated with a finite element model as described in paper 2.

The projects

I am involved in three different projects to a varying amount, two European projects which are account for most of the time and one local Swedish project. Both European projects started when I started my PhD studies in January 2010 and run for four years. The Swedish project started in 2009 and will be finished in November 2012.

The first European project is called "Nanopatterned scaffolds for active myocardial implants", abbreviated as NanoCARD. The NanoCARD project is funded by the European Union Seventh Framework Program (FP7/2007-2013) under grant agreement n° NMP3-SL-2009-229294 NanoCARD. The project is coordinated by Joachim Spatz at Max Planck Institute for Intelligent Systems, Stuttgart, Germany, and involves eight academic research institutes and four companies.

The aim of the project is to design, fabricate, characterize and evaluate a biomimetic heart implant to form myocardial tissue *in vitro*. By tailoring material properties to present cells with specific biochemical, topographical and mechanical cues, stem and progenitor cells should selectively adhere, proliferate and differentiate on the scaffold to form myocardial tissue. The project covers the optimization of each parameter and its evaluation *in vitro* using cell culture and high throughput screening. The acquired knowledge will then be translated into the fabrication of the implant which will be tested in an animal model.

The second European project is called "Nanoscopically-guided induction and expansion of regulatory hematopoietic cells to treat autoimmune and inflammatory processes", abbreviated as NanoII. The NanoII project is funded by the European Union Seventh Framework Program (FP7/2007-2013) under grant agreement n° NMP4-LA-2009-229289 NanoII. The project is also coordinated by Joachim Spatz at Max Planck Institute for Intelligent Systems, Stuttgart, Germany, and involves ten academic research institutes and five companies.

The aim is to develop new approaches to control cell differentiation and proliferation of hematopoietic cells by using advanced nanofabricated surfaces, chemical modifications and microfluidics. In particular, differentiation and proliferation of regulatory immune cells will be investigated to treat diverse inflammatory diseases and autoimmune disorders. The cell culture platform developed within the project will allow the ex vivo generation of microenvironments that closely resemble *in vivo* conditions in specific organs. It will allow detailed investigations and high

throughput screening of cell-cell and cell-matrix interactions, as well as the effects of soluble cues. Cells produced in this *in vitro* platform will be used for *in vivo* experiments in an animal model and the generated knowledge will be translated into human cell applications.

The third project local Swedish project is called "Scaffolding nanomaterials for stem cell proliferation, migration and neural differentiation". The project is funded by Vinnova under grant agreement number 2008-02948. The project is coordinated by Georg Kuhn at University of Gothenburg Center for Brain Repair and Rehabilitation, Gothenburg, Sweden and involves four academic research groups and one company.

The aim of this project was to combine nanotechnology and stem cell biology to find new treatments for neurodegenerative diseases. The key to increase the self-healing potential in the brain is to gain deeper knowledge about the specific conditions found in the brain stem cell niche. This project will explore the possibility to use biocompatible nanofibers to create an artificial stem cell niche *in vitro* that allows detailed cell studies. The aligned nanofibers mimic radial glial cells which act as important contact guidance cues in the developing brain to guide neural progenitor cells from the proliferation zone to their destination. By using nanofibers with the right chemical modification it should be possible to stimulate stem cells to proliferate and migrate along the fibers. The knowledge about the underlying processes will help to design treatments with injectable fiber material to stimulate proliferation and migration of adult brain stem cells to cure neurodegenerative diseases.

[1] C. M. Bohun, J. E. Potts, B. M. Casey, and G. G. S. Sandor, "A population-based study of cardiac malformations and outcomes associated with dextrocardia.," The American journal of cardiology, vol. 100, no. 2, pp. 305-9, Jul. 2007.

[2] N. Garg, B. L. Agarwal, N. Modi, S. Radhakrishnan, and N. Sinha, "Dextrocardia: an analysis of cardiac structures in 125 patients.," International journal of cardiology, vol. 88, no. 2–3, pp. 143-55; discussion 155-6, Apr. 2003.

[3] M. Levin, "Left-right asymmetry in embryonic development: a comprehensive review.," Mechanisms of development, vol. 122, no. 1, pp. 3-25, Jan. 2005.

[4] I. Capdevila and J. C. Izpisúa Belmonte, "Knowing left from right: the molecular basis of laterality defects.," Molecular medicine today, vol. 6, no. 3, pp. 112-8, Mar. 2000.

[5] E. N. Olson, "Gene regulatory networks in the evolution and development of the heart.," Science (New York, N.Y.), vol. 313, no. 5795, pp. 1922-7, Sep. 2006.

[6] B. Alberts, A. Johnson, J. Lewis, M. Raff, K. Roberts, and P. Walter, Molecular Biology of the Cell, 5th ed. New York: Garland Science, 2007.

[7] S. F. Gilbert, Developmental Biology, 9th ed. Sunderland: Sinauer Associates, 2010.

[8] B. O. Palsson and S. N. Bhatia, Tissue Engineering, 1st ed. Upper Saddle River: Pearson Prentice Hall, 2004.

[9] E. W. K. Young and D. J. Beebe, "Fundamentals of microfluidic cell culture in controlled microenvironments.," Chemical Society reviews, vol. 39, no. 3, pp. 1036-48, Mar. 2010.

[10] J. A. Burdick and G. Vunjak-Novakovic, "Engineered microenvironments for controlled stem cell differentiation.," Tissue engineering. Part A, vol. 15, no. 2, pp. 205-19, Feb. 2009.

[11] H. Yu, I. Meyvantsson, I. A. Shkel, and D. J. Beebe, "Diffusion dependent cell behavior in microenvironments.," Lab on a chip, vol. 5, no. 10, pp. 1089-95, Oct. 2005.

[12] J. Becerra, L. Santos-Ruiz, J. A. Andrades, and M. Marí-Beffa, "The stem cell niche should be a key issue for cell therapy in regenerative medicine.," Stem cell reviews, vol. 7, no. 2, pp. 248-55, Jun. 2011.

[13] A. Spradling, D. Drummond-Barbosa, and T. Kai, "Stem cells find their niche," Nature, vol. 414, no. November, 2001.

[14] Kshitiz, D.-H. Kim, D. J. Beebe, and A. Levchenko, "Micro- and nanoengineering for stem cell biology: the promise with a caution.," Trends in biotechnology, vol. 29, no. 8, pp. 399-408, Aug. 2011.

[15] E. Dejana, "Endothelial cell-cell junctions: happy together.," Nature reviews. Molecular cell biology, vol. 5, no. 4, pp. 261-70, Apr. 2004.

[16] S. P. Herbert and D. Y. R. Stainier, "Molecular control of endothelial cell behaviour during blood vessel morphogenesis," Nature Reviews Molecular Cell Biology, vol. 12, no. 9, pp. 551-564, Aug. 2011.

[17] E. C. Lai, "Notch signaling: control of cell communication and cell fate.," Development

(Cambridge, England), vol. 131, no. 5, pp. 965-73, Mar. 2004.

[18] K. Niessen and A. Karsan, "Notch signaling in the developing cardiovascular system.," American journal of physiology. Cell physiology, vol. 293, no. 1, pp. C1-11, Jul. 2007.

[19] J.-P. Frimat et al., "A microfluidic array with cellular valving for single cell co-culture.," Lab on a chip, vol. 11, no. 2, pp. 231-7, Jan. 2011.

[20] J. T. Groves and M. L. Dustin, "Supported planar bilayers in studies on immune cell adhesion and communication," Journal of Immunological Methods, vol. 278, no. 1–2, pp. 19-32, Jul. 2003.

[21] T. D. Perez, W. J. Nelson, S. G. Boxer, and L. Kam, "E-cadherin tethered to micropatterned supported lipid bilayers as a model for cell adhesion.," Langmuir : the ACS journal of surfaces and colloids, vol. 21, no. 25, pp. 11963-8, Dec. 2005.

[22] F. T. Bosman and I. Stamenkovic, "Functional structure and composition of the extracellular matrix.," The Journal of pathology, vol. 200, no. 4, pp. 423-8, Jul. 2003.

[23] S. F. Badylak, "The extracellular matrix as a scaffold for tissue reconstruction," Online, vol. 13, no. 02, pp. 377-383, 2002.

[24] K. E. Brown and K. M. Yamada, "The role of integrins during vertebrate development," Seminars in Developmental Biology, vol. 6, no. 2, pp. 69-77, Apr. 1995.

[25] F. G. Giancotti, "Integrin Signaling," Science, vol. 285, no. 5430, pp. 1028-1033, Aug. 1999.

[26] C. Bökel and N. H. Brown, "Integrins in development: moving on, responding to, and sticking to the extracellular matrix.," Developmental cell, vol. 3, no. 3, pp. 311-21, Sep. 2002.

[27] M. M. Stevens and J. H. George, "Exploring and engineering the cell surface interface.," Science (New York, N.Y.), vol. 310, no. 5751, pp. 1135-8, Nov. 2005.

[28] J. Takagi, K. Strokovich, T. a Springer, and T. Walz, "Structure of integrin alpha5beta1 in complex with fibronectin.," The EMBO journal, vol. 22, no. 18, pp. 4607-15, Sep. 2003.

[29] S. L. Goodman, "Alpha 6 beta 1 integrin and laminin E8: an increasingly complex simple story.," Kidney international, vol. 41, no. 3, pp. 650-6, Mar. 1992.

[30] R. Haubner, R. Gratias, B. Diefenbach, S. L. Goodman, A. Jonczyk, and H. Kessler, "Structural and Functional Aspects of RGD-Containing Cyclic Pentapeptides as Highly Potent and Selective Integrin R V 3 Antagonists," Analysis, no. 8, pp. 7461-7472, 1996.

[31] J. D. Humphries, A. Byron, and M. J. Humphries, "Integrin ligands at a glance.," Journal of cell science, vol. 119, no. Pt 19, pp. 3901-3, Oct. 2006.

[32] G. E. Plopper, H. P. McNamee, L. E. Dike, K. Bojanowski, and D. E. Ingber, "Convergence of integrin and growth factor receptor signaling pathways within the focal adhesion complex.," Molecular biology of the cell, vol. 6, no. 10, pp. 1349-65, Oct. 1995.

[33] K. T. Tran, L. Griffith, and A. Wells, "Extracellular matrix signaling through growth factor receptors during wound healing.," Wound repair and regeneration : official publication of the Wound

Healing Society [and] the European Tissue Repair Society, vol. 12, no. 3, pp. 262-8.

[34] C. M. Consortium, "Cell Migration Gateway," EISSN: 1747-7883, 2012. [Online]. Available: http://www.cellmigration.org/. [Accessed: 10-Aug-2012].

[35] R. Zaidel-Bar, M. Cohen, L. Addadi, and B. Geiger, "Hierarchical assembly of cell-matrix adhesion complexes.," Biochemical Society transactions, vol. 32, no. Pt3, pp. 416-20, Jun. 2004.

[36] B. Geiger, "A 130K protein from chicken gizzard: its localization at the termini of microfilament bundles in cultured chicken cells.," Cell, vol. 18, no. 1, pp. 193-205, Sep. 1979.

[37] T. M. Svitkina and G. G. Borisy, "Arp2/3 complex and actin depolymerizing factor/cofilin in dendritic organization and treadmilling of actin filament array in lamellipodia.," The Journal of cell biology, vol. 145, no. 5, pp. 1009-26, May 1999.

[38] D. Vignjevic and G. Montagnac, "Reorganisation of the dendritic actin network during cancer cell migration and invasion.," Seminars in cancer biology, vol. 18, no. 1, pp. 12-22, Feb. 2008.

[39] G. Giannone et al., "Lamellipodial actin mechanically links myosin activity with adhesion-site formation.," Cell, vol. 128, no. 3, pp. 561-75, Feb. 2007.

[40] C. K. Choi, M. Vicente-Manzanares, J. Zareno, L. a Whitmore, A. Mogilner, and A. R. Horwitz, "Actin and alpha-actinin orchestrate the assembly and maturation of nascent adhesions in a myosin II motor-independent manner.," Nature cell biology, vol. 10, no. 9, pp. 1039-50, Sep. 2008.

[41] P. Hotulainen and P. Lappalainen, "Stress fibers are generated by two distinct actin assembly mechanisms in motile cells.," The Journal of cell biology, vol. 173, no. 3, pp. 383-94, May 2006.

[42] D. R. Critchley, "Biochemical and structural properties of the integrin-associated cytoskeletal protein talin.," Annual review of biophysics, vol. 38, pp. 235-54, Jan. 2009.

[43] A. Horwitz, K. Duggan, C. Buck, M. C. Beckerle, and K. Burridge, "Interaction of plasma membrane fibronectin receptor with talin--a transmembrane linkage.," Nature, vol. 320, no. 6062, pp. 531-3, 1986.

[44] A. P. Gilmore and K. Burridge, "Regulation of vinculin binding to talin and actin by phosphatidyl-inositol-4-5-bisphosphate.," Nature, vol. 381, no. 6582, pp. 531-5, Jun. 1996.

[45] K. A. DeMali, C. A. Barlow, and K. Burridge, "Recruitment of the Arp2/3 complex to vinculin: coupling membrane protrusion to matrix adhesion.," The Journal of cell biology, vol. 159, no. 5, pp. 881-91, Dec. 2002.

[46] W. Huang, N. Sakamoto, R. Miyazawa, and M. Sato, "Role of paxillin in the early phase of orientation of the vascular endothelial cells exposed to cyclic stretching.," Biochemical and biophysical research communications, vol. 418, no. 4, pp. 708-13, Feb. 2012.

[47] M. Yoshigi, L. M. Hoffman, C. C. Jensen, H. J. Yost, and M. C. Beckerle, "Mechanical force mobilizes zyxin from focal adhesions to actin filaments and regulates cytoskeletal reinforcement.," The Journal of cell biology, vol. 171, no. 2, pp. 209-15, Oct. 2005.

[48] E. H. Hall, A. E. Daugherty, C. K. Choi, A. F. Horwitz, and D. L. Brautigan, "Tensin1 requires protein phosphatase-1alpha in addition to RhoGAP DLC-1 to control cell polarization,

migration, and invasion.," The Journal of biological chemistry, vol. 284, no. 50, pp. 34713-22, Dec. 2009.

[49] J. T. Parsons, "Focal adhesion kinase: the first ten years," Journal of Cell Science, vol. 116, no. 8, pp. 1409-1416, Apr. 2003.

[50] H. C. Ott et al., "Perfusion-decellularized matrix: using nature's platform to engineer a bioartificial heart.," Nature medicine, vol. 14, no. 2, pp. 213-21, Feb. 2008.

[51] H. C. Ott et al., "Regeneration and orthotopic transplantation of a bioartificial lung," Nature Medicine, vol. 1, no. July, pp. 1-8, Jul. 2010.

[52] T. H. Petersen et al., "Tissue-engineered lungs for in vivo implantation.," Science (New York, N.Y.), vol. 329, no. 5991, pp. 538-41, Jul. 2010.

[53] C. J. Bettinger, R. Langer, and J. T. Borenstein, "Engineering substrate topography at the micro- and nanoscale to control cell function.," Angewandte Chemie (International ed. in English), vol. 48, no. 30, pp. 5406-15, Jan. 2009.

[54] M. A. Serban and G. D. Prestwich, "Modular extracellular matrices: solutions for the puzzle.," Methods (San Diego, Calif.), vol. 45, no. 1, pp. 93-8, May 2008.

[55] N. Li and A. Folch, "Integration of topographical and biochemical cues by axons during growth on microfabricated 3-D substrates.," Experimental cell research, vol. 311, no. 2, pp. 307-16, Dec. 2005.

[56] W.-J. Li, C. T. Laurencin, E. J. Caterson, R. S. Tuan, and F. K. Ko, "Electrospun nanofibrous structure: a novel scaffold for tissue engineering.," Journal of biomedical materials research, vol. 60, no. 4, pp. 613-21, Jun. 2002.

[57] S. K. W. Dertinger, X. Jiang, Z. Li, V. N. Murthy, and G. M. Whitesides, "Gradients of substrate-bound laminin orient axonal specification of neurons.," Proceedings of the National Academy of Sciences of the United States of America, vol. 99, no. 20, pp. 12542-7, Oct. 2002.

[58] R. C. Gunawan, J. Silvestre, H. R. Gaskins, P. J. a Kenis, and D. E. Leckband, "Cell migration and polarity on microfabricated gradients of extracellular matrix proteins.," Langmuir, vol. 22, no. 9, pp. 4250-8, Apr. 2006.

[59] M. Arnold et al., "Activation of integrin function by nanopatterned adhesive interfaces.," Chemphyschem : a European journal of chemical physics and physical chemistry, vol. 5, no. 3, pp. 383-8, Mar. 2004.

[60] K. A. Hing, "Bone repair in the twenty-first century: biology, chemistry or engineering?," Philosophical transactions. Series A, Mathematical, physical, and engineering sciences, vol. 362, no. 1825, pp. 2821-50, Dec. 2004.

[61] A. J. Engler, S. Sen, H. L. Sweeney, and D. E. Discher, "Matrix elasticity directs stem cell lineage specification.," Cell, vol. 126, no. 4, pp. 677-89, Aug. 2006.

[62] A. L. Zajac and D. E. Discher, "Cell differentiation through tissue elasticity-coupled, myosin-driven remodeling.," Current opinion in cell biology, vol. 20, no. 6, pp. 609-15, Dec. 2008.

[63] E. Cimetta et al., "Microfluidic device generating stable concentration gradients for long term cell culture: application to Wnt3a regulation of catenin signaling.," Lab on a chip, vol. 10, no. 23, pp. 3277-83, Dec. 2010.

[64] M. Katoh and M. Katoh, "WNT signaling pathway and stem cell signaling network.," Clinical cancer research : an official journal of the American Association for Cancer Research, vol. 13, no. 14, pp. 4042-5, Jul. 2007.

[65] M. J. Sutherland and S. M. Ware, "Disorders of left-right asymmetry: heterotaxy and situs inversus.," American journal of medical genetics. Part C, Seminars in medical genetics, vol. 151C, no. 4, pp. 307-17, Nov. 2009.

[66] A. Carreau, B. El Hafny-Rahbi, A. Matejuk, C. Grillon, and C. Kieda, "Why is the partial oxygen pressure of human tissues a crucial parameter? Small molecules and hypoxia.," Journal of cellular and molecular medicine, vol. 15, no. 6, pp. 1239-53, Jun. 2011.

[67] M. V. Chakravarthy, E. E. Spangenburg, and F. W. Booth, "Culture in low levels of oxygen enhances in vitro proliferation potential of satellite cells from old skeletal muscles.," Cellular and molecular life sciences : CMLS, vol. 58, no. 8, pp. 1150-8, Jul. 2001.

[68] M. Skolimowski et al., "Microfluidic dissolved oxygen gradient generator biochip as a useful tool in bacterial biofilm studies.," Lab on a chip, pp. 2162-2169, Jun. 2010.

[69] S. H. McKiernan and B. D. Bavister, "Environmental variables influencing in vitro development of hamster 2-cell embryos to the blastocyst stage.," Biology of reproduction, vol. 43, no. 3, pp. 404-13, Sep. 1990.

[70] J. Pouysségur, F. Dayan, and N. M. Mazure, "Hypoxia signalling in cancer and approaches to enforce tumour regression.," Nature, vol. 441, no. 7092, pp. 437-43, May 2006.

[71] L. E. Gerweck and K. Seetharaman, "Cellular pH gradient in tumor versus normal tissue: potential exploitation for the treatment of cancer.," Cancer research, vol. 56, no. 6, pp. 1194-8, Mar. 1996.

[72] I. K. Zervantonakis, C. R. Kothapalli, S. Chung, R. Sudo, and R. D. Kamm, "Microfluidic devices for studying heterotypic cell-cell interactions and tissue specimen cultures under controlled microenvironments.," Biomicrofluidics, vol. 5, no. 1, p. 13406, Jan. 2011.

[73] D. C. Dorn and A. Dorn, "Structural characterization and primary in vitro cell culture of locust male germline stem cells and their niche.," Stem cell research, vol. 6, no. 2, pp. 112-28, Mar. 2011.

[74] T. Vazin and D. V. Schaffer, "Engineering strategies to emulate the stem cell niche.," Trends in biotechnology, vol. 28, no. 3, pp. 117-24, Mar. 2010.

[75] D. E. Discher, D. J. Mooney, and P. W. Zandstra, "Growth factors, matrices, and forces combine and control stem cells.," Science, vol. 324, no. 5935, pp. 1673-7, Jun. 2009.

[76] S. Krause, M. V. Maffini, A. M. Soto, and C. Sonnenschein, "The microenvironment determines the breast cancer cells' phenotype: organization of MCF7 cells in 3D cultures.," BMC cancer, vol. 10, p. 263, Jan. 2010.

[77] D. Wlodkowic and J. M. Cooper, "Tumors on chips: oncology meets microfluidics.," Current opinion in chemical biology, vol. 14, no. 5, pp. 556-567, Sep. 2010.

[78] N. A. Raof, W. K. Raja, J. Castracane, and Y. Xie, "Bioengineering embryonic stem cell microenvironments for exploring inhibitory effects on metastatic breast cancer cells.," Biomaterials, vol. 32, no. 17, pp. 4130-9, Jun. 2011.

[79] J. Liu et al., "Mast cell: insight into remodeling a tumor microenvironment.," Cancer metastasis reviews, vol. 30, no. 2, pp. 177-84, Jun. 2011.

[80] N. T. Elliott and F. Yuan, "A review of three-dimensional in vitro tissue models for drug discovery and transport studies.," Journal of pharmaceutical sciences, vol. 100, no. 1, pp. 59-74, Jan. 2011.

[81] Y. Lai, A. Asthana, and W. S. Kisaalita, "Biomarkers for simplifying HTS 3D cell culture platforms for drug discovery: the case for cytokines.," Drug discovery today, vol. 16, no. 7–8, pp. 293-7, Apr. 2011.

[82] L. Sujata and S. Chaudhuri, "Stem cell niche, the microenvironment and immunological crosstalk.," Cellular & molecular immunology, vol. 5, no. 2, pp. 107-12, Apr. 2008.

[83] A. Sica, C. Porta, E. Riboldi, and M. Locati, "Convergent pathways of macrophage polarization: The role of B cells.," European journal of immunology, vol. 40, no. 8, pp. 2131-3, Aug. 2010.

[84] N. C. Talbot and L. A. Blomberg, "The pursuit of ES cell lines of domesticated ungulates.," Stem cell reviews, vol. 4, no. 3, pp. 235-54, Sep. 2008.

[85] T. Winslow, "Regenerative Medicine 2006 © 2006," 2006.

[86] A. Khademhosseini, R. Langer, J. Borenstein, and J. P. Vacanti, "Microscale technologies for tissue engineering and biology.," Proceedings of the National Academy of Sciences of the United States of America, vol. 103, no. 8, pp. 2480-7, Mar. 2006.

[87] P. Wallin, C. Zandén, B. Carlberg, N. Hellström Erkenstam, J. Liu, and J. Gold, "A method to integrate patterned electrospun fibers with microfluidic systems to generate complex microenvironments for cell culture applications," Biomicrofluidics, vol. 6, no. 2, p. 024131, 2012.

Chapter 2

Mobile and immobile cues for cells

Contents

I started my PhD by traveling to the kick-off meetings for the NanoCARD and NanoII European projects (page 14), which I would be involved in, together Julie. During the meetings Julie and I came up with a couple of ideas what we could contribute to the projects and what my research project should be about. In the next couple of weeks, we refined those ideas and decided that I would start to work on a system that Julie had a lot of experience with and I also had been working with before. We wanted to combine supported lipid bilayers ("BOX 2.1" on page 24) with gold nano patterned surfaces from Joachim Spatz's laboratory ("BOX 2.2" on page 26). The idea was to generate a special cell growth substrate that provides cells with laterally mobile, but also with immobile cues (Figure 2.1). On such a substrate a cell can rearrange and change the distribution of one cue dynamically and in dependence of its state, but on the other hand it is provided with a rigid, immobile part that it can attach to and exert a force on. Furthermore, the mobile part of the system not necessarily needed to be a cue to stimulate the cell, but could also serve as a reporter to study the accumulation of a certain cell receptor at the interface between the cell and the substrate [1].

Supported lipid bilayers

Julie had worked on using supported lipid bilayers as cell culture substrates for a couple of years, mainly to study initial attachment of neural progenitor cells to peptide functionalized bilayers [2]. I also had some experience with the system from my work with Nina Tymchenko which we were about to submit as a communication to Journal of the American Chemical Society. We worked on understanding the processes of cell attachment to a laterally mobile substrate and tried to show if the lipid bilayer was still intact and mobile underneath a cell, or if it was disrupted and cells were attaching to the underlying glass surface [3 manuscript

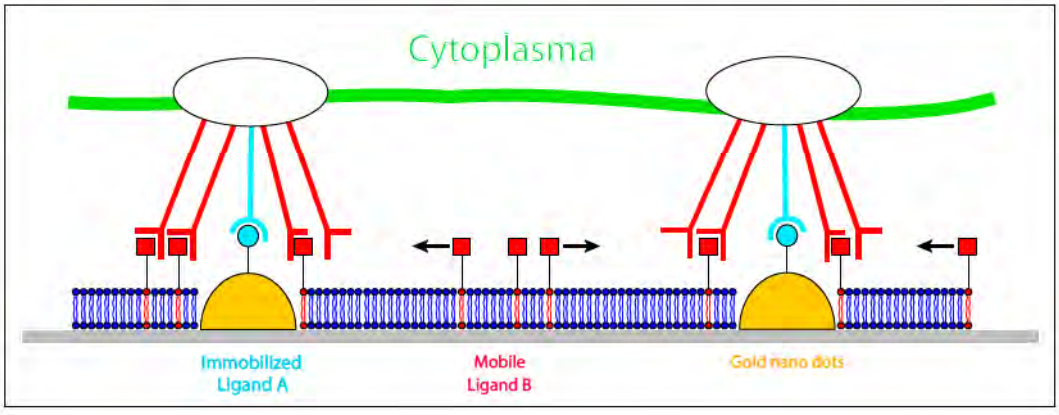

Figure 2.1
Schematic showing the idea of combining mobile and immobile cues in an cell culture platform by using gold nano dots and lipid bilayers

Supported lipid bilayers

BOX 2.1

Lipid bilayers play a very important role in biology and are essential for the life as we know it. The cell plasma membrane separates the inside of a cell from the surrounding environment and many intra-cellular compartments are formed by lipid bilayers. A lipid bilayer is a self-assembled thin membrane formed by two layers of lipid molecules this arrangement occurs due to the molecular properties of phospholipids. Phospholipids are amphiphilic molecules with a hydrophilic head group and a hydrophobic tail. This means that when lipids are placed in water they will assemble in a special way to minimize the contact of hydrophobic tales with water and thus may form a lipid bilayer sheet, where the tails are buried at the inside and the hydrophilic head-groups are facing the aqueous environment on both sides. Other molecular structures to minimize free energy include micelles, compact round structures with the tails facing inwards and the head groups outwards towards the water, and liposomes, a closed lipid bilayer structure which can vary in size from a several nanometers to a few micrometers in diameter. [13]

One way to study lipid bilayers and their properties *in vitro* is to form them on a solid substrate, so called supported lipid bilayers. They can be formed by vesicle adsorption; first intact lipid vesicles will adsorb on the surface until they reach a critical coverage, subsequently the vesicles will start to rupture and form a lipid bilayer at the surface [14]. The lipid vesicles used in this method are normally unilaminar and 70-150 nanometer in size, they can be formed from different lipid mixtures with a variety of properties.

Lipid behavior is defined by its molecular composition; in particular, the head group and two fatty acid tails play an important role. There are more than 500 different known forms of fatty acids (tails) and they can be either saturated or unsaturated; unsaturated fatty acids have one or more carbon-carbon double bonds. Fatty acids found in phospholipids in the cell membrane normally have acyl chains that are between 10 and 24 carbons long, and are either saturated or mono-unsaturated, poly-unsaturated fatty acids occur, but are less common in the membrane. The length and number of double bonds in the fatty acid chains of phospholipids defines their melting/phase-transistion temperature and thus lateral mobility and overall membrane elasticity. Below the melting temperature lipid bilayers are in the gel state where the acyl chains are ordered and mobility is limited, upon rising the temperature above the melting temperature lipid bilayers enter the liquid crystalline state where lipids can rotate more freely and mobility is higher, which can be measured with fluorescence recovery after photobleaching (FRAP) "BOX 2.4" on page 31. The melting temperature increases with increasing chain length, due to higher van der Waals forces between the chains, and decreases with an increasing number of carbon-carbon double bonds. The kink formed by a double bond increases the occupied volume and hinders van der Waals forces between neighboring chains. The lipid head group on the other side is responsible for the lipid bilayer charge, with lipid head groups that are anionic (net negative), zwitterionic (net neutral) or cationic (net positive).

In addition to the lipid composition, the surface plays an important role and will greatly influence bilayer formation [15], under normal conditions lipid bilayers can be formed on SiO_2 [15], glass [16], mica [17], TiO_2 [18] and oxidized PDMS [19]. The bilayer formation can be followed by for example quartz crystal microbalance with dissipation monitoring (QCM-D) measurements "BOX 2.3" on page 29.

Name	Structure	Comments
POPC	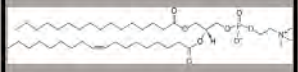	16:0-18:1 PC (GMP) Transition temperature: -2°C Charge: Zwitterionic 1-palmitoyl-2-oleoyl-sn-glycero-3-phosphocholine (POPC) C42H82NO8P
Rhod-PE	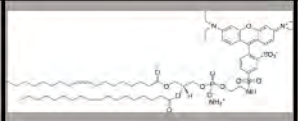	18:1 Liss Rhod PE Transition temperature: — (DOPE: -16°C) Charge: Negative 1,2-dioleoyl-sn-glycero-3-phosphoethanolamine-N-(lissamine rhodamine B sulfonyl) C68H109N4O14PS2
NBD-PC	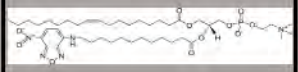	18:1-12:0 NBD PC Transition temperature: — Charge: Zwitterionic 1-Oleoyl-2-[12-[(7-nitro-2-1,3-benzoxadiazol-4-yl)amino]dodecanoyl]-sn-Glycero-3-Phosphocholine C44H76N5O11P
Maleimide-PE	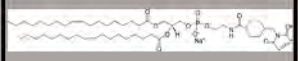	18:1 PE MCC Transition temperature: — (DOPE: -16°C) Charge: Negative 1,2-dioleoyl-sn-glycero-3-phosphoethanolamine-N-[4-(p-maleimidomethyl) cyclohexane-carboxamide] C53H90N2NaO11P
Biotinyl-PE	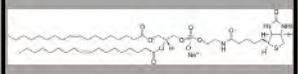	18:1 Biotinyl PE Transition temperature: — (DOPE: -16°C) Charge: Negative 1,2-dioleoyl-sn-glycero-3-phosphoethanolamine-N-(biotinyl) C51H91N3O10PNaS

Table 2.1
Table showing the different lipids used in this thesis with their name, chemical structure, composition, charge and transition temperature.

Gold nano dot structured surfaces

BOX 2.2

Joachim Spatz published 2003 in Nanotechnology [20] a way to produce surfaces with defined nano structures, using the self-assembly of diblock copolymer micelles. Block copolymer micelle nanolithography is a powerful technique to control the distance on the nanometer scale between small (2-8 nm) particles on a surface by changing the molecular weight of the block copolymers. Figure 2.2 illustrates the general principle. The method is very interesting for cell culture substrates, because it allows control in the nanometer range from 15-300 nanometers, thus mimicking length scales found in native extracellular matrix and at the same time it is possible to coat large surface areas of a couple square centimeters due to self-assembly.

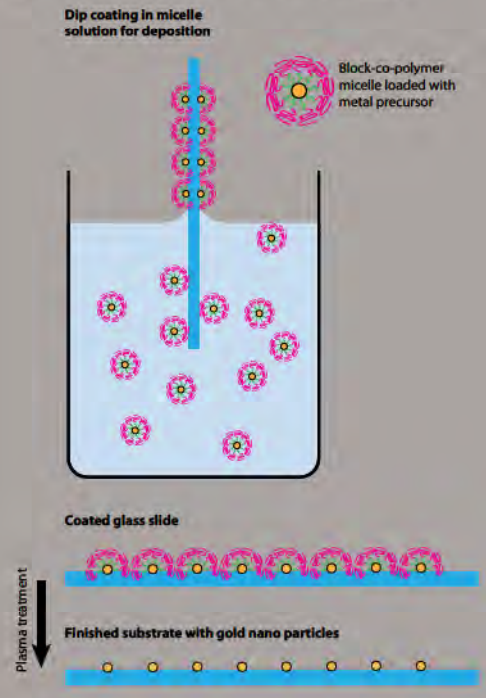

Substrates with different spacings have been used in many different studies to investigate mainly focal adhesion formation in cells in response to different inter particle distances of gold nano dots functionalized with a cell adhesion peptide. The results show that different cell types prefer different spacings and that focal adhesion formation is very tightly controlled in response to changes of a couple of nanometers. The optimal range for focal adhesion formation is between 50 to 70 nanometers [21], which is in correspondence with typical binding epitope spacing found *in vivo*, collagen and fibronectin binding epitope periodicity is around 65 nanometer [22], [23]. For larger spacings (above 100 nanometers) cells show delayed attachment, a faster turnover of focal complexes, rapid changes in cell morphology in the form of extension and retraction and higher cell mobility [24]. Thus, cells are definitely able to distinguish between different spacings and sense their environment on the nanometer length scale. Through signal integration within the cell, this ability will eventually result in global changes in cell gene expression patterns and cell fate determination, effecting cell differentiation, proliferation, migration and apoposis [21].

Figure 2.2
Schematic of the production process for glass slides with gold nano dots by dip coating. The glass slide is slowly retracted from a container filled with block-co-polymer micelle solution. The polymer ensures an equal spacing between particles and is removed with a plasma treatment in the second step. The end product are glass slides with equally spaced gold nano dots in a hexagonal order.

in preparation]. Others had demonstrated the potential of supported lipid bilayers to mimic cell-cell interactions by decorating the lipid bilayer with different ligands and molecules to simulate a cell [4–12] and we wanted to extend on that research.

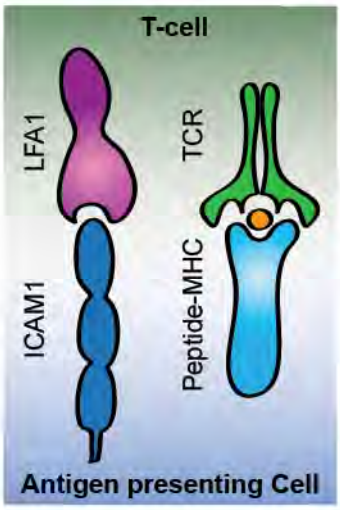

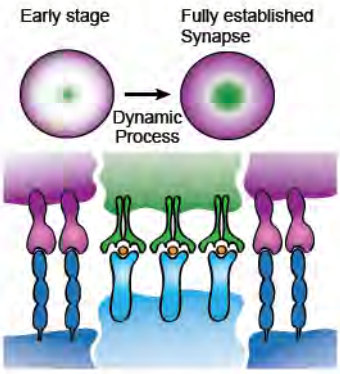

In particular, the work of Michael Dustin and Jay Grooves should be highlighted here. They focused on using supported lipid bilayer and cell interactions to study the formation of immunological synapses [1], [10], [12], [25]. An immunological synapse is formed between a T cell and an antigen-presenting cell; it is a very important part in the antigen recognition process of T cells. It involves various receptor-ligand interactions including T Cell Receptor (TCR) binding to peptide:major histocompatibility complex (pMHC), as well as leukocyte function-associated antigen-1 (LAF-1) on the T cell binding to intracellular adhesion molecule-1 (ICAM-1) present in the cell membrane of antigen-presenting cells. The ability to provide a cell with certain cues by functionalizing the supported lipid bilayer with molecules is of importance because it enables studies to mimic cell-cell interactions and study them in more detail. By using particular molecules, interactions can be separated from each other and underlying mechanism can be investigated to explore cellular pathways. Grooves and Dustin together with co-workers did a lot of work on bilayers functionalized with peptide:major histocompatibility complex (pMHC) and intracellular adhesion molecule-1 (ICAM-1) to understand how antigen recognition in a T cell works [10], [25]. The supported lipid bilayer is also a very practical system to study the dynamics of such interactions and the time dependent formation and reorganization of immunological synapses [12], [26], something that is very difficult to study when looking at real cell-cell interactions with two cells.

I was a bit hesitant at the beginning to use lipid bilayers in combination with gold nano structured surfaces as cell culture substrate. Despite that I thought that it would be really interesting, I was not convinced that it would work so well. The advantage of working with immune cells and the formation of the immunological synapse is that those cells do not apply large lateral forces on the substrates, and that experiments normally do not last longer than a couple of hours [10]. In contrast, we wanted to work with attachment dependent cells like cardiomyocytes or endothelial cells, which are known to exert lateral forces and wanted to study them over several days. From my previous experience I did know that it was a difficult system to work with and I was still unsure from our previous experiments, if the lipid bilayer was intact and mobile and if spreading cells were attaching to the bilayer or penetrating through it - a question that would follow me over a long time and even today we are not sure what the answer is. There were

a lot of uncertainties about this system and results varied even on the same substrate depending on the cells, there current state and their density. It was not a reliable system at the time. On the other hand, it was a very exciting project and both Joachim Spatz and Benjamin Geiger were very positive to the idea. The plan was to test some approaches in our laboratory and develop a robust protocol, once that was available I would go down to Israel and work in Benny Geiger's lab to study cell attachment to these substrates in detail. I was enthusiastic to have the opportunity to work together with Benjamin Geiger on this project, who I think is a great scientist and also a great person. This is how my first project started.

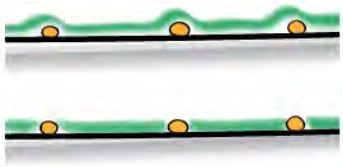

We decided to first focus on the formation of support lipid bilayers on substrates with gold nano dots without any functionalization. The main question at this early stage was if it is possible to form a bilayer at all and if the bilayer would cover the gold nano dots or form around them. For our future application, it was necessary to find a way to form the bilayer exclusively around the gold, leaving the nano dots accessible to present immobile cues. Roiter et al. had shown 2009 that a lipid bilayer could be formed around silica nanoparticles, when the particles were between 1.2 and 22 nanometer in diameter, once the particles became bigger or smaller the bilayer would envelop them [27]. Although, silica particles were used in that case, it offered a starting point for us and I was hopeful that it would work with gold nano particles as well.

I was also planning to look into different ways to functionalize the lipids at the same time, something which had been done before in our group and was supposed to be fairly straight forward. I thought it would be good to start working from both ends simultaneously to reach the goal of a complete platform presenting mobile and immobile cues to cells, faster. Things, however, proved to be more difficult than I had first imagined when I eagerly started.

Bilayers around Au dots

I wanted to study bilayer formation with two different techniques, quartz crystal microbalance with dissipation monitoring (QCM-D) and fluorescence recovery after photobleaching (FRAP). QCM-D is a surface sensitive technique that monitors the change in hydrated mass on a surface, for a more detailed description of the technique see "BOX 2.3" on page 29. With QCM-D, it is possible to follow vesicle adsorption to the surface until reaching full coverage and subsequently rupture of vesicle and formation of a supported lipid bilayer. In this way, QCM-D gives you data about the process of bilayer formation over a large

Quartz crystal microbalance with dissipation monitoring

BOX 2.3

Quartz crystal microbalance with dissipation monitoring (QCM-D) is a label-free surface sensitive technique that can detect mass changes down to 0.5 ng/cm^2 on a sensor surface (one sensor with a sampling rate of five seconds). If all 4 sensors of an E4 are used the sensitivity is 2 ng/cm^2 at sampling rate of one second. The sensor is a piezoelectric quartz crystal (14 mm in diameter) and by applying an alternating electrical potential across the crystal, it will start to oscillate at its resonant frequency (typical 5 MHz for Q-sense crystals). Upon mass increase on the surface this resonant frequency will decrease which can be detected, and thus changes at the interface can be followed. The detection depth, the distance from the crystal surface where changes are still measured, is approximately 250 nanometers, but is depending on the film structure. For rigid films that are closely coupled to the sensor surface the penetration depth is deeper. [28], [30]

The coupled mass can be calculated using the Sauerbrey model, which describes the linear relation between changes in frequency caused by changes in mass. This model is valid as long as the film on the sensor is fairly rigid (low dissipation) and closely coupled. If the film is too soft or high the frequency is no longer linear related to the mass, an addition have new molecules to the sensor will not generate the same frequency response as the first ones or the overall mass of a molecule is underestimated, because it is not closely coupled.

$$\triangle m = -\frac{C \cdot \triangle f}{n}$$

C = 17.7 ng Hz^{-1} cm^{-2} for a 5 MHz quartz crystal.

n = 1,3,5,7 is the overtone number.

Therefore, QCM-D does not only measure the frequency shift, but can also monitor energy dissipation by stopping the excitation of the crystals and following the decay in amplitude. The energy dissipation contains interesting information about the viscoelastic properties of the layer on a sensor surface. A rigid layer will that is closely coupled to the sensor will have less energy dissipation than a soft layer over the same time. The mass and thickness of soft films that do not fulfill the requirements of the Sauerbrey equation can be modeled with the Voigt-Voinova model [31] to give adequate results.

Because QCM-D is a surface sensitive technique, no labels are required and measurements can be followed in real-time, it is very suitable to study bilayer formation and the different steps associated with it. A typical measurement for POPC lipid vesicles on a SiO2 crystals resulting in bilayer formation with a final frequency shift of -25 Hz and dissipation below 0.5.

part of the sensor surface without the requirement of any labels in the lipid vesicle solution. Because the technique was developed in our laboratory in 1995 [28], [29] and has been used tremendously to monitor bilayer formation [15], there is a lot of knowledge how to interpret the data.

Whereas QCM-D tells you something about the processes occurring during bilayer formation, FRAP is used to look at the bilayer quality and mobility. In order for FRAP to work, a small portion of the lipid molecules need to be labeled with a fluorophore. Once the bilayer is formed, images are taken with a fluorescence microscope, a small spot in the center of an image frame is bleached with a high intensity light source and subsequently images are taken for a couple of minutes to follow recovery of the bleached spot. Recovery is possible, because the lipid bilayer is mobile and new fluorescence molecules diffuse into the bleached spot. The technique is described in more detail in "BOX 2.4" on page 31. The image data is analyzed to calculate the mobility of the lipid bilayer. If the lipid molecules in the bilayer are mobile the black spot in the center of the image will disappear over time, because other fluorescently labeled lipids will diffusive into the area. The time it takes for the spot to disappear will be depending on the diffusion coefficient of the laterally mobile lipids and is therefore a measure of their mobility. It is, however, important to keep in mind that FRAP is mainly a measure for the mobility of the labeled lipid and does not measure the unlabeled lipids.

In the first experiments to study bilayer formation on gold nano dot surfaces, I used a lipid mixture with 2% NBD-PC lipids and 98% POPC lipids and vesicles were approximately 90-100 nanometer in diameter. The fluorescently labeled lipid was even used in the QCM-D experiments, so results could be directly compared. I first started with Rhodamine head group labeled lipids, but switched to NBD tail labeled lipids very early on, because the Rhodamine was causing problems which I will come back to later.

For FRAP measurements I used glass slides coated with gold nano dots on one half of the sample and plain glass on the other half. The aim was to have an internal control and compare bilayer properties in the same dish, on the same glass surface with and without nano dots. For the QCM-D measurements the entire SiO_2 crystal was coated with gold dots. All surfaces were prepared at the Max Planck Institute for Intelligent Systems in Stuttgart by Yvonne Schön from Joachim Spatz group. Two different inter particle distances were used in this phase of the project, 65 and 250 nanometer, to see if the spacing between gold dots would influence the ability to form a bilayer. The gold nano particles themselves were around 6 to 8 nanometer in diameter and 4 to 5 nanometer high.

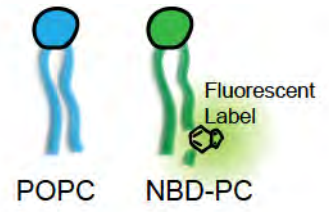

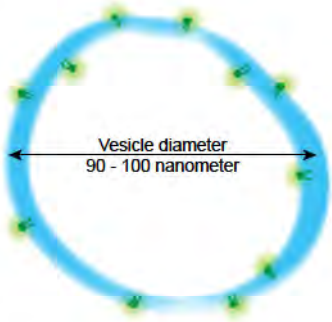

Fluorescence recovery after photobleaching

BOX 2.4

FRAP stands for fluorescence recovery after photobleaching and is a technique that can be used to measure lateral lipid mobility in bilayers. It requires having a fluorescence label on some the lipid molecules, commonly 1 to 2 weight percent is sufficient, but with more sensitive cameras lower concentrations are possible. It is important to keep in mind that FRAP is only able to detect the fluorescence lipids, therefore it is important that those lipids behave similar to the rest of the lipid matrix to extract data that is relevant for the whole bilayer. FRAP measurements use bleaching, the destruction of fluorophores due to illumination, and the subsequent recovery to extract the diffusion coefficient of a lateral mobile lipids, a typical FRAP series is shown in Figure 2.3.

In a first step, a couple of images are taken, this data is later needed to calculate the overall change in intensity over time due to general bleaching. In a second step, a spot of several tens of micrometers is illuminated with a higher intensity to locally quench the fluorophores in the center of the sample. It is important to use the maximum intensity to bleach the spot as fast as possible and achieve a sharp bleach spot. If it takes too long time diffusion will become significant even under the bleaching and the data will be more difficult to analyze. For this reason lasers are commonly used for bleaching, however we do not have a laser setup for the microscope I used for my FRAP measurements. The third step is the actually measurement. Images are taken in short intervals (5 seconds) over the whole field of view with low illumination power for 3 or 4 minutes to follow the recovery of the bleached spot. The lipid bilayer is present on the whole surface the entire time, but during bleaching the fluorescently labeled lipids are locally depleted, but due to diffusion and the lateral mobility within a bilayer this area recovers and an equal distribution of fluorescent lipids is reestablished.

The diffusion coefficient can be calculated from the intensity changes over time. During the recovery fluorescence lipids will constantly diffuse into the area and the intensity in the bleached spot will increase. By analyzing this change of intensity in the whole image sequence, one can get the coefficient. Peter Jönsson, a former group member, wrote a matlab program to automate this kind of analysis, which allows to quickly getting diffusion coefficients. In a first step, the program calculates the circular average with respect to r (distance from the center) to minimize spatial noise and afterwards transforms the data into the frequency domain, using a Hankel transform. The program also corrects for temporal noise and drift; drift occurs due to unintended photo bleaching during monitoring recovery of the intentional bleached spot. The advantage of this program is the robustness of the analysis to variations of the size or shape of the bleached spot, temporal drift, and spatial noise. The fact that only isotropic diffusion can be monitored is not limiting for lipid bilayer analysis, because diffusion in lipid bilayers is normally direction independent. [32]

Figure 2.3
Example of a typical FRAP image series for a recovering bilayer, showing selected images

I started with fluorescence microscopy experiments, because it took some time before I got coated QCM-D crystals and I thought that it would be easier to get an idea about bilayer formation by looking at the samples with fluorescence microscopy.

From the first experiments, it was obvious that there was a difference between the glass surfaces and surfaces covered with gold nano dots. Figure 2.4 shows two fluorescence images at the border between the glass part of the sample and the side coated with gold nano dots, either with a inter particle distance (IPD) of 65 or 250 nanometer. The illumination power (32.8 mW/cm^2 with FITC filter [33]) was the same for both images and the fluorescence intensity on the glass side is comparable between both samples, however, the intensity on the modified side is highest for the short spacing, but is also increased for the wider spacing. There is a bright line directly at the border visible on the 250 nanometer spacing sample, this is most likely an effect from the production process and is attributed to a higher density of gold nano dots directly at the dipping edge. Furthermore, the image is much more homogenous on the glass side compared to the gold structured part.

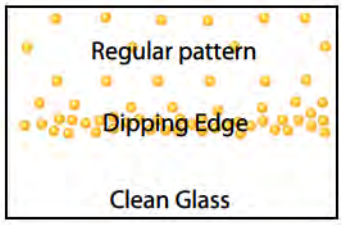

At this point, I had two possible explanations for this effect, either the gold was influencing the fluorescence signal in some way or more fluorescence lipid material was present on the structured side. Taking into account that the fluorescence on that side was much more inhomogeneous compared to the glass side, it could mean that lipid vesicles were adsorbing intact on the gold structured surfaces. This theory was further supported by the fact that the surface with more gold dots (IPD 65 nm) was brighter than the one with fewer dots (IPD 250 nm). If the vesicles would adsorb on the gold dots, there should be a relation between lipid material and thus fluorescence intensity and the number of gold particles per area.

After getting this initial data I wanted to look at the system in more detail and try to understand if my theory was right or if there was something else happening. I also wanted to know if

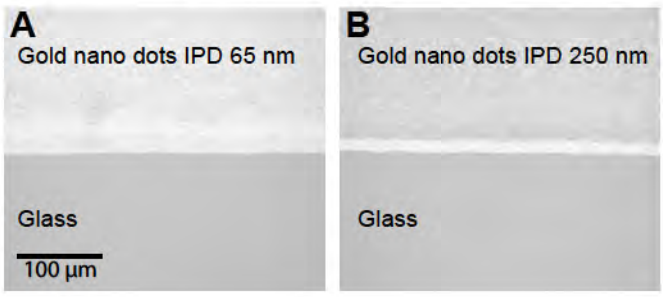

Figure 2.4
Fluorescence micrographs of NBD lipids at the border between the glass substrate and gold nano dot coated substrate, for both 65nm IPD and 250nm IPD.

there was a bilayer forming at all, although vesicles were adsorbing on the gold nano dots, there was still a possibility that a bilayer was formed in between the dots as well.

In order to test those ideas, I performed FRAP measurements both on two different gold nano structured surfaces, as well as on glass. I used 4 samples for each surface and the results are summarized in Table 2.2. The diffusion coefficient is very similar for all three surfaces, but lower on the gold structured part. The data was analyzed with a student's t-test and the resulting p-value is p=0.001 (glass – 250 nm spacing), p=0.02 (glass – 65 nm spacing) and p=0.008 (250 nm – 65 nm spacing). It is important to note that even though statistical significant the difference is very small. The diffusion coefficient reported in literature varies and values depend on lipid composition, fluorescence label, FRAP setup, analysis approach and surface properties, amongst others [34], [35]. The values presented here are comparable to values measured previously on glass substrates under the same conditions with the same procedure between.

	Mean Diffusion coeffcient	Standard Deviation
Glass	1.81	0.04
IPD 65 nm	1.76	0.02
IPD 250 nm	1.72	0.01

Table 2.2
Diffusion coeffcient and standard deviation for lipid bilayers formed on glass and gold nano dot coated substrates (IPD 65nm and 250nm)

Overall, this is interesting data, because it means that a mobile lipid bilayer is formed even on the gold nano dot structured surfaces, where I thought I was observing intact lipid vesicles before. One explanation would be that, although, intact lipid vesicles are adsorbing on the gold nano dots, which has been observed by others [14], there is a bilayer forming on the glass surface between the dots too, which recovers after bleaching.

All the fluorescence microscopy data pointed towards the fact that I did have a mixture of absorbed intact vesicles and lipid bilayer on the gold nano structured surface. This was not optimal for the final application, but it was also promising tom some extent. At least, I could show that the lipid bilayer remained mobile between the gold dots and that offered a starting point to improve the system further. The task was to find a solution to avoid vesicle adsorption.

At this point, I felt that I needed another experimental technique to validate the results I got from the fluorescence microscopy measurements. I had gotten the gold nano structured SiO2 crystals by now and was ready to test my theory with QCM-D. In the first measurements, I focused on the densely packed gold nano dots with a inter particle distance of 65 nanometer, because from the previous experiments I thought that the effect would be larger for those samples and therefore would be easier to measure with QCM-D.

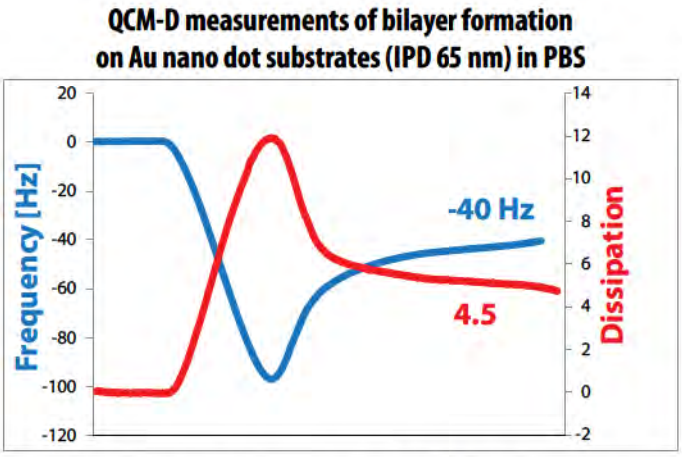

Figure 2.5
QCM-D measurement data for bilayer formation of POPC vesicles in PBS buffer on gold nano dot coated crystals with an interparticle distance of 65 nm

Both control samples and samples with gold dots showed the same qualitative behavior typical for bilayer formation (see Box QCM-D), but values differed. The control sample without any modifications had a frequency shift of 25 Hz and a dissipation shift of 0.3 which is expected for bilayer formation. On the other hand, the sample with gold nano dots (Figure 2.5) had a frequency shift of 40 Hz and a dissipation shift of 4.5. The increase in the frequency shows that more mass is coupled to the sensor surface, but more significant is the increase in dissipation, which is related to a higher viscoelasticity.

The qualitative similarity of the data for plain crystals and crystals with gold nano dots suggested that a bilayer is formed on both surfaces. The typical signal increase at the beginning showing intact vesicle adsorption until critical coverage is reached, follow by rupture of the vesicles and formation of a bilayer. It also fitted well with the FRAP data I had measured previously. The higher dissipation pointed towards the presence of intact vesicles, because vesicles are much more elastic and seen as a substantial increase in dissipation [36].

Everything seemed to come together nicely, the fluorescence microscopy measurements, the FRAP data and the QCM-D experiments all supported the theory shown in Figure 2.6. The only problem was that this was not what I was really aiming for. I needed the gold dots to be accessible for functionalization to present immobile cues to cells that I wanted to culture on these substrates. With all the vesicles still sitting on the surface, there was little chance the system would work in the end. Thus, I needed to get rid of the vesicles but keep the bilayer. I had previously tested to flush away the remaining vesicles by rigorous rinsing or later with high flow rates in the QCM-D liquid cell, but it did

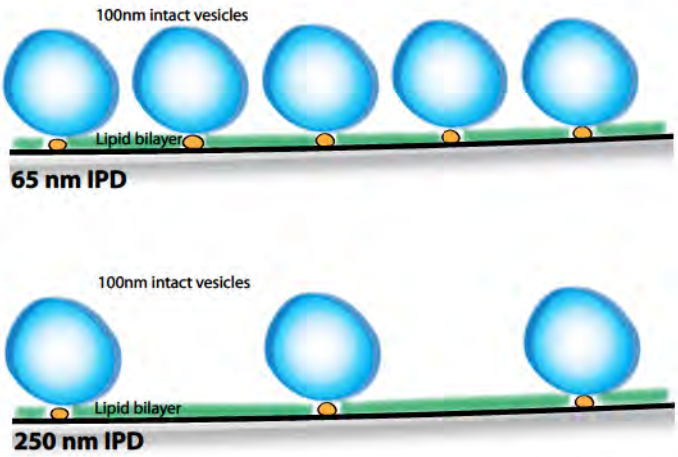

Figure 2.6
Schematic of intact vesicles on gold nano dots with a bilayer formed in-between as a possible explanation of the FRAP and QCM-D data.

not really help. After talking to some other people in the group, I learned that you can use buffers containing multivalent ions to assist vesicle rupture and I thought this is exactly what I should try.

I took the same lipid composition as before, but diluted the vesicles in a buffer containing 10mM $MgCl_2$, which should have the strongest promoting effect in bilayer formation [37]. Figure 2.7 shows the QCM-D results and it looks like bilayer formation is considerably improved by the addition of magnesium cations. At the beginning, the behavior is similar to the measurement before, but upon rinsing the frequency shift decreases to 26 Hz and the dissipation shift to 0.3, which is within the range for a normal bilayer. Especially, the large decrease in dissipation shift from 2.7 without the magnesium ions to 0.3 with them confirmed that the number of absorbed vesicles was highly reduced.

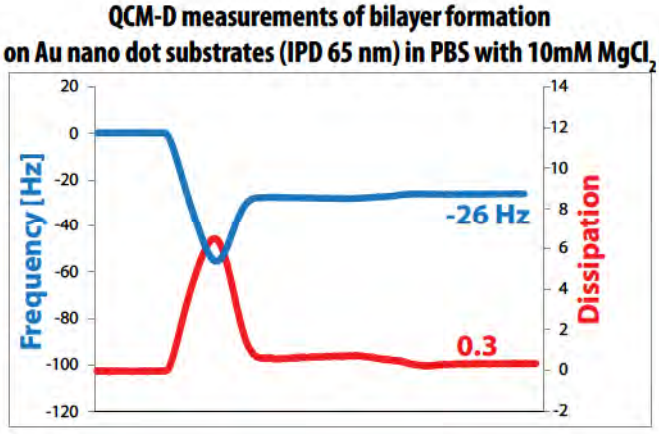

Figure 2.7
QCM-D measurement data for bilayer formation of POPC vesicles in PBS with 10mM $MgCl_2$ buffer on gold nano dot coated crystals with an interparticle distance of 65 nm

Bastien Seantier and Bengt Kasemo, who work on the same floor as we, have suggested that Mg^{2+} divalent cations interact with the phosphate in the lipid head group and converting it from a dipole into a positive monopole [37]. They, furthermore, showed that fewer vesicles need to adsorb on a surface before bilayer formation starts in comparison to conditions without magnesium cations. The conversion of the lipid headgroup leads to a stronger vesicle-surface interaction, because the vesicles are now positive and the surface negative charged. Another effect that they described in their paper is that the repulsion forces between vesicles will increase, due to the fact that both are positive charged. This second effect is very interesting in my particular case. My idea was that vesicles will adsorb on the small nano dots, this interaction will most likely be very weak because the gold nano dots are only 6 to 8 nanometer in diameter and are hopefully surrounded by a lipid bilayer. If the repulsion force between lipids increases only slightly that might be enough to break the weak interaction between the vesicles and the gold, thus vesicles will no longer adsorbing on the nano dots.

So, I did know from the QCM-D measurements that there was a chance that Mg^{2+} or divalent cations in general could help in getting rid of the vesicles on the gold nano dots. The next logical step would have been to go back to the fluorescence microscope and re-run the experiments to see if I could observe the same beneficial effect there and how the FRAP data would change. I do not remember why I never went back and did those experiments, but I did not do it. Probably, it was because at that time other projects were advancing faster and I did not have the time and peace to just go back and do the re-runs. Looking back at it now, I think it would have been good and worthwhile to do them.

There was, however, one additional problem. It was very difficult to evaluate if the bilayer was forming around the gold nano dots or if it was covering them underneath. I thought of two different ways to explore where the bilayer was forming, atomic force microscopy as a direct method or the adsorption of something to the gold as an indirect method.

With atomic force microscopy, it would be possible to measure the height and see if there were any bumps on the surface where the bilayer was formed on top of gold nano dots. This technique would have been great and I still think that it is required to clearly understand where the bilayer is formed. The problem was that I did not know enough about atomic force microscopy and could not run it on my own, and it was difficult to find someone who could run it for me.

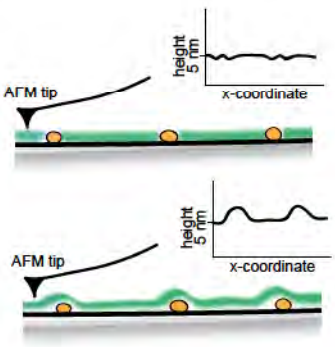

Therefore, I tried to use an indirect method and couple something to the gold. At the end of the day, that was what I was aiming for in the first place. As long as it was possible to couple something to the gold, it would allow us to use the substrate for its intended purpose. Instead of going directly to a thiol-gold coupling chemistry, I assumed it would be easier to adsorb proteins on the gold. My idea was, that a POPC bilayer is inert to protein adsorption [38], [39], hence if I would see a signal with QCM-D by introducing protein solution it would mean that the bilayer was not covering the whole surface. It is possible to argue that this not necessarily needed to be attributed to the gold nano dots, but that the bilayer in itself could have a lot of defects, but taking all the data into account I thought it would be worthwhile doing those experiments. I did know that I eventually needed to show that it was possible to covalently couple something specifically to the gold, but the protein approach offered me a simpler entry point to the problem.

I formed the bilayer with buffer containing magnesium chloride to avoid vesicle adsorption on gold structured crystals with 65 and 250 nanometer spacing. After successful bilayer formation bovine serum albumin (BSA) was injected at a concentration of 1 mg/ml for 15 minutes and subsequently rinsed with buffer. Figure 2.8 shows the QCM-D data for the bovine serum albumin injection. The signal for frequency and dissipation increases upon injection of the protein solution, but returns to its original value after rinsing; the response is very similar for both inter particle distances.

It was a bit difficult to interpret the data, the problem was that QCM-D measurements are not only sensitive to the effects directly at the surface, but are also influenced by the bulk solution up to a couple of hundred nanometers above the surface [36]. This, so called bulk shift, will result in a reversible shift in frequency and dissipation. It is difficult to distinguish between a weak interaction with a transient adsorption of BSA to the gold and a bulk shift, but there are two parts that were pointing more towards a bulk shift. If BSA was adsorbing on the gold, a difference in amplitude should be visible between the two different spacing. The number of gold dots and possible binding sides on the sample with 65 nanometer spacing are much higher than a sample with 250 nanometer inter particle distance. The other consideration was that the gold nano dots are very small (6-8 nm) and that the BSA (5-7 nm in diameter) might not even be able to adsorb on the gold in this case.

Overall the QCM-D experiments gave me some additional information about what was happening on the surface, but there still

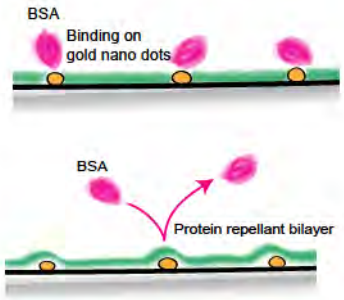

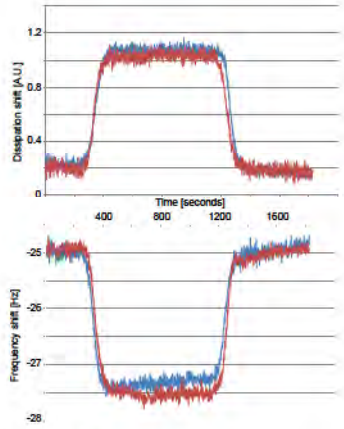

Figure 2.8
QCM-D data of BSA injection and rinsing step to show protein repellence of the substrate. Substrate with gold nano dots and successfully formed POPC lipid bilayer (not shown).
Top curve: Dissipation
Bottom curve: Frequency
Red: IPD65 nm Blue: IPD250 nm

were open questions. It was possible to get rid of the adsorbed vesicles with bivalent Mg^{2+} ions, or at least this is what the QCM-D measurements suggested, the ultimate test would be to use this approach with fluorescence microscopy as mentioned previously. If the bilayer under this conditions was forming over or around the gold nano particles was still unclear to me at this point. My experiment with the BSA adsorption was not really successful and in retro-perspective, it was not well designed from the beginning to answer this question. I did not have enough knowledge about surface chemistry and molecular surface interactions at this point to design a proper experiment. I did not consider the fact that the interactions between BSA and gold might be too weak on such small nano dots. Looking back, I should have coupled a thiol-biotin to the gold dots and afterwards detect successful coupling by injection of a large streptavidin molecule that binds to the biotin.

Taking into account both the fluorescence microscopy and QCM-D data I was still positive that the system could work, but I never went any further with this approach, because other things happened in the meantime to which I will come back at the end of this chapter.

Lipid tubes

At the beginning of all the bilayer experiments, I considered to use rhodamine head-labeled vesicles instead of the NBD tail-labeled lipids that I used in the end. Rhodamine is known to promote cell attachment [40] and I thought it would be interesting to see if rhodamine head-group labeled lipids would have a similar effect. The reason why I did all experiments with NBD-PC in the end were the initial results that I got with the Rhodamine label - I saw something that looked a little bit like fluorescence grass (Figure 2.9) on the lipid bilayer upon bleaching. I and other in the group had observed this kind of lipid structure previously, and we normally did everything to avoid getting them in our samples. Thus, I switched to NBD labeled lipids and could run my experiments without this problem. There was, however, some literature available about this kind of lipid structures and even people in our own group had been working on this previously. All of those approaches used some kind of special molecule to form lipid tubes, for example the polyunsaturated long fatty acid docosahexaenoic acid [41] or antimicrobial peptides temporins B and L [42], [43].

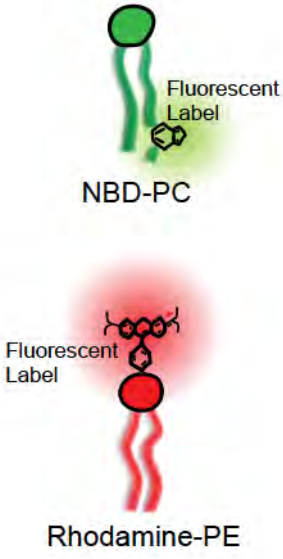

I have to admit that I was not really aware of this literature when I started my experiments, I was just curious to know what caused the formation of those lipid structures, under which conditions they are formed without intentional adding certain molecules and

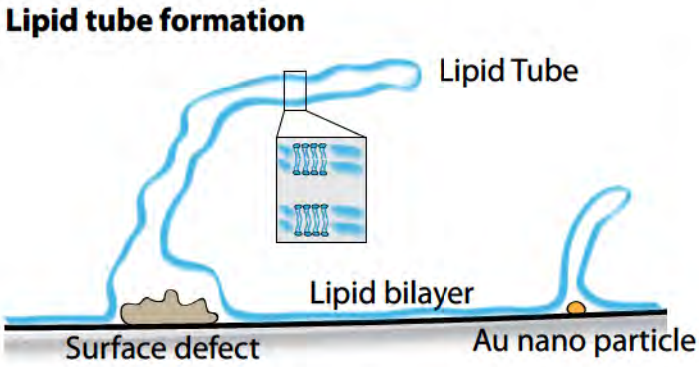

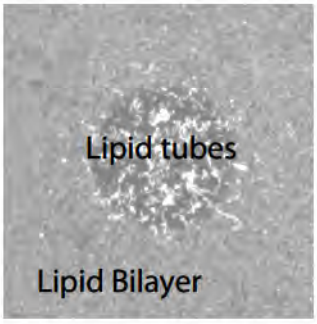

Figure 2.9
Schematic of lipid tube formation and an possible explanation for their formation. On the right: Lipid tubes formed on an gold nano dot coated substrate with Rhodamine-PE containing vesicles after bleaching.

what the underlying principle was. Figure 2.9 shows a schematic of one possible way what lipid tubes could look like and how they could assemble. There were different opinions ranging from surface contamination over liquid contamination to bilayer ageing, but all the options could not really explain what I saw in my measurements. So, I started a little side project to look into this issue in more detail and tried to understand what was happening.

The effect was very much limited to the bleaching area and I was able to change the size by varying the spot size (Figure 2.10). I could even place several spots next to each other by multiple exposures. So for me, it was clear that the effect was triggered by fluorescence light in combination with the gold nano structures, because I could not observe anything on plain glass substrates. I did, however, have no idea what the underlying principles could be and what I was actually seeing. Although, I did not have any particular application or use for such lipid structures, I thought it would be worthwhile to spend some time to investigate where they were coming from.

Figure 2.10
Effect of variations in bleachs spot size and position on lipid tube formation. Micrographs taken with 40x magnification of bilayer containing Rhodamine-PE lipids on gold nano dot structured substrates.

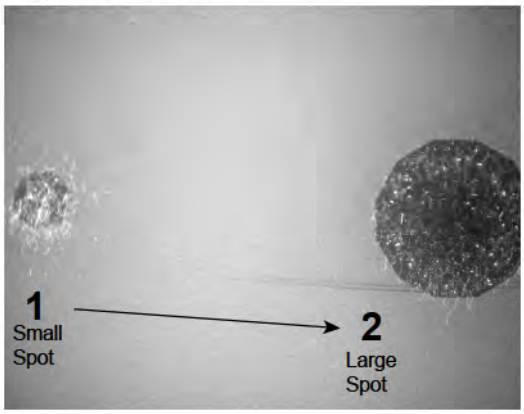

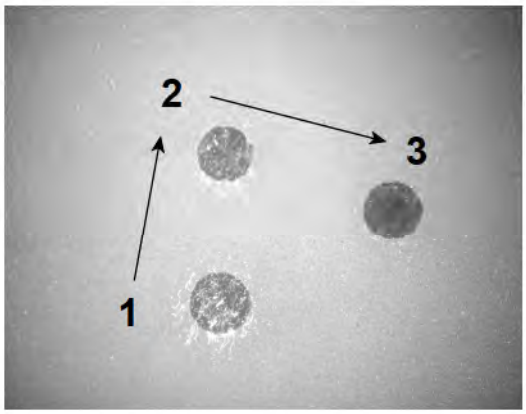

The first thing I considered was if the effect was in any way related to the time between bilayer preparation and measurements. I incubated gold structured surfaces with an inter particle distance of 65 nanometer with 2% Rhodamine-PE 98% POPC containing lipid vesicles for one and a half hours, before I rinsed them with PBS. I kept the samples in PBS after rinsing for 90, 150, 240 or 330 minutes before measuring. I found no correlation between the age of a bilayer and the formation of lipid tubes; they formed on all samples with gold nano dots independent from the time in buffer, but did not form on any of the plain glass surfaces. I did not check if even longer times in buffer solution in the range of days would have any effect, but the data showed at least that there was no influence within hours.

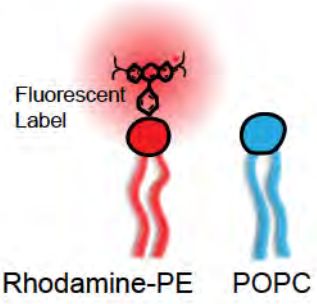

Another argument that is often brought up when bilayer formation is impaired in some way, is contaminations. Lipid bilayers are very sensitive to contaminations on the surface, as well as, impurities in solution [15]. In my measurements, I used glass surfaces were half of the area was modified with gold nano dots and the other half was empty. I could only observe the formation of lipid tubes on the gold structured side, because the liquid covered the whole surface including both sides, this meant that liquid contamination was highly unlikely. I could, however, not exclude that the surface itself was contaminated during the gold deposition process. One possibility to investigate surface contamination further would have been to use for example x-ray photoelectron spectroscopy to look at the atomic composition at the surface. But, I thought before going into such an extensive analysis, it would be better to see if there were other factors that influenced tube formation.

The next parameter on the list was the light itself, I was wondering if the wavelength of the light would have any impact on lipid tube formation. I used the same light source for all experiments, but selectively choose only parts of the spectrum for illumination during bleaching (Table 2.3). After the bleaching the bilayer was always imaged with a lower light intensity in the Rhodamine channel to be able to see the lipid bilayer and if present lipid tubes. The results showed that lipid tube formation was not an effect of light in general, but rather an effect that was only observed

Channel	Excitation wavelength [nm]	Bleching?	Lipid tubes?
DAPI	Bandpass 360-370	NO	NO
FITC	Bandpass 450-490	NO	NO
Rhodamine	Bandpass 540-550	YES	YES
Brightfield	Full spectrum	YES	NO

Table 2.3
Experimental scheme for different light excitations and their effect on bleaching and lipid tube formation.

when the sample is illuminated with a high intensity of the excitation wavelength of the rhodamine labeled lipid head groups. One part that was surprising with this data was that even brightfield illumination did not show the same effect; bleaching was observed, but not tube formation. This result was unexpected, because brightfield illumination contains all wavelengths including the part of the light that was used in the rhodamine channel. I still do not have any good explanation for this behavior and it would be good to repeat those experiments to confirm the results.

Once, I did know that lipid tubes were formed only during excitation in the rhodamine channel, the next logical step was to explore how different durations of illumination would correlate with tube formation. I was not only interested in the pure illumination time, but also if there were differences when light was entirely given at once versus the same amount given in chopped up intervals. The experiments included two different cumulative bleaching times, 10 seconds or 60 seconds. The illumination was either given at once or in intervals with 1 second of illumination and 4 seconds darkness, thus illumination in intervals was spread out over 50 seconds instead of 10 or 300 seconds instead of 60, but importantly the amount of light was similar for the "interval" and "at once" condition. Katarina Logg et al. showed in a completely different context that light-induced stress in yeast cells is related not only to the amount of light, but also to temporal scheme in which it is delivered [44]. Therefore, I thought it would be interesting to look if this could also be observed for my system. The samples were imaged 2 minutes after bleaching and the results are shown in Figure 2.11.

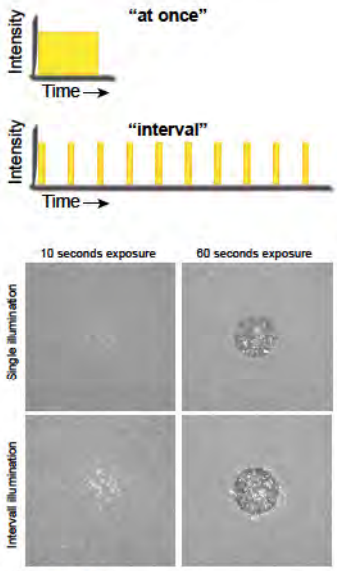

Figure 2.11
Effect of single or intervall illumination of lipid bilayers on gold nano dot coated substrates for two different accumulative exposure times.

Obviously, there is a difference depending on the exposure duration, more extensive lipid tube formation can be observed for 60 seconds than for 10. The images also show that there is a difference between samples illuminated a single time or in intervals. For the samples were the illumination is chopped up with short 1 second pulses of light and 4 seconds of darkness lipid tubes are longer and more numerous. One problem with this experimental scheme was that I had observed previously, lipid tubes grow over time even in darkness, because the bleaching procedure took differntly long, lipid tubes in the "interval" condition had more time to grow. One possibility to address this problem would have been to image the samples at many time points after bleaching and compare the results accordingly.

My initial thought that the lipid tube formation was connected to fluorescence illumination was more and more confirmed, but I still had no idea about the underlying process. It could be that the illumination itself was causing the effect, but it could also be

a secondary, more indirect effect of the illumination. I did know that the energy concentrated on a small part of the sample during illumination was quite high and that this would also lead to local heating. Since, the extent of lipid tube formation was related to illumination time and the effect was stronger when energy was delivered in intervals, I thought that local heating was one likely cause for tube formation. In order to test this hypothesis, I needed to decouple illumination and heating from each other in the next experiment.

I used an on-stage incubator that allowed me to step-wise increase the temperature in a petri dish which contained a lipid bilayer sample. I used both gold nano dot substrates, with interparticle distances of 65 and 250 nanometer, and a glass surface as control. The bilayers were formed at room temperature and the temperature was afterwards increased from 30°C to 50°C in two degree steps. Images were taken at each temperature point with low illumination power to minimize effects from the light.

Figure 2.12 shows fluorescence images at different temperatures for all three substrates. At room temperature (22°C) no lipid tubes are present, and even increasing the temperature to 30°C does not change the behavior of the lipid bilayer. Increasing the temperature further to 34°C, lipid tube formation begins to become visible on the glass substrate and the structured surface with 65 nanometer inter particle spacing, but not for the large 250 nanometer spacing where the first lipid tubes are visible at 36°C. At even higher temperatures the amount and length of lipid tubes increases for all samples, but there are fundamental differences in shape and length of lipid tubes between the glass surfaces and the gold nano structured surfaces.

On the glass, there are two distinct populations of lipid tubes. The first population of easiely visible long tubes, which can reach lengths of several hundrets of mirometers and are unevenly distributed over the sample. The other population is more difficult to see in the images (Figure 2.12 Glass 44°C), but are composed of small (1-2 micrometer) tubes that are evenly distributed over the entire surface. The situation on the surfaces with gold dots is different, here only short (3-15 micrometer) lipid tubes can be observed. These tubes are longer than the small ones on glass surfaces, but do not reach the length of the long ones and they are fairly evenly distributed over the whole surface. There is no significant difference between the two inter particle distances, it might be that the average length is slightly longer for 65 nanometer spacing, but it is difficult to judge from the available images.

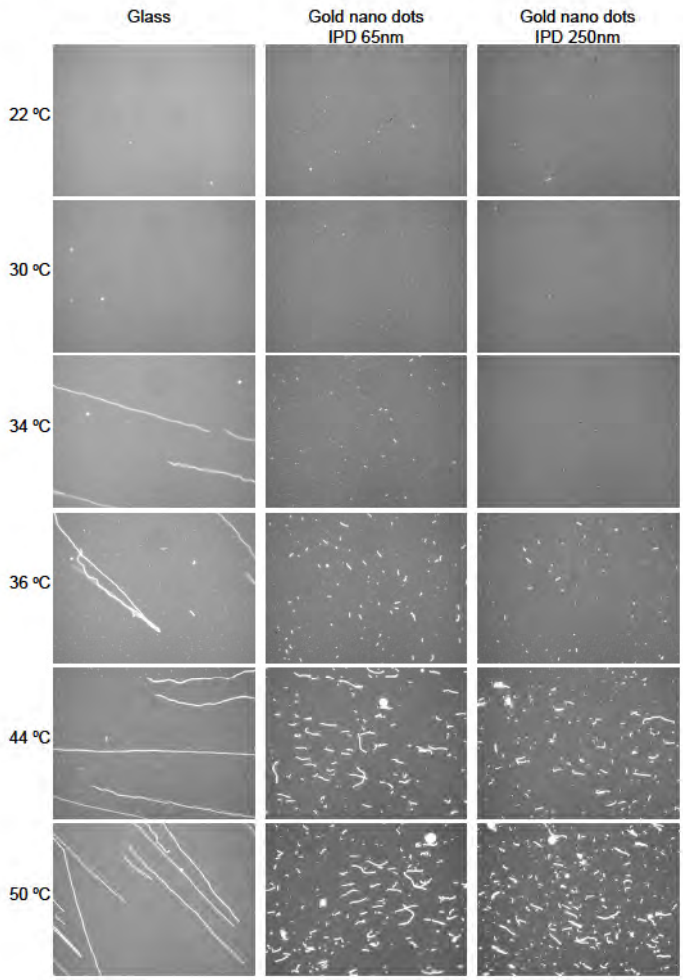

Figure 2.12
Temperature series from 22°C to 50°C of lipid bilayers formed on three different substrates: glass, gold nano dots IPD65 nm, and gold nano dots IPD200 nm. Lipid tube formation is visible on all samples, but the on-set temperatures varies for the thee substrates.

To me this data clearly showed that an increase in temperature would lead to lipid tube formation and that the transition temperature was around 34°C, but the underlying principle was still unclear. I thought that the difference in tube length and distribution could be a starting point, especially the two populations on glass substrates were unexpected and very interesting in this context. One observation at 34°C on the glass substrate (Figure 2.12) was further shaping an idea I got previously. The lipid tubes in Figure 2.13 are all originating from a straight line, which suggests a surface defect. It is quite common to have scratches on the glass surfaces that I used resulting in vesicle adsorption at those places instead of bilayer formation. Under normal circumstances, this does not pose any problems for bilayer experiments, but under my special conditions it was a very exciting fact.

Figure 2.13
Localized lipid tube formation on a glass substrate at 34°C

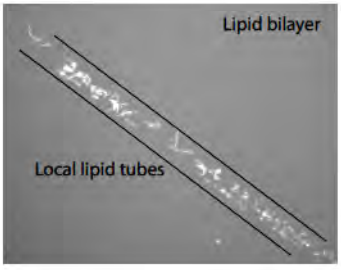

From all the data and different experiments, I came to the conclusion that three important preconditions needed to be fulfilled to see lipid tube formation, the presence of vesicles, energy in the form of heat and the right lipids. I observed tubes only with rhodamine-PE containing vesicles, but not when I used NBD-PC as a fluorescence label.

This could either be due to the fact that the rhodamine in general behaves differently or maybe more likely that the rhodamine label is sitting in the lipid head group. Due to its location the rhodamine can easily interact with the substrates and in particular the gold nano dots. For very close distances (100-150 Ångström), surface energy transfer (SET) between rhodamine as a donor dipole and the free conduction electrons of the gold nano dots might occur and the electromagnetic field might further enhance interactions [45]. Furthermore, the rhodamine is attached to a PE lipid. It is known that DOPE can undergo a phase transition from lamellar to hexagonal phase and form lipid tubes, in a pH-, composition- and temperature-dependent manner [46]. There are no reports on the composition that I used in my experiments, but other studies report 40°C [47] and 56°C [48] as a phase transition temperature. This is around the temperature I saw lipid tube formation in my system.

Heat could either be delivered to the sample directly as shown with the last experiment or it could be a consequence of high intensity illumination and the associated local heating on the substrate. This effect might be further increased by the gold nano dots, gold nano particles are known to adsorb light at specific wavelengths, depending on their size and shape [49],and are used for localized heating in cancer therapy [50]. The reason why I thought that intact lipid vesicles were needed was supported by several small observations. During the illumination experiments, I was not able to get lipid tube formation on the plain glass substrates where I had a smooth bilayer without intact vesicles, conversely, I did know that I had adsorbed vesicles on the gold nano dots where I saw tubes. For the heating experiment the long lipid tubes all originated most likely from defects in the lipid bilayer where lipid vesicles had not ruptured, meaning that intact vesicles were always present when lipid tubes could be formed.

The tube length in itself is also interesting to consider in this context, my assumption was that additional lipid material was required, in order to form lipid tubes. A scratch on the glass that will effect bilayer formation and can be observed with fluorescence microscopy is likely to be at least a few micrometers wide. This means that there is enough space for numerous vesicles to adsorb, in comparison to gold nano dots where the maximum

is one vesicle per dot, which is most likely not even reached due to weak interactions. Thus much more lipid material is available at a scratch, allowing longer lipid tubes to be formed. Because scratches on the surface are individual, unconstrained defects the long lipid tubes are not evenly distributed over the whole sample, but are clustered in areas with scratches. On the other hand the gold nano dots are present over the entire area and will therefore result in a more even distribution of tube lengths.

There is a fourth precondition, which I think needs to be fulfilled, but I do not have direct experimental prove that this is the case. I think besides energy, intact vesicles and the right lipids, a supported lipid bilayer is required as well and that the tubes are connected to the bilayer on the surface. During the bleaching experiments, I observed that the fluorescence intensity in the tubes is increasing. The bilayer spot is completely bleached and over time bright fluorescent tubes are appearing which are limited to the area of the black spot. In order for this to happen, labeled lipids need to diffuse from the surrounding lipid bilayer and accumulate in the tubes. Similar to normal FRAP experiments were the mobility of the lipid bilayer is proven by the recovery of the bleached spot, the intensity increase in the tubes can be seen as a proof for the ability of lipids to pass from the bilayer into the tubes. The reason why I am not able to say that this third precondition needs to be fulfilled for lipid tube formation in general is that I do not know if it is required or optional. One simple way to prove this would be to adsorb intact lipid vesicles for example on a titanium oxide surface and increase the temperature similar to the experiments described here. Because only intact vesicles and no lipid bilayer will be present on this surface, I would be able to answer the question if a surrounding bilayer is a necessity or an option, but I have not performed this experiment yet.

Another interesting observation was made when cooling down samples after heating them to 50°C.During cooling the lipid tubes collapsed and formed large lipid blobs on the surface. I was fascinated when I saw this effect for the first time under the microscope, how the lipids tubes started to roll up from one end and within a few seconds completely collapsed. I quickly took several movies and Figure 2.14 shows a time sequence of what was happening on the surface. Interestingly, this was not observed for the small evenly distributed population of lipid tubes on glass substrates, which just disappeared without any signs of accumulation of lipid material. These tubes contain much less lipid material and once the temperature is lowered the bilayer might relax and the short tubes disappear without leaving anything behind. On the other hand the long tubes contain so much lipid material, that they collapse and the extra lipid material is accumulated on one spot resulting in bright lipid assemblies.

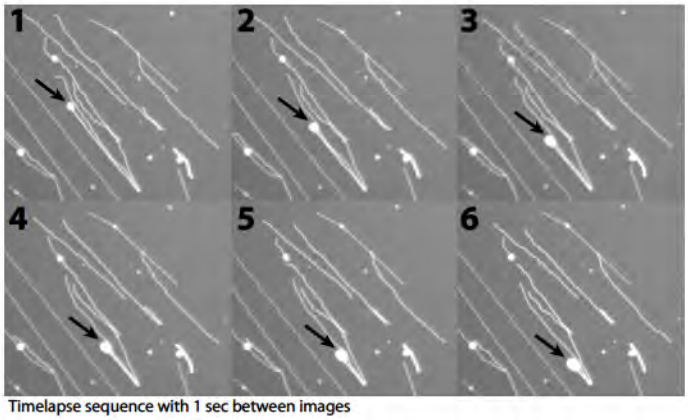

Timelapse sequence with 1 sec between images

Figure 2.14
Timelapse sequence of lipid tubes with 1second between images at 22°C. Lipid tubes are collapsing during cooling and form large lipid accumulates.

I, now, had a pretty good idea how lipid tubes could be formed, that three necessary preconditions were energy in the form of heat, intact lipid vesicles and the right lipids and that there was a fourth precondition of a surrounding lipid bilayer where I was not sure if it was necessary or optional. This way is systematically different from the methods described previously to form lipid tubes, because no additional molecules are needed and lipid tubes can be patterned with light. There were several experiments I thought needed to be done to get further insight into the underlying principles, but the main problem was that I still had no idea about the molecular effects. I was almost certain that some form of simulation, either molecular dynamics [51–53] or Monte Carlo [54], [55], was needed to fully understand how the lipid tubes were formed. So, I decided to present my data, during a group meeting to get some input from others – with limited success. During an additional meeting with Fredrik Höök, I was discouraged to continue to work on the lipid tubes, because I did not have any application for them in mind and I was told to focus on the original questions of forming a bilayer around the gold nano dots and the functionalization of the lipid bilayer. I thought it was a bit sad, I had come quite far, but I also realized that I could not continue the work on my own, since I lacked the knowledge to further investigate the molecular mechanisms behind tube formation. In general, I still think it was worthwhile to work on this side project, it was a project entirely driven by curiosity and even though I did not come all the way to a full explanation of the process and still do not have an application, I learned a lot during the process. I now know how to produce lipid tubes and developed a possible underlying theory. My curiosity was at least partially satisfied.

Lipid functionalization

Despite the fact that it was still unclear if the lipid bilayer formed around gold nano dots or over them, and the lipid tube side experiment took some time, I was still working on strategies to functionalize the lipid bilayer in parallel. One consideration was that in case I would not be able to form the bilayer on the gold nano substrates, I could still use functionalized bilayers on plain glass surfaces as cell culture substrates. We would not be able to reach our final goal of combining mobile and immobile cues on one substrate, but there were still a lot of interesting questions to investigate.

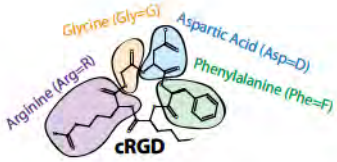

One main question that both we and Benjamin Geiger were keen to investigate was, if cells could form focal adhesions ("BOX 1.3" on page 6) on laterally mobile lipid bilayers. Other people had previously suggested that it was impossible for a cell to spread on a laterally mobile substrate and exert a force to it. They argued that in this case the cells were actually penetrating the lipid bilayer and attaching to the underlying glass substrate [4]. From our previous measurements, we still were not sure if that was the case and had come up with an alternative theory that cells are stabilizing the interface and cross-link the lipid bilayer to some extent [3manuscript in preparation].In order to answer this question, we decided to use the very common and well-studied attachment peptide cyclic RGD. Cyclic RGD is a small peptide sequence found in many extra cellular matrix proteins [56]. RGD is the one-letter amino acid code for Arginine-Glycine-Aspartic acid. The integrin receptors $ALPHA_vBETA_3$ and $ALPHA_{IIb}BETA_3$ found in many cells can bind selectively to the cyclic RGD sequence to form attachment points [57], [58].

Nearly independent of the molecule of interest, lipid bilayers can be functionalized by using different coupling chemistries, for example, maleimide-thiol [2], amine-coupling with N-Hyroxysuccinimide (NHS) [59] or biotin-streptavidin [60]. The independency of coupling chemistry to the molecule of interest is a large advantage, because although we were focusing on cyclic RGD for the first experiments, it meant that it would be easy to use similar protocols for other substances in the long run. It also meant that we could reuse old protocols from within the group [2] as a good starting point; unfortunately it was much more complicated than I first thought.

Julie and I decided to start with a maleimide-thiol coupling chemistry, which had been used previously in the group to couple IKVAV peptides to lipid bilayers [2]. We had lipids with maleimide head-groups left from those earlier studies and got some

thiolated cyclic RGD from Horst Kesslers' group in Germany. Everything was setup and ready and I started my experiments in July 2010, in the middle of summer vacation when everyone was away.

PE-MCC

I used the previous data as a starting point and work with a mixture of lipids, where 5% are PE-MCC with a maleimide in the head group, 2% are fluorescently tail-labeled NBD-PC lipids and the rest were POPC lipids. While, I planned to study the coupling chemistry with QCM-D first, I thought it would be good to include a fluorescently labeled lipid again right from the beginning to easily correlate data with later FRAP measurements. Here it was even more important to use a tale-labeled lipid like the NBD-PC, because I wanted to study cell attachment to a specific peptide and did not want to have any other entity like head-group labeled lipids to interfere with this interaction.

I started to look at bilayer formation with QCM-D, because it is impossible to label the cyclic RGD with a fluorophore without compromising the binding properties. And we did not have any antibodies against the peptide; therefore, QCM-D offered a good way to follow first the bilayer formation and afterwards the subsequent coupling of the peptide.

There were some initial problems, because I could not form bilayers from lipid vesicles containing maleimide lipids. I tested different batches of those lipids that we had in the freezer, changed the amount of PE-MCC lipids in the mixture down to 1% and modified the cleaning procedures for the crystals. In the end, I remembered what I learned from the bilayer formation experiments on gold nano structured surface and after adding 10mM magnesium chloride things worked. This should normally not be required, but I was happy to get the bilayers after all.

The next step was to couple the thiolated cRGD peptide to the lipid bilayer and it did not really work. I was running several QCM-D experiments and was unable to detect any reliable signal upon injection of cRGD peptide solution, I expected a small but detectable shift of -5 Hz similar to the IKVAV coupling [2]. There were two major obstacles at this time that complicated the whole situation. First, it was in the middle of summer and basically everybody was on vacation, so it was very tricky to ask other people for help. I did not have so much experience in chemistry and functionalization at that point to judge the importance of all the different steps and troubleshooting became a difficult task. Second, I had gotten a very limited amount of cRGD peptide from Benjamin Geiger's group and I did not wanted to waste it, but QCM-D measurements required quite a lot of material due

to the comparable large liquid cell. So, I was very limited in the number of experiments that I could run. In the end, it was probably due to thiol oxidation that I could not measure any response. One problem with with thiol-coupling chemistry is that disulfide bonds, the binding of two thiol groups together, can easily form by oxidation and exposure of solutions to air should therefore be reduced as much as possible. I did know that and tried my best working in a glove box under a nitrogen atmosphere, when preparing the solutions, but it did not help so much.

During this summer, I learned the hard way that some things are much more difficult than they look like, that it is very important to have other people around to ask for help and that you should do things either right or not at all. Because I did not have enough cRGD, I tried all different kinds of stuff for example to couple other thiols or to use reducing agents like TCEP (Tris(2-carboxyethyl)phosphine HCl) to open up BSA proteins and use their cysteine for coupling. It was not really worth it, instead of doing and testing all these things, I should have sat down, read through the literature and plan experiments that had a chance to be successful. But at least I learned this important lesson during one summer and will always remember it.

After all the problems, I had with the maleimide-thiol coupling-chemistry, I thought it would be wise to use a more robust method and after summer I discussed this with Julie. Julie was first hesitant to switch to a Biotin-Neutravidin-Biotin sandwich chemistry, because she was worry about the mobility of the bilayer and that the neutravidin might interfere with cell attachment. In the end, we agreed to give it a try to see if it was in general a possible route to go.

For this coupling chemistry the bilayer contains a low amount of biotinylated lipids, once a bilayer is formed neutravidin is coupled to the biotin in the lipids head-groups, because the neutravidin has four binding sites one of the remaining binding sites can be used to couple a biotinylated cyclic RGD on top in a subsequent step. There is no covalent bond formed between biotin and streptavidin, but the binding affinity is very high (K_D ~ 10^{-14} mol/L) [61] and remains stable for conditions used during cell culture [62].

I used two different concentrations of biotinylated lipids (Biotinyl PE) 0.1 and 1 % to investigate the effect of concentration on bilayer formation and lateral mobility. For the purpose to measure bilayer mobility, I again included 2% NBD-PC as a fluorescently labeled lipid in all experiments and used POPC lipids as a matrix.

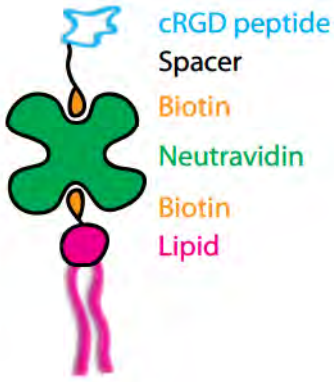

This time the bilayer formation did not pose any problems and the two step functionalization could easily be followed with QCM-D. The data in Figure 2.15 shows the formation of the lipid bilayer at the beginning, followed by coupling of the large neutravidin molecule and binding of the peptide in the last part. I used three different conditions to make sure the observed effect was true, condition one had 1% biotinylated lipids and neutravidin was injected at a concentration of 25 µg/ml, condition two had 0.1% biotinylated lipids and neutravidin and condition three had 1% biotinylated lipids again, but instead of neutravidin pure buffer was injected. Under all conditions peptide solution at a concentration of 25 µg/ml RGD-Biotin peptide in PBS was injected in the last stage.

The data very nicely showed that the amount of neutravidin that was binding to the lipid bilayer is correlated to the amount of biotinylated lipids, as I was expecting, the frequency shift upon neutravidin injection was 36 Hz for the 1% condition, whereas it was only 11 Hz for the 0.1% condition.

Detection of the peptide coupling step was much more difficult, because the peptide is very small and thus will increase the overall mass only a little bit. Importantly a shift was clearly detected for

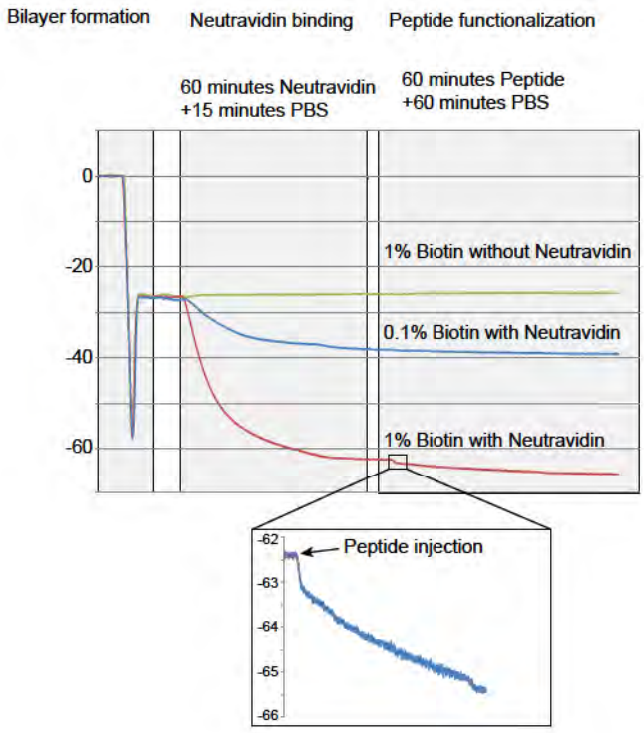

Figure 2.15
QCM-D data on bilayer formation, neutravidin binding and peptide functionalization under three different conditions.

the 1% condition with neutravidin, but not without neutravidin, showing that the shift is due to successful coupling. If the neutravidin is not present on the lipid bilayer the peptide has nothing to bind to and thus there is no frequency shift. For the 0.1% condition, it was a bit tricky to distinguish between noise and signal drift and successful coupling of the peptide. I assumed that the system worked even for this condition and that it was only difficult to probe the effect with the setup I used. I still think that is reasonable, because the control condition clearly showed that it worked.

After successful QCM-D measurements, I wanted to characterize the system further and see if the bilayer mobility was influenced by the large neutravidin. The small fraction of fluorescently labeled lipids allowed me to monitor the overall bilayer mobility using FRAP and I extended this approach by adding CY3-labeled streptavidin at a low concentration to the neutravidin solution to measure its mobility at the same time. Neutravidin and streptavidin are very similar, but streptavidin has an isoelectric point of 5 whereas neutravidin has a near neutral isoelectric point and thus basically no charge in cell culture conditions. The only reason to use labeled streptavidin was that we had that in the fridge, but did not have any labeled neutravidin. Because the cyclic RGD is coupled to both of them I assumed that the mobility for the peptide and the linker would be the same and I, therefore, could get information about the diffusion coefficient of the part I was most interested in.

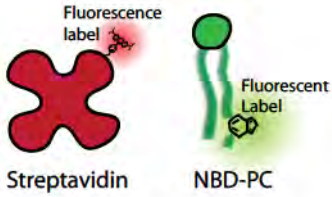

One problem when translating the experimental protocols from the QCM-D measurements to FRAP was that I normally used standard petri dishes to form bilayers on glass substrates or SiO2 crystals and looked at them with an immersion objective. This process required several ml of solution for each step and it was difficult to wash the surfaces efficiently, since I was limited to partial exchange of the liquid to keep the bilayer wet at all times. The QCM-D liquid cell had the advantage of being a closed system, where liquids could be injected in a simple manner and rinsing was not a problem. For some unknown reason I did not use the liquid chamber that our lab had designed for this particular situations. Instead, I worked on a microfluidic channel to minimize the liquid volume needed for each experiment down to a couple of microliter. At the same time, it was important that the bilayer in the channel was large enough to allow multiple and reliable FRAP measurements. The channel I used in the end was not optimal and I exchanged liquids with a pipette always trying to avoid air bubbles, but it worked and I was able to run the measurements. It, also, was the starting point to get deeper into microfluidics (see Chapter 3 & 4).

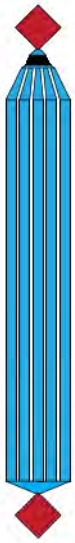

	Mean diffusion coefficient	Standard deviation
Bilayer	1.04	0.02
Bilayer with linker (Bilayer)	1.04	0.10
Bilayer with linker (Streptavidin)	1.01	0.08
Bilayer with linker and peptide (Bilayer)	1.03	0.09
Bilayer with linker and peptide (Streptavidin)	0.92	0.30

Table 2.4
Diffusion coefficient and standard deviation for all steps during bilayer functinalization for both the lipids and the linker.

Table 2.4 shows the diffusion coefficient calculated from the FRAP measurements for all different steps. I used 0.1% biotinylated lipids in this experiment and measured the lateral mobility both for the lipid bilayer and the linker after each step of the functionalization. There was no substantial difference for the diffusion coefficient of the lipid bilayer and the neutravidin or any change during the whole procedure. The value went down a little bit for the last measurement after peptide coupling, but it was still within the same range. Overall the values were lower than in previous measurements on larger glass substrates, but this is most likely attributed to the small channel size with limits the ability for recovery as illustrated in Figure 2.16. On the glass substrate, lipid material can diffuse freely over the entire surface which is several square millimeters. In the microfluidic on the other hand, the area is much more restricted, especially in one direction; the distance from the center to the channel wall is only around 400 micrometers. This constriction limits free diffusion in the lipid bilayer and has most likely an effect on the measured diffusion coefficient, but since the main objective was to compare diffusion coefficients for the different functionalization steps under similar conditions, this should not be a problem.

Figure 2.16
FRAP in microlfuidic channel with limited diffusion due to geometrical restrications from the channel.

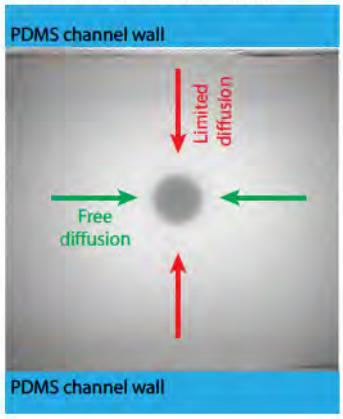

Important is that the measured values do not change during binding of the neutravidin and that the linker is as mobile as the rest of the bilayer. In a previous experiment, I had used 1% biotinylated lipids and under those conditions I saw a severe reduction of mobility upon binding of the neutravidin. Chengfei Lou et al. reported that streptavidin forms crystals at biotin-lipid concentrations over 1.5%, but that already before mobility was reduced for 1% biotinylated lipids compared to 0.75% in their study [63]. Thus, the measured difference in mobility that I saw between 0.1% and 1% biotinylated lipids is reasonable.

So this seemed to work, both the FRAP experiments and the QCM-D experiments showed promising results and I thought, great, finally I have a system that I can use in combination with my cells. When we were in Israel in June 2010 I had gotten transfected HeLa cells from Benjamin Geiger, which by the way is a very interesting story in itself how I transported those cells to

the lab alive in a flask, going through one of the most thorough airport security checks in the world at Ben Gurion international airport in Israel. Those HeLa cells, however, were transfected in a way that paxilin a small protein associated with focal adhesion formation ("BOX 1.3" on page 6) was tagged with a green fluorescence maker. I thereby could follow cell attachment and focal adhesion formation on lipid bilayers in living cells.

Cells on lipid bilayers

The last experiments with cells on bilayers, I did together with Nina T. and we were mainly focusing on the interaction of cells with lipid bilayers containing a small fraction of lipids with a positive charged head group. We looked at early attachment and spreading of cells happening within hours. As I mentioned before, we had some problems to get reliable and reproducible data with that approach, but were able to see a difference in cell morphology depending on the bilayer charge. When the bilayer was doped with positive charged head groups cells spread out, where as they were rounded on plain POPC bilayers.

Now that I had a working system to couple cRGD to a bilayer, I wanted to see how cells would behave on such a substrate. With the cRGD, we had a much more defined system than with the charged head groups; it was clear how cells interact with peptide and it was a direct interaction of cell integrins and peptide sequence. One problem though was to prepare the bilayers since the microfluidic channels that I had used before were not suitable for cell culture and I did not even have the equipment to maintain cells in microfluidic channels for longer periods, at that time. This meant I was forced to do run the experiments on normal glass substrates in wells and hope that everything would work. The major obstacle for that process was the large liquid volumes and associated with that the problem to wash the samples. In order to avoid de-wetting of the bilayer, the liquid could only be exchanged in partial rinses, which is very time-consuming and risk filled, because the liquid might not be completely exchanged or bubbles are destroying the bilayer.

Another problem was that the paxilin would show up in the green fluorescence channel, similar to the NBD lipid labeled that I normally used. I included the NBD-PC in the bilayer anyways, because it should be homogenously distributed in the bilayer and the focal adhesions would be localized having a much higher intensity. I hoped that I could still get some idea about both parts even though they were in the same channel. It would have been optimal to have a blue tail-labeled lipid, but I did not have that.

At the end I got everything to work and seeded HeLa cells on POPC bilayers (2% NBD-labeled PC) with 0.1% biotinylated lipids that were functionalized with cRGD via a neutravidin (5% Cy-3 labeled streptavidin) linker. The cells were incubated (37°C 5% CO_2) for 48 hours on the substrates and I just hoped that everything would work.

After the incubation I took the samples and looked at them under the microscope to see if the cells were spreading and if there still was a bilayer underneath them. Figure 2.17 shows a composite fluorescence micrograph with the cells in bright green (Paxilin GFP), the bilayer in green (NBD-PC) and red (streptavidin Cy-3). Cell morphology differs for the individual cells; the two cells in the center seem to be fairly spread out and the localized accumulation of paxilin is a clear sign for cell attachment and the

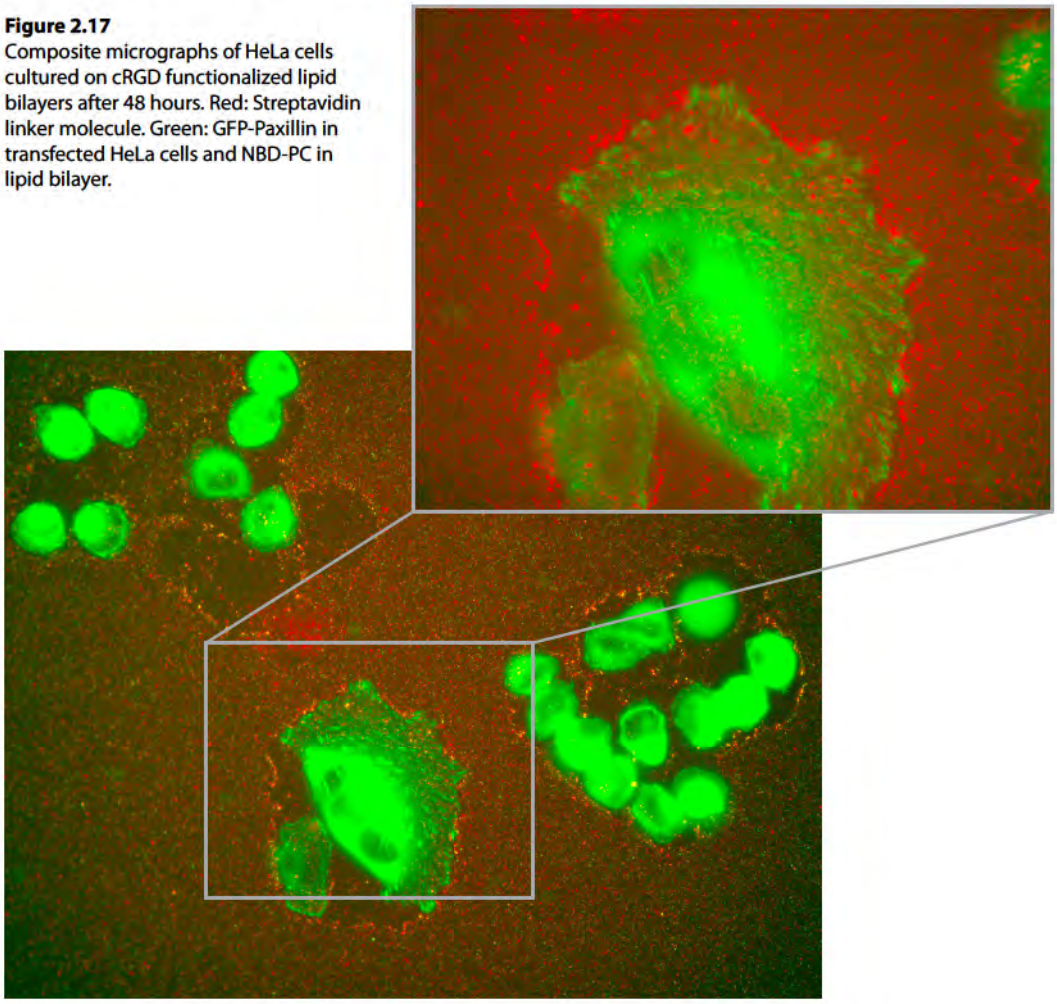

Figure 2.17
Composite micrographs of HeLa cells cultured on cRGD functionalized lipid bilayers after 48 hours. Red: Streptavidin linker molecule. Green: GFP-Paxillin in transfected HeLa cells and NBD-PC in lipid bilayer.

formation of attachment points ("BOX 1.3" on page 6). The other cells are much more rounded and it is difficult to judge if there is a higher local concentration of paxlin at the outer rim of some the cells or not. One very apparent fact is that the bilayer looks very different around the cells and far away from the cells. Directly next to the cells the fluorescence signal from the bilayer is fairly smooth and low in intensity, but far away the signal is much spottier and the overall intensity is higher. There is a clear boundary between those two areas with a thin line of even higher fluorescence intensity and a higher density of spots.

This result did not really look so promising; the bilayer did not seem to be intact after 48 hours in the incubator with cells seeded on top. An intact bilayer would have looked much smoother and homogenous, as the picture I took before during FRAP measurements. The samples with the cells looked more like intact vesicles adsorbed on the surface. This would also explain the two different areas and the rim at the border. If the surface was not covered with a lipid bilayer, but instead with intact lipid vesicles, a cell likely is able to attach to the underlying substrate and either internalize the lipid vesicles or push them away. During cell attachment, the cell will move and thereby creating an area with less vesicles larger than its own footprint, which can be seen as a smoother low intensity fluorescence signal in close proximity to the cells. Furthermore, the pushing of lipid vesicles could explain the formation of a rim, at the boundary where the cell has been pushed lipid vesicles will accumulate and be seen as a higher intensity rim.

The problem was just that this was not what I wanted. I needed an intact lipid bilayer to study how a cell could interact with it and what effect lateral mobility had on cell attachment, spreading and adhesion formation. I repeated this experiment twice, but got the same results again. Unfortunately, I did not look at the lipid bilayer prior to putting cells on top and thus was unable to know if there was a bilayer at the beginning or if there were vesicles from the start. I think one reason for the problems was the liquid handling and that I was not able to rinse efficiently enough between all the different functionalization steps.

I felt that I was not moving forward in this project, the problems were basically the same that I had already during my first experiments with cells on lipid bilayers together with Nina T. The system was not reliable, lacked the desired robustness and it was difficult to optimize it. In October 2011, Lohmüller et al. published a paper in NanoLetters which nearly exactly described what I had tried to achieve over the last one and a half years. It is a great paper and they characterized the system in a lot of detail,

functionalizing both the lipid bilayer and the gold nano dots with different proteins, testing different spacings of the gold nano dots and looking a cell attachment to those substrates. It really was precisely what we wanted to do, but did not succeed with. I was a little bit shocked at the beginning, but I quickly realized that they probably had better expertise, more resources, more people and a higher commitment for the project than we had. And I thought – it shows at least one thing, the idea that we had at the beginning was very good, even though we did not get it to work and others did. This paper also made it much easier for me to move away from lipid bilayers and I was happy about that. I was very eager to focus more on microfluidics which I thought was a fascinating field and the next chapters will tell you more about it and how to use them to study cells in defined microenvironments.

[1] Y. Kaizuka, A. D. Douglass, R. Varma, M. L. Dustin, and R. D. Vale, "Mechanisms for segregating T cell receptor and adhesion molecules during immunological synapse formation in Jurkat T cells.," Proceedings of the National Academy of Sciences of the United States of America, vol. 104, no. 51, pp. 20296-301, Dec. 2007.

[2] D. Thid et al., "Issues of ligand accessibility and mobility in initial cell attachment.," Langmuir : the ACS journal of surfaces and colloids, vol. 23, no. 23, pp. 11693-704, Nov. 2007.

[3] N. Tymchenko, P. Wallin, A. Kunze, and J. Gold, "Probing supported phospolipid bilayer mobility under adherent cells." 2012.

[4] T. D. Perez, W. J. Nelson, S. G. Boxer, and L. Kam, "E-cadherin tethered to micropatterned supported lipid bilayers as a model for cell adhesion.," Langmuir : the ACS journal of surfaces and colloids, vol. 21, no. 25, pp. 11963-8, Dec. 2005.

[5] B. Ananthanarayanan, L. Little, D. V. Schaffer, K. E. Healy, and M. Tirrell, "Neural stem cell adhesion and proliferation on phospholipid bilayers functionalized with RGD peptides.," Biomaterials, pp. 1-10, Aug. 2010.

[6] P. Y. Chan, M. B. Lawrence, M. L. Dustin, L. M. Ferguson, D. E. Golan, and T. a Springer, "Influence of receptor lateral mobility on adhesion strengthening between membranes containing LFA-3 and CD2.," The Journal of cell biology, vol. 115, no. 1, pp. 245-55, Oct. 1991.

[7] D. Stroumpoulis, H. Zhang, L. Rubalcava, J. Gliem, and M. Tirrell, "Cell Adhesion and Growth to Peptide-Patterned Supported Lipid Membranes," Cell, no. 5, 2007.

[8] A. E. Oliver et al., "Cell attachment behavior on solid and fluid substrates exhibiting spatial patterns of physical properties.," Langmuir : the ACS journal of surfaces and colloids, vol. 25, no. 12, pp. 6992-6, 2009.

[9] V. Marchi-Artzner, B. Lorz, U. Hellerer, M. Kantlehner, H. Kessler, and E. Sackmann, "Selective adhesion of endothelial cells to artificial membranes with a synthetic RGD-lipopeptide.," Chemistry (Weinheim an der Bergstrasse, Germany), vol. 7, no. 5, pp. 1095-101, Mar. 2001.

[10] J. T. Groves and M. L. Dustin, "Supported planar bilayers in studies on immune cell adhesion and communication," Journal of Immunological Methods, vol. 278, no. 1–2, pp. 19-32, Jul. 2003.

[11] J. T. Groves, L. K. Mahal, and C. R. Bertozzi, "Control of Cell Adhesion and Growth with Micropatterned Supported Lipid Membranes," Langmuir, vol. 17, no. 17, pp. 5129-5133, 2001.

[12] K. D. Mossman, G. Campi, J. T. Groves, and M. L. Dustin, "Altered TCR signaling from geometrically repatterned immunological synapses.," Science (New York, N.Y.), vol. 310, no. 5751, pp. 1191-3, 2005.

[13] M. Luckey, Membrane Structural Biology. Cambridge: Cambridge University Press, 2008.

[14] C. a Keller and B. Kasemo, "Surface specific kinetics of lipid vesicle adsorption measured with a quartz crystal microbalance.," Biophysical journal, vol. 75, no. 3, pp. 1397-1402, Sep. 1998.

[15] E. Reimhult, F. Ho, and B. Kasemo, "Intact Vesicle Adsorption and Supported Biomembrane Formation from Vesicles in Solution : Influence of Surface Chemistry , Vesicle Size , Temperature , and Osmotic Pressure †," Biomembranes, no. 18, pp. 1681-1691, 2003.

[16] H. Schönherr, J. M. Johnson, P. Lenz, C. W. Frank, and S. G. Boxer, "Vesicle adsorption and lipid bilayer formation on glass studied by atomic force microscopy.," Langmuir : the ACS journal of surfaces and colloids, vol. 20, no. 26, pp. 11600-6, Dec. 2004.

[17] R. P. Richter and A. R. Brisson, "Following the formation of supported lipid bilayers on mica: a study combining AFM, QCM-D, and ellipsometry.," Biophysical journal, vol. 88, no. 5, pp. 3422-33, May 2005.

[18] F. F. Rossetti, M. Bally, R. Michel, M. Textor, and I. Reviakine, "Interactions between titanium dioxide and phosphatidyl serine-containing liposomes: formation and patterning of supported phospholipid bilayers on the surface of a medically relevant material.," Langmuir : the ACS journal of surfaces and colloids, vol. 21, no. 14, pp. 6443-50, Jul. 2005.

[19] C. Satriano, M. Edvardsson, G. Ohlsson, G. Wang, S. Svedhem, and B. Kasemo, "Plasma oxidized polyhydroxymethylsiloxane--a new smooth surface for supported lipid bilayer formation.," Langmuir : the ACS journal of surfaces and colloids, vol. 26, no. 8, pp. 5715-25, Apr. 2010.

[20] R. Glass, M. M ller, and J. P. Spatz, "Block copolymer micelle nanolithography," Nanotechnology, vol. 14, no. 10, pp. 1153-1160, Oct. 2003.

[21] B. Geiger, J. P. Spatz, and A. D. Bershadsky, "Environmental sensing through focal adhesions.," Nature reviews. Molecular cell biology, vol. 10, no. 1, pp. 21-33, Jan. 2009.

[22] F. Jiang, H. Hörber, J. Howard, and D. J. Müller, "Assembly of collagen into microribbons: effects of pH and electrolytes.," Journal of structural biology, vol. 148, no. 3, pp. 268-78, Dec. 2004.

[23] W. C. Little, M. L. Smith, U. Ebneter, and V. Vogel, "Assay to mechanically tune and optically probe fibrillar fibronectin conformations from fully relaxed to breakage.," Matrix biology : journal of the International Society for Matrix Biology, vol. 27, no. 5, pp. 451-61, Jul. 2008.

[24] E. A. Cavalcanti-Adam, T. Volberg, A. Micoulet, H. Kessler, B. Geiger, and J. P. Spatz, "Cell spreading and focal adhesion dynamics are regulated by spacing of integrin ligands.," Biophysical journal, vol. 92, no. 8, pp. 2964-74, Apr. 2007.

[25] S.-J. E. Lee, Y. Hori, J. T. Groves, M. L. Dustin, and A. K. Chakraborty, "The synapse assembly model.," Trends in immunology, vol. 23, no. 10, pp. 500-2, Oct. 2002.

[26] S. Y. Qi, J. T. Groves, and a K. Chakraborty, "Synaptic pattern formation during cellular recognition.," Proceedings of the National Academy of Sciences of the United States of America, vol. 98, no. 12, pp. 6548-53, Jun. 2001.

[27] Y. Roiter, M. Ornatska, A. R. Rammohan, J. Balakrishnan, D. R. Heine, and S. Minko, "Interaction of lipid membrane with nanostructured surfaces.," Langmuir : the ACS journal of surfaces and colloids, vol. 25, no. 11, pp. 6287-99, 2009.

[28] M. Rodahl, F. Höök, A. Krozer, P. Brzezinski, and B. Kasemo, "Quartz crystal microbalance setup for frequency and Q-factor measurements in gaseous and liquid environments," Review of Scientific Instruments, vol. 66, no. 7, p. 3924, 1995.

[29] M. Rodahl, F. Höök, A. Krozer, and B. Kasemo, "Piezoelectric crystal microbalance for weighing small amounts of matter i.e. deposited on or removed from quartz electrodes - measures resonant frequency and dissipation factor using oscillation of crystal and measurement of," U.S. Patent 1996-506277 [80]1996.

[30] Technologynote, "Quartz crystal microbalance with dissipation (qcm-d)."

[31] M. V. Voinova, M. Rodahl, M. Jonson, and B. Kasemo, "Viscoelastic Acoustic Response of Layered Polymer Films at Fluid-Solid Interfaces: Continuum Mechanics Approach," Physica Scripta, vol. 59, no. 5, pp. 391-396, May 1999.

[32] P. Jönsson, M. P. Jonsson, J. O. Tegenfeldt, and F. Höök, "A method improving the accuracy of fluorescence recovery after photobleaching analysis.," Biophysical journal, vol. 95, no. 11, pp. 5334-48, Dec. 2008.

[33] C. S. Murphy and M. W. Davidson, "Light Source Power Levels," 2012.

[34] G. M. Lee and K. Jacobson, "Lateral Mobility of Lipids in Membranes," Current Topics in Membranes, vol. 40, pp. 111-142, 1994.

[35] C. Scomparin, S. Lecuyer, M. Ferreira, T. Charitat, and B. Tinland, "Diffusion in supported lipid bilayers: influence of substrate and preparation technique on the internal dynamics.," The European physical journal. E, Soft matter, vol. 28, no. 2, pp. 211-20, Feb. 2009.

[36] M. V. Voinova, M. Jonson, and B. Kasemo, "'Missing mass' effect in biosensor's QCM applications," Biosensors and Bioelectronics, vol. 17, no. 10, pp. 835-841, Oct. 2002.

[37] B. Seantier and B. Kasemo, "Influence of mono- and divalent ions on the formation of supported phospholipid bilayers via vesicle adsorption.," Langmuir : the ACS journal of surfaces and colloids, vol. 25, no. 10, pp. 5767-72, May 2009.

[38] A.-S. Andersson, K. Glasmästar, D. Sutherland, U. Lidberg, and B. Kasemo, "Cell adhesion on supported lipid bilayers.," Journal of biomedical materials research. Part A, vol. 64, no. 4, pp. 622-9, Mar. 2003.

[39] K. Glasmästar, C. Larsson, F. Höök, and B. Kasemo, "Protein adsorption on supported phospholipid bilayers.," Journal of colloid and interface science, vol. 246, no. 1, pp. 40-7, Feb. 2002.

[40] J. M. de la Fuente, A. Andar, N. Gadegaard, C. C. Berry, P. Kingshott, and M. O. Riehle, "Fluorescent aromatic platforms for cell patterning.," Langmuir : the ACS journal of surfaces and colloids, vol. 22, no. 13, pp. 5528-32, Jun. 2006.

[41] D. Thid, J. J. Benkoski, S. Svedhem, B. Kasemo, and J. Gold, "DHA-induced changes of supported lipid membrane morphology.," Langmuir : the ACS journal of surfaces and colloids, vol. 23, no. 11, pp. 5878-81, May 2007.

[42] Y. a. Domanov and P. K. J. Kinnunen, "Antimicrobial Peptides Temporins B and L Induce Formation of Tubular Lipid Protrusions from Supported Phospholipid Bilayers," Biophysical Journal, vol. 91, no. 12, pp. 4427-4439, Dec. 2006.

[43] R. Machán, A. Miszta, W. Hermens, and M. Hof, "Real-time monitoring of melittin-induced pore and tubule formation from supported lipid bilayers and its physiological relevance.," Chemistry and physics of lipids, vol. 163, no. 2, pp. 200-6, Feb. 2010.

[44] K. Logg, K. Bodvard, A. Blomberg, and M. Käll, "Investigations on light-induced stress in fluorescence microscopy using nuclear localization of the transcription factor Msn2p as a reporter.," FEMS yeast research, vol. 9, no. 6, pp. 875-84, Sep. 2009.

[45] T. Sen and A. Patra, "Resonance Energy Transfer from Rhodamine 6G to Gold Nanoparti-

cles by Steady-State and Time-Resolved Spectroscopy," Journal of Physical Chemistry C, vol. 112, no. 9, pp. 3216-3222, Mar. 2008.

[46] A. S. Ulrich, "Biophysical aspects of using liposomes as delivery vehicles.," Bioscience reports, vol. 22, no. 2, pp. 129-50, May 2002.

[47] D. Oliveira and L. N. Coelho, "Correlation of the effects of cryoprotectants over the supramolecular organization of bilayers and liposomes size composed by 1 , 2-dioleoylphosphatidylethanolamine (DOPE)," vol. 30, no. 2006, p. 2007, 2007.

[48] S. Linser, J. Andrä, M. Kumpugdee, S. S. Funari, and R. Willumeit, "The antimicrobial peptide NK-2 enhances the negative curvature strain in phosphatidylethanolamine model membranes," pp. 2-3.

[49] G. Baffou, R. Quidant, and C. Girard, "Heat generation in plasmonic nanostructures: Influence of morphology," Applied Physics Letters, vol. 94, no. 15, p. 153109, 2009.

[50] X. Huang, P. K. Jain, I. H. El-Sayed, and M. a El-Sayed, "Plasmonic photothermal therapy (PPTT) using gold nanoparticles.," Lasers in medical science, vol. 23, no. 3, pp. 217-28, Jul. 2008.

[51] V. Kothekar, "Molecular dynamics simulation of hydrated phospholipid bilayers.," Indian journal of biochemistry & biophysics, vol. 33, no. 6, pp. 431-47, Dec. 1996.

[52] P. Huang, J. J. Perez, and G. H. Loew, "Molecular dynamics simulations of phospholipid bilayers.," Journal of biomolecular structure & dynamics, vol. 11, no. 5, pp. 927-56, Apr. 1994.

[53] J. J. Wendoloski, S. J. Kimatian, C. E. Schutt, and F. R. Salemme, "Molecular dynamics simulation of a phospholipid micelle.," Science (New York, N.Y.), vol. 243, no. 4891, pp. 636-8, Feb. 1989.

[54] O. Lenz and F. Schmid, "A simple computer model for liquid lipid bilayers," Journal of Molecular Liquids, vol. 117, no. 1–3, pp. 147-152, Mar. 2005.

[55] S. O. Nielsen, C. F. Lopez, G. Srinivas, and M. L. Klein, "Coarse grain models and the computer simulation of soft materials," Journal of Physics: Condensed Matter, vol. 16, no. 15, p. R481-R512, Apr. 2004.

[56] B. Alberts, A. Johnson, J. Lewis, M. Raff, K. Roberts, and P. Walter, Molecular Biology of the Cell, 5th ed. New York: Garland Science, 2007.

[57] E. Ruoslahti and M. D. Pierschbacher, "New perspectives in cell adhesion: RGD and integrins.," Science (New York, N.Y.), vol. 238, no. 4826, pp. 491-7, Oct. 1987.

[58] E. Ruoslahti, "RGD and other recognition sequences for integrins.," Annual review of cell and developmental biology, vol. 12, pp. 697-715, Jan. 1996.

[59] C.-J. Huang, P.-Y. Tseng, and Y.-C. Chang, "Effects of extracellular matrix protein functionalized fluid membrane on cell adhesion and matrix remodeling.," Biomaterials, vol. 31, no. 27, pp. 7183-95, Sep. 2010.

[60] K. Shen, J. Tsai, P. Shi, and L. C. Kam, "Self-aligned supported lipid bilayers for patterning the cell-substrate interface.," Journal of the American Chemical Society, vol. 131, no. 37, pp. 13204-5, Sep. 2009.

[61] N. M. Green, "Avidin," Advances in protein chemistry, vol. 29, pp. 85-133, Jan. 1975.

[62] D. Falconnet, G. Csucs, H. M. Grandin, and M. Textor, "Surface engineering approaches to micropattern surfaces for cell-based assays.," Biomaterials, vol. 27, no. 16, pp. 3044-63, Jun. 2006.

[63] C. Lou, Z. Wang, and S.-W. Wang, "Two-dimensional protein crystals on a solid substrate: effect of surface ligand concentration.," Langmuir : the ACS journal of surfaces and colloids, vol. 23, no. 19, pp. 9752-9, Sep. 2007.

Chapter 3

Controlling liquid environments

Contents

After all the problems that I had with the lipid bilayers, my belief in that project was fading and I was looking for alternatives to form controlled environments on the cellular length scale. I was 10 months into my PhD and felt that something needed to change; I wanted to switch the focus of my research away from lipid bilayers. During those first months, I had worked a little bit with microfluidics on the side and used some simple channels in the bilayer experiments to reduce the liquid volume and simplify liquid exchange. There were a lot of problems with those channels and liquid handling was primitive and difficult, but I had a lot of ideas how to improve the system to get better results. I was fascinated by microfluidics with all their possibilities to alter fluid flow [1–3], control chemical mixing [4–6], the integration of sensors onto chips [7–13] and all the other things one could do. I really wanted to work with this kind of systems and concentrate my research in that area.

There were a few people in our division that were working with microfluidics, using small channels to drive bilayers [14], rapidly exchange liquid around lipid vesicles [15] or for sample handling in localized surface plasmon resonance (LSPR) measurements [16]. Although, those approaches were not very closely related to what I wanted to do, they helped me and offered a starting point into the world of microfluidics. So there was some base knowledge available nearby and I could easily get access to all the equipment that I needed to start working. However, there was no one who was working with cells in microfluidics channels in the division and the kind of systems that I was interested in. Julie had worked a long time ago, during her own PhD studies, with a shear flow cell which is the closest she had come to microfluidics, but I thought that the lack of background knowledge would not be such a big problem. I thought it would be worthwhile to invest some time to acquire the knowledge and build up all the necessary resources that I needed to perform experiments - and in the end Julie agreed. I was very optimistic and excited to start.

I started with reading the literature to get a better overview of what other people had done, what designs had been tested and what challenges people were facing. Basically, I needed to get an idea what the field of microfluidics was about and what was happening. I realized very quickly that there were a lot of articles in the area, at the beginning I was not so focused in my literature search and was reading articles that had to do with microfluidics in a very broad sense. I was overwhelmed by all the different things that had been already realized, and I thought it was difficult to come up with new ideas. Every time, I had an idea, that I thought was novel, I realized that people had already done it in some way. Looking back now, I think it was naïve to consider that

I would come up with something completely new within a couple of weeks without the experience from working in the field for some time. It was, nevertheless, a very interesting time and I am happy that I spend the time in getting into everything by reading all the articles, some more relevant than others, but at the end I had an idea what to do and where to start. I had not followed the same approach for my first research project on the lipid bilayers, because there was so much knowledge already available by the people working close to me that I never really sat down and went through all the literature. I think that was a mistake and things might have turned out differently with the bilayers if I had done a proper literature study first, but this time I did know better and I can say that it helped me a lot in my coming projects.

Microfluidic designs

There are different ways to produce microfluidic chips, but the most common procedure in academia, where small numbers of chips are needed and designs get changed often, is soft lithography with PDMS [17–20]. The process is described in detail in "BOX 3.2" on page 67; in general, you need a chrome mask with your channel design which is used to produce a SU-8 master, PDMS is molded and cured on the master, afterwards, the replicate in PDMS is detached from the master and bonded to a bottom substrate. This is a very convenient way to produce microfluidic channels and costs are limited, once you have an SU-8 master, which can be used over and over again, you only need an oven and plasma cleaner. Fortunately, our division has access to a PDMS lab with all the needed equipment and tools.

I have designed a variety of microfluidic channels in AutoCAD for different applications, most of them based on principles and designs from literature. For some of the channels, I did not have an immediate need, but thought they would be useful for future applications. Because the chrome mask is one of the expensive parts for microfluidic channels, I always tried to fit as many designs as possible on each of the four masks I have ordered until now. My idea was that, even though, the designs were often not very original, but rather close to designs others had used before, I could use those channels in a new context. For me it was also part of building up a library of different microfluidic networks that I and other could use in the future. The designs are shown and briefly describe in "BOX 3.3" on page 68.

Microfluidic principles

BOX 3.1

Microfluidics is a term used to describe systems that contain micrometer sized channels to transport liquids. Even though many different microfluidic systems have been realized and are used for a large variety of applications they all have some properties in common. Due to the small dimensions of the channels fluids behave differently at this length scale and microfluidic systems can take advantage of certain fluid mechanical properties not observed in larger liquid volumes. A common way to describe fluidic systems and their intrinsic properties is by using dimensionless numbers that give the ratio between two competing physical phenomena. The two most important numbers for microfluidic systems are the Reynolds number (Re) eq.1 that gives the ratio between viscous forces and inertial forces and the Péclet number (Pe) eq.2 that gives the ratio between convection and diffusion.[21]

$$Re = \frac{\rho \cdot U_0 \cdot L_0}{\eta} = \frac{f_i}{f_v} \qquad \textbf{eq.1}$$

ρ = *Density* ($1 \frac{g}{cm^3}$ *for water at* 20°C)
η = *Shear viscosity* ($1 \cdot 10^{-2} \frac{g}{cm \cdot s}$)
U_0 = *Flow velocity* (*typical* $1 - 1000 \frac{\mu m}{s}$)
L_0 = *Typical length scale* ($1 - 500 \mu m$)

At a typical length scale (L_0) of microfluidic channels that is between a few micrometers up to several hundreds of micrometers in diameter and flow velocities (U_0) in the micrometer to centimeter per second regime, the Reynolds number is normally below 100. This means that viscous forces are typically much larger than inertial forces in microfluidic channels and in many cases the nonlinear effects of inertial forces completely disappear. Therefore, microfluidic fluid system can often be described with linear Stokes equations eq. 3 and fluid flow is predictable and deterministic. Another important effect is that fluid flow in microfluidic channels is laminar without turbulences, the transition

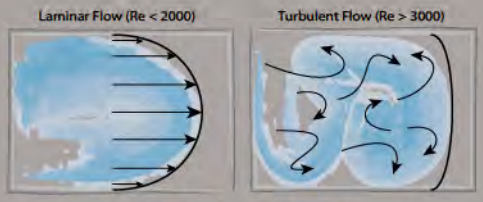

between laminar and turbulent flow occurs around a Re of 2000-3000. As a result, mixing of two parallel fluid streams in microfluidic channels is limited to diffusion at the interface between the streams. Such conditions are difficult to realize in larger fluid systems and offer some big advantages for cell biology applications of microfluidics as described in this thesis, but it also means that mixing is limited and might take very long time.

$$Pe = \frac{U_0 \cdot L_0}{D} = \frac{Z}{w} \qquad \textbf{eq.2}$$

U_0 = *Flow velocity* (*typical* $1 - 1000 \frac{\mu m}{s}$)
L_0 = *Typical length scale* ($1 - 500 \mu m$)
D = *Diffusion coefficient*
Z = *Length traveled down stream*
w = *Length traveled along the width of the channel*

The relation between convection, by which molecules in a fluid are travelling with a certain velocity in one direction and diffusion, by which they randomly travel in all direction, is given by the Péclet number. It can be used to estimate how long a channel needs to be in respect to its width to achieve complete mixing for a certain flow velocity and diffusion constant. For example Pe of 100 means that complete mixing within the channel is achieved after a distance that is 100 times the width of the channel. Péclet numbers can vary significantly in microfluidic systems depending on the molecule of interest, channel size and flow velocity and

$$\nabla p = \mu \nabla^2 \mathrm{u} + \mathrm{f} \qquad \textbf{eq.3}$$

p = *Pressure*
μ = *Dynamic viscosity*
u = *Flow velocity*
f = *Body forces acting on the fluid*
∇ = *Vector field operator*

are important to consider during the design process to either reach complete mixing between different streams or to avoid diffusive mixing in other systems.

The small dimensions of microfluidic channels, furthermore, result in a large surface area to volume ratio which means that surface properties become very important. The boundary conditions at the interface between the liquid and the channel wall have a severe effect on flow properties and the effect of hydrophobic walls will be much larger in a microfluidic system than in a large tube. Therefore, special measures need to be used to reduce the hydrophobicity of PDMS, a common material for microfluidic systems; most commonly oxidation of the surface via plasma treatment is used to get a hydrophilic layer on the PDMS and the channels are filled with water immediately afterwards to maintain hydrophilicity. An area of microfluidics that actually exploits the large surface area to volume ratio is electrokinetics, like electro-osmotic driven flow or on-chip electrophoresis. In electro-osmotic driven flow ionized liquids move relative to a charged surface (channel walls) when an electric field is applied [22]. In on-chip electrophoresis on the other hand, charged particles or molecules move relative to a stationary liquid in response to a electric field [23].

Besides the fact that fluid mechanical properties change at the small dimensions of microfluidic system, it also means that sample volumes are very small and are normally in the nanoliter or low microliter regime. The ability to control these volumes with high spatial and temporal resolution allows for experiment otherwise difficult to conduct. The use of microfluidic chips allows the delivery of a variety of signaling molecules to the cells in a highly controlled manner [1], [3], and the precise delivery allows generation of defined and controllable microenvironments [21], [24], as discussed in this thesis. Furthermore, reagent volumes are much smaller with is for example important when working with rare samples, to minimize waste, and to reduce costs.

Relation of surface to volume in different sized channels

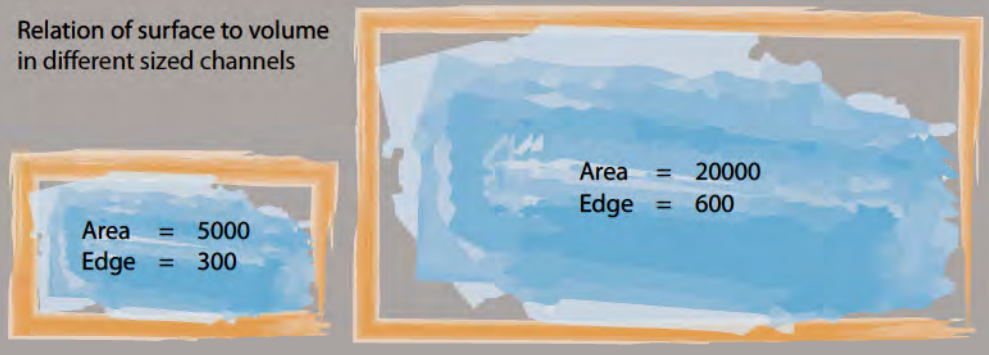

Microfluidic chip production

BOX 3.2

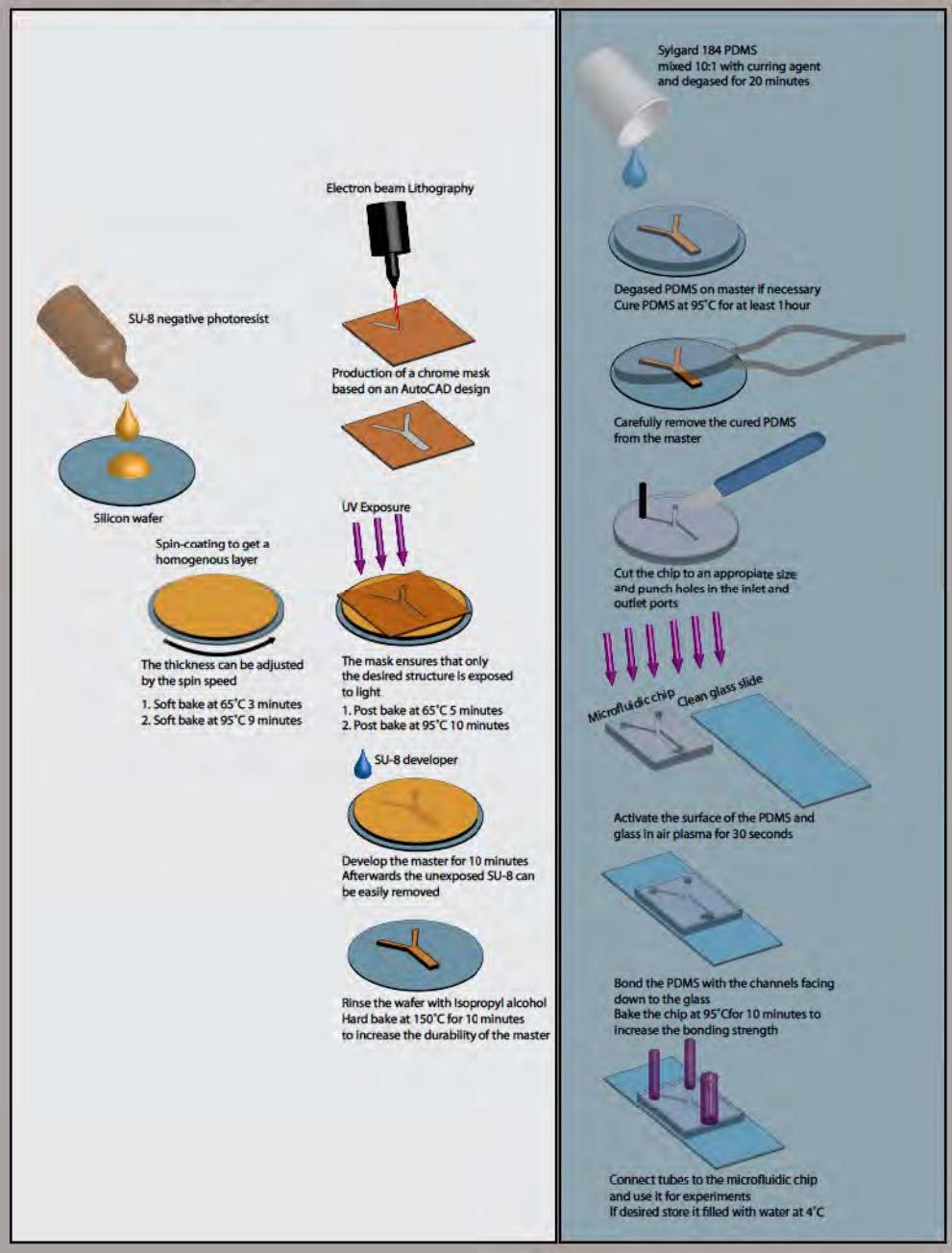

Microfluidic designs

BOX 3.3

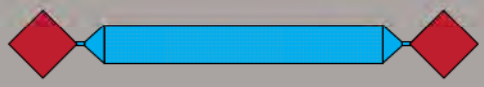

Channel 1 is a simple straight channel with one inlet and one outlet and a large cell culture area (2x14.4 mm). The cell culture area is supported by pillars (octagon shaped with a span of 60 µm) spaced 200 µm(center-to-center). The pillars can also be used for increasing the integrity and stability of an in situ cross-linked hydrogel, but this has not been tested so far. Similar pillar structures have been used and published previously for the aforementioned reasons [25], [26].

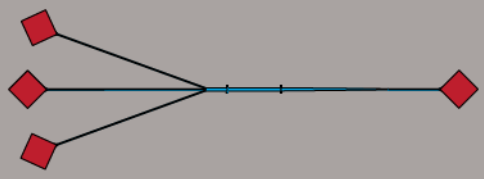

Channel 2 is a modified cross-channel with three inlets and one outlet, however inlet and outlet configurations can vary and connected as needed. The main channel is 300 µm wide and 7mm long before, whereas the inlet channels are only 100 µm wide. Four small structural features outside the microfluidic network are used as markers. Different revisions of the general channel layout have been produced, one with an improved outlet channel that is kept at a width of 300 µm all the way, and one with three rows of pillars (50x50 µm with 20 µm openings in-between) at the beginning and end of the main channel that were used as sieves. The universal design of a cross-channel has been used in many different applications and in this work was used in the image-based feedback microfluidic experiments (page 82) and for early cell culture experiments.

Channel 3 is a straight channel with one inlet and one outlet. There are five main channels each 800 µm wide and 30mm long. At the inlet a pillar structure with varying pillar dimensions is used to trap obstacles and air bubbles [27]. The main aim with this channel was to design a microfluidic network with a maximum surface area that could easily be operated using a pipette and avoid air bubbles as much as possible. To support the large surface area the main channel was divided into five channels to avoid a collapse and

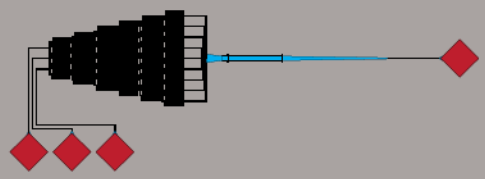

binding of the PDMS roof to the glass bottom. The channel was mainly used for lipid bilayer functionalization experiments (page 47) and simple cell experiments.

Channel 4 is a flow based gradient generator microfluidic network, adapted from Noo Li Jeon's design [28]. It has three inlets which allows the formation of complex gradients, six mixing stages and nine outlets after the last stage of the gradient network. These outlets are combined into a single probing channel that is 400 µm wide and 5 mm long. The outlet channel becomes narrower towards the end (100 µm), the inlets are 50 µm wide, as are the serpentines in the gradient network, but the mixing channels of the network are 100 µm wide. This design is discussed in more detail in chapter 4 ("Electrospun fibers in microfluidic channels" on page 102).

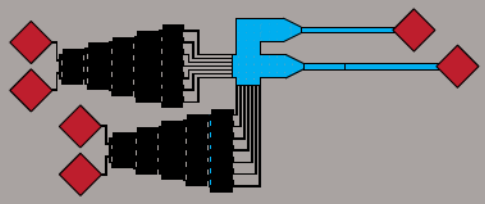

Channel 5 is a flow based double gradient microfluidic design. The gradient generating network is similar to the one of channel 4, but with only two inlets each, five mixing stages and seven outlets from the gradient networks. The outlets from the two gradient networks are combined perpendicular to each other in a square sized main chamber (2x2mm) and liquids leave the network through two outlets (500 µm wide). Pillars (100x100 µm) are placed in the main chamber at a distance of 650 µm (center-to-center) to support the roof. This channel design was developed and used by the Tissue Engineering course students 2011, supervised by me (Patric Wallin). The aim was to have system where a surface bound gradient can be applied in a first step and afterwards a second soluble gradient can be applied perpendicular to the first one. It is important to note that the two gradients cannot be applied simultaneously. The general microfluidic design of this chip worked and it might be used again in future studies ("Surface immobilized gradients of molecules" on page 120).

Channel 6 is a diffusion based gradient generator microfluidic network, similar to the one used by Amir Shamloo [29]. It has two inlets, one for the source and one for the sink channel, which each has two outlets. In addition, the main cell culture chamber (14x2mm) can be accessed via four universal ports. The main chamber is supported by a single row of pillars (120x120 µm) spaced at 1mm (center-to-center). The sink and source channels are connected to the main cell culture chamber through small channels (50x50x500 µm); the rest of the channels has a height of 200 µm. The design and application of this microfluidic network is described in detail in chapter 4 ("Cell migration and ligand spacing" on page 122).

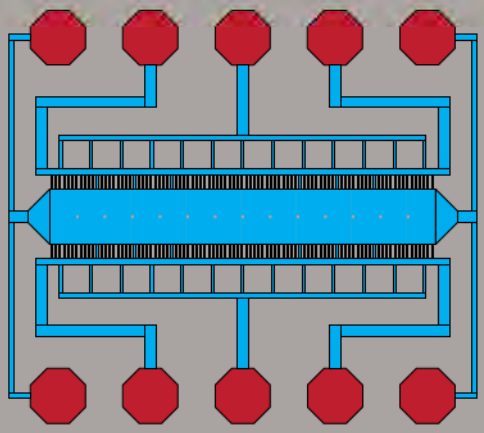

Liquid handling

The first thing, I decided to do was to improve the liquid handling, the way to control fluid flow in microfluidic channels. Until then everybody in our division working with microfluidics used either syringe pumps, peristaltic pumps or vacuum suction to drive liquids through channels. I wanted a system that was more suitable and adjusted to the demands of microfluidic cell culture, a system with better control of flow rates and a system that could be automated and controlled by a computer.

I, first, looked into commercial systems that offered completely integrated solutions adapted for microfluidic channels, the most advanced systems are normally based on pressure driven flow (MFCS series, Fluigent, France or Mitos P-Pumps, Dolomite, UK). In these systems, the liquid reservoir is pressurized to pump fluids; solutions can only get out through the tubes connected to a microfluidic chip. The flow rate is controlled by changing the pressure above the liquid and in the most advanced systems a flow meter is coupled into the fluid flow between the reservoir and microfluidic chip to have a feedback control. It is similar to gravity driven flow, where a large amount of liquid is placed higher than a connected channel and thereby creates a pressure that drives the fluid [30], [31]. You can think of water towers that do the same thing in the macro world, they pressurize the water supply and make sure water is coming out of your water tap when you open it. The benefit of systems like the ones from Fluigent and Dolomite is that the pressure above the liquid can be controlled and changed very fast to adjust flow rates, in comparison to gravity flow, where alteration of flow rates is more difficult.

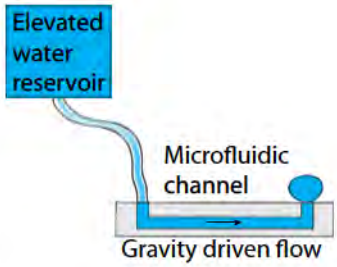

Pressure driven flow has certain advantages over using syringe or peristaltic pumps due to the design. Especially its pulseless pumping performance is important to generate smooth liquid flows in microfluidic channels which are difficult to achieve with other systems. In syringe pumps for example, a stepper motor is used to slowly compress the syringe to drive the liquid, because a stepper motor has discrete steps the resulting flow will pulsate. This pulsation is dampened by tubing and elastic PDMS microfluidic channels, but can still cause problems in certain application areas. [31–33] In pressure driven systems, the pressure can be adjusted continuously and thus pulsation is eliminated [3], [31].

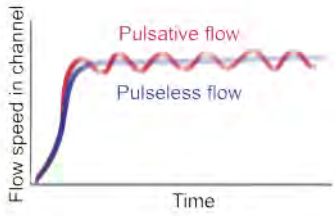

On the other hand, the available pressure driven systems have certain limitations and disadvantages. One main limitation that those systems share with syringe pumps is that restricted access to the liquid reservoir; you cannot refill nor change the solution during continuous operation once the system is loaded and started.

This is particular limiting for long term cell culture experiments were, even though the channel volume is small, larger volumes are needed for continuous perfusion or if you want to recycle cell culture media to keep cell produced cytokines in the system [34–36]. Furthermore, quick exchange between different solutions is not possible in the same way as with other systems using selections valves to control the feeding solution. There are certainly ways to solve that problem for example by briefly interrupting perfusion to exchange or refill solution, but it is nonetheless a restriction that might cause problems for certain experimental schemes.

For me not only the performance itself was important to consider, but also the price for a whole setup and its flexibility. I wanted to have a system that could be adapted to different kinds of microfluidic platforms, from long term cell culture, over short term cell stimulation, to integrated microfluidic biosensing, covering flow rates from a few nanoliter to a couple of microliter per minute. I started to read all the specifications from the different manufacturers and got quotes from both Fluigent and Dolomite. I have to admit that I was a surprised to learn that a Fluigent system with the ability to control 4 channels individually was around 200.000 SEK, when I got the quote in 2010. I did not think it was, or is, worth the money, it is a very good system with many advantages, but it has its limitations.

I was, therefore, looking for an alternative and in the meantime, Julie had talked with her husband, Michael Rodahl, about our wish to buy a liquid handling system. Michael he was testing some pumps for Q-Sense at that time. He suggested that I could come to his office and take a look at one of the pumps we was working with, because he thought it might be suitable for our application. I am very grateful for his advice and help, because it laid the foundation for my current liquid handling system and I probably would not have known about the pumps I am now using without his recommendation.

The pump that Michael had in his office was a milliGAT pump from GlobalFIA (Global Fia, Inc., USA) [37] and I did know right from the beginning that I wanted to use this kind of pump for my microfluidic chips. The milliGAT pump can be operated continuously, the feeding solution can be changed and refilled during operation, it offers a wide range of flow rates from 30 nanoliter per minute up to 10 milliliter per minute and even though pulsation is not eliminated, it is minimized. The underlying technique used in milliGAT pumps is described in "BOX 3.4" on page 73.

milliGAT pump

BOX 3.4

The milliGAT pump (Global FIA Inc., USA) is a computer controlled bi-directional rotating four piston pump. Each pump consist of a pump head with fluid connectors, a stepper motor and gearbox, a stepper motor controller and a power supply. The milliGAT pump is a self-priming pump, it can tolerate gas in the fluids lines and remains operational.

There are two different versions of the pump, with different gear boxes, a low flow (LF) version and a high flow (HF) version. In our system, the LF version is used, which displaces 100 microliter under a full turn of the stepper motor. A full turn has 200 steps, 1.8° per step, and each step is further divided into 256 micro-steps, thus the resolution is 51200 steps per turn, because the of the 4.75x gearbox each micro step equals 0.4 nanoliter. The stepper motor controller (MicroLynx, Schneider Electric Motion, USA) has a velocity resolution of 0.0005 full steps per second and an acceleration resolution of 0.711 full steps per seconds^2. The acceleration and deceleration type can be changed between, linear, triangle, s-curve, parabolic, sinusoidal s-curve or user-defined; in this setup a linear type was used. The controller communicates via RS-232 with a computer.

The milliGAT pump is based on a very special pump head design, which insures that liquids can be pumped continuously and with minimal pulsation. The head contains four liquid compartments with pistons, similar to small syringes (Figure 3.1). Each compartment has a volume of 25 microliter for the LF version. All four syringes are rotating around the center of the pump head. During this rotation the pistons are moved upwards for the releasing compartments and downwards for the drawing compartments. Continuous pumping is achieved, because there are four syringes and at least one is always connected to the outlet and one to the inlet. The small volume of each compartment enables the high precision and slow flow rates.

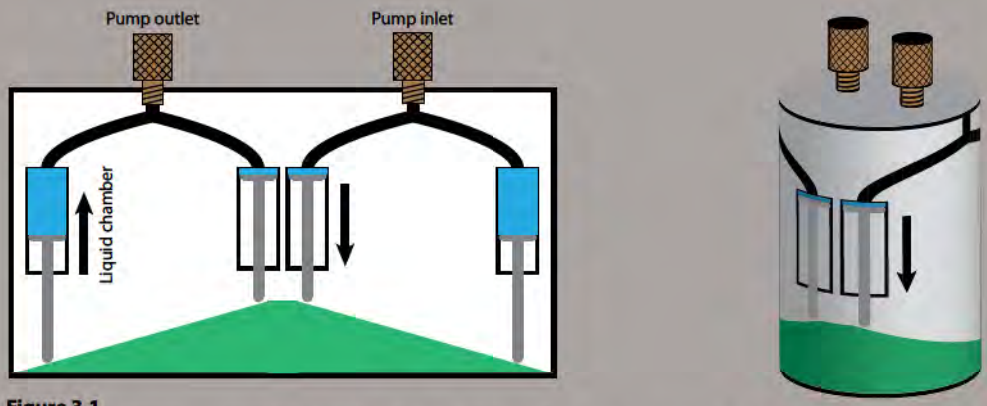

Figure 3.1
Schematic of the operation principle of the milliGAT pumps, in a two-dimensional represenation and a second representation to show how the actually pump head looks like.

I discussed all the different options with Julie and we decided to go for a self-made system build around milliGAT pumps. It was clear that it would take some time to put everything together and get a working setup, but we both also felt that we would gain by having a flexible system that could be adjusted to our needs and was nevertheless cheaper than a commercial one. The material for the final design included four milliGAT pumps and three selection valves that all could be controlled from a computer was around 115.000 SEK at the end. The idea was to build the setup in a modular way and to include more pumps and valves if needed later on, but four pumps and three valves would be sufficient for the beginning. I placed the order for the pumps at GlobalFIA in the end of October 2010 and thought everything would go smoothly, but I greatly underestimated the bureaucratic complexity of the whole thing. I was in constant contact with GlobalFIA and Chalmers financial department until mid-December before everything was sorted out. In the end, everything was fine and I got everything that I needed.

Software for liquid handling system

One of my main wishes was to control the pumps from a computer and automate the whole liquid handling. I thought that automatization could help to increase reproducibility, simplify operation and allow for more complex experimental schemes. Fortunately, GlobalFIA provided LabView (more information "BOX 3.5" on page 75) drivers both for the pumps and selection valves. This was great and saved me a lot of time, because I could start with high-level programming right from the beginning, instead of having to program the RS-232 comport interface to the pumps from scratch. I had been programming with LabView previously, and it felt good to be able to use some of the things I learned a long time ago when I studied mechanical engineering in Hannover, but it took some time to get used to it again. By programming everything myself, I was able to fit the software exactly to my needs and demands, which I regarded as an advantage over the other pump systems that I look into, where this was not possible to the same extent.

In the first version of the software the main aim was to simply interface the pumps and see if I could get them to pump liquid at different flow rates. An example of the LabView code for a single pump is shown in Figure 3.2. In the first step, the pump is initialized with its comport and address to start the communication between the computer and the pump. Afterwards, the program enters a while-loop in which it remains until the stop button is pressed to ensure continuous operation. The slew-command is used to tell the pump to pump liquid at a given flow rate until it

Labview

BOX 3.5

LabVIEW is a development environment from National Instruments based on the visual programming language G and stands for Laboratory Virtual Instrumentation Engineering Workbench. It is specially designed for data acquisition, instrument control, test automation, signal processing, industrial control and related tasks, and offers a wide variety of pre-defined elements to support the user in the design of those tasks. [38–40]

Every LabVIEW program has two parts: the front-panel with the user interface and the back-panel with the executable code. In LabVIEW Virtual Instruments (VIs) represent subroutines for specific tasks or might even represent more complex operations; they consist of a block diagram on the back-panel and a front-panel element. Data can be either supplied or retrieved via the front-panel element by the user. On the back-panel all the different VIs forming the LabVIEW code are connected by wires to propagate variables and information from on VI to the next VI. The LabVIEW library has many different predefined VIs for all sorts of tasks, from simple mathematical operations to complex signal processing, all to facilitate data acquisition, processing and control. This library can be further extended by the user, who can combine several low-level VIs to solve a specific task and save the routine as a new VI, thereby greatly improving the ability to re-use code during the development process. The large amount of available VIs, the graphical programming approach and the extensive support to interface laboratory instrumentation hardware helps the user to quickly program powerful applications even with limited programming background knowledge. Furthermore, it is possible to compile code into standalone executable programs that can be distributed and do only require the free LabVIEW runtime engine to work on any computer.

One fundamental element in LabVIEW programming is the State Machine. It is a very useful architecture to interface systems that progress through different states, for example, initiation, idle, user interaction, operation and close-down. Each state gets input either from the user, configuration files or previous states and leads to the execution of the next state. The ability to add new states during the development of an application is a very helpful and keeps complex algorithms readable.

LabVIEW has been used to control microfluidic systems in several experiments, one example is the work from Sahai et al. who used a custom made LabVIEW program to control the pressure of fluids and opening and closing of microfluidic valves to form temporal and spatial concentration gradients. One positive effect of using LabVIEW in our setup was that Global FIA is providing the necessary VIs to interface and operate the milliGAT pumps and Valco selection valves, thus they can be easily controlled from a LabVIEW program.

National Instruments offer also a large variety of data acquisition systems (DAQ) and input/output (I/O) interfaces. The NI USB-6008 and NI USB-6501 are two very interesting in the product range, because they offer low cost interfaces. The USB-6501 (979 SEK) is a digital I/O interface with 24 channels and the USB-6008 (1699 SEK) has 8 analogue inputs (12-bit, 10 kS/s), 2 analogue outputs (12-bit, 150 S/s) and 12 I/O channels. Even though, other microcontrollers are even cheaper, the big advantage of the National Instruments DAQ systems is the seamless integration into LabVIEW. It is, therefore, straight forward to incorporate measurement and control tasks into each application. The I/O ports for example could be coupled to a very simple sensor to detect if there is still fluid in the main reservoir and otherwise stop the pumps and inform the operator.

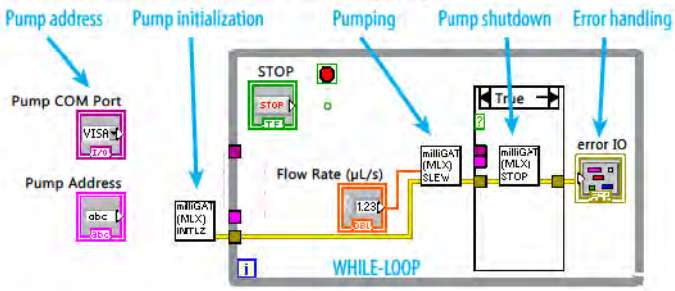

Figure 3.2
Labview block diagram to operate a single pump from a computer

receives a new command, this is the main operation mode: you tell the pump at which flow rate to operate and it does it until you tell it to change flow rate or stop. The last part is to stop the pumps before the program is closed, it is important to close the connection between the computer and the pump before shutting everything down to avoid undefined operational states. Once the stop button is pressed the case-structure changes to the true-state and the connection is stopped by the stop-command. Throughout the whole code, errors are passed on from the initialization to the pumping to the close down and are displayed in an error interface to assist in trouble shooting and error detection. Error handling is an essential part in all programming and is particular important in an application which heavily interacts with users and the environment. Each error needs to get an individual code and be reported on. Fortunately, LabVIEW has some powerful tools for error handling which helps to automate those processes. [38–41]

In subsequent versions of the program, I incorporated more and more functionality to run more complex operations. I added the ability to control pumps individually as well as all together, a better user interface which shows how much liquid has been pumped and graphs monitoring flow rate changes and I also added the selection valves to be controlled from the computer. Selection valves are initialized in the same way as pumps and a "Go-2-Port" command is used to select a particular port of the valve. Furthermore, I developed a special version which offered the possibility to use function generators to control the flow rate for each pump. I used this functionality to manipulate flows both spatially and temporally and to form different kinds of fluid plugs, Figure 3.3. Sequence 1 shows the formation of a small red fluid plug in a channel using a square function, whereas sequence 2 shows the alternating switching between two streams using a sine function.

I even used the remote control feature integrated in LabView to control the whole system via WiFi from another computer and tested possibilities to do this from my iPhone as well. I was just

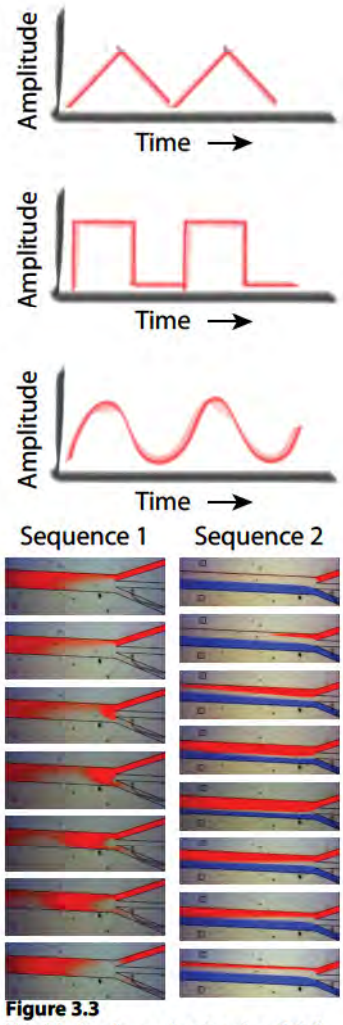

Figure 3.3
Liquid plug formation in microfluidic channel using function generators to control flow rates.

curious what was possible and how much functionality you could add. Although, I had a little bit of experience in LabView programming, I had never used it to this extent and with all the possibilities that were available - I was fascinated by it.

After adding all kinds of functions and testing different alternatives, I realized that the final program had grown uncontrollable in all different directions and was far away from being user-friendly. At this point, I decided to make a very simple version with limited functionality, it could only control four pumps, and the flow rate could either be adjust for each point individually or for all at the same time (Figure 3.4). Even though, this version had limited capabilities it was exactly what I needed to run my first cell experiments, it was stable and running without problems. Furthermore, the operation was easy to learn for other people as well which become more important later and I will come back to that in chapter 5.

I learned that it is really important to keep a balance between mere amount of functions and usability, especially when programming something that might not only be used by you, but has potential for other people. It was, however, valuable to test the different options and see potential functions that could be integrated. I am still planning to go back and completely rewrite the LabView code to make software that is both user-friendly, even helping the user actively in parameter definition, and at the same time offers complex functionality. I truly believe that this is possible, but I am also aware of the fact that it will take time to find the right balance. The reason why I think it is necessary to rewrite the whole code is that I want to build it in a modular way using LabView state machines [42–44], see "BOX 3.5" on page 75.

Figure 3.4
Labview block diagram for the pumpcenter application 1.4, a stable version to control four pumps simultaneously with a simple user interface

Labview Block diagram for the pumpcenter application 1.4

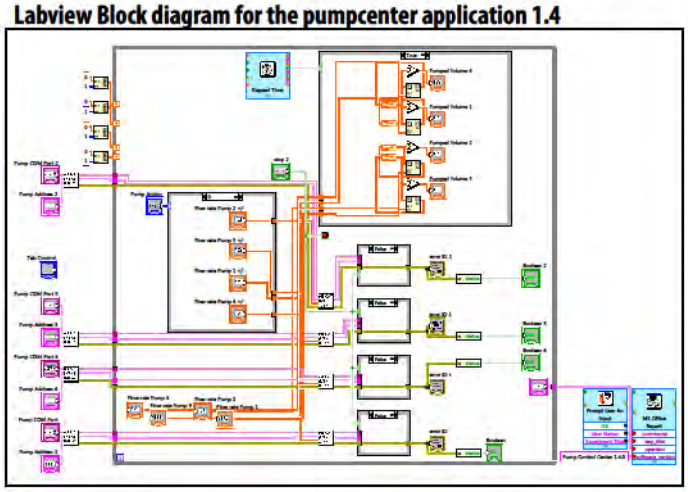

Front panel user interface

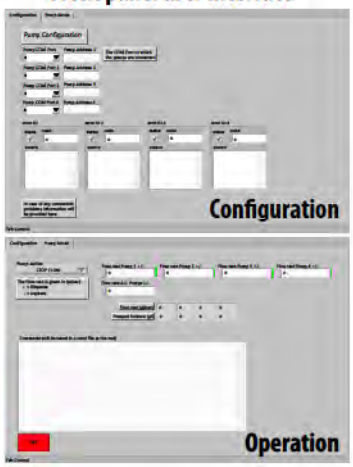

State machines have the advantage that the resulting code is easier to maintain and extend; new functions can be added subsequently by still keeping the main framework intact. It might have been wise to use a state machine structure right from the beginning, but my main goal at the beginning was to get the pumps to work and I did not consider all options carefully enough when starting to program. Nevertheless, I think the experience that I gained when testing different functions and used them in combination with the pumps will be very useful, once I am reprogramming the whole software.

The plans for an updated version include automatic report generation of flow rates and other parameters, interactive user guidance to set up experiments and programmed sequences that will dispense different liquids at certain flow rates over a given time in a pre-programmed way. One example for such a sequence could be injection of cells, pause the flow for the cells to settle, perfusion with media, injection of a bioactive molecule for a given amount of time, fixation of the cells and staining. This is one of my dreams that you can plug in a microfluidic chip and all the solutions that you need and then you just need to press the start button and the whole experiment is performed in a highly reproducible manner [2], [45–47]. This ability in combination with interactive user guidance might be able to make microfluidics more accessible for cell biologist and other non-engineers to unveil the full potential of the technology [1], [48]. But I am also aware that this might be a task better left to companies who have already started to this [48], because it does not offer much scientific value in itself. It might just be a very useful tool and enabling technology for other experiments. Right now, I think I will focus on using the pumps more than on programming a better software, because the current version works for me right now, but if other functions are needed down the road I will need to reconsider the options.

Hardware of the liquid handling system

I noticed quite soon after I got the pumps and valves and did my first experiments that I would need some kind of frame to keep everything together. It was horrible at the beginning, each pump or valve comes with its own controller box and power supply, plus the fact that I needed a converter from RS232-to-USB to connect everything to the computer. Taking into account the microfluidic chip itself, all tubes and solutions, it was just not very practical, especially when running experiments with three pumps. Therefore, I sat down and designed a metal frame (Figure 3.5) that could accommodate all the electronics and also add special holders for different types of liquid containers. I talked to Rune Johansson from our workshop, a person that I really appreciate,

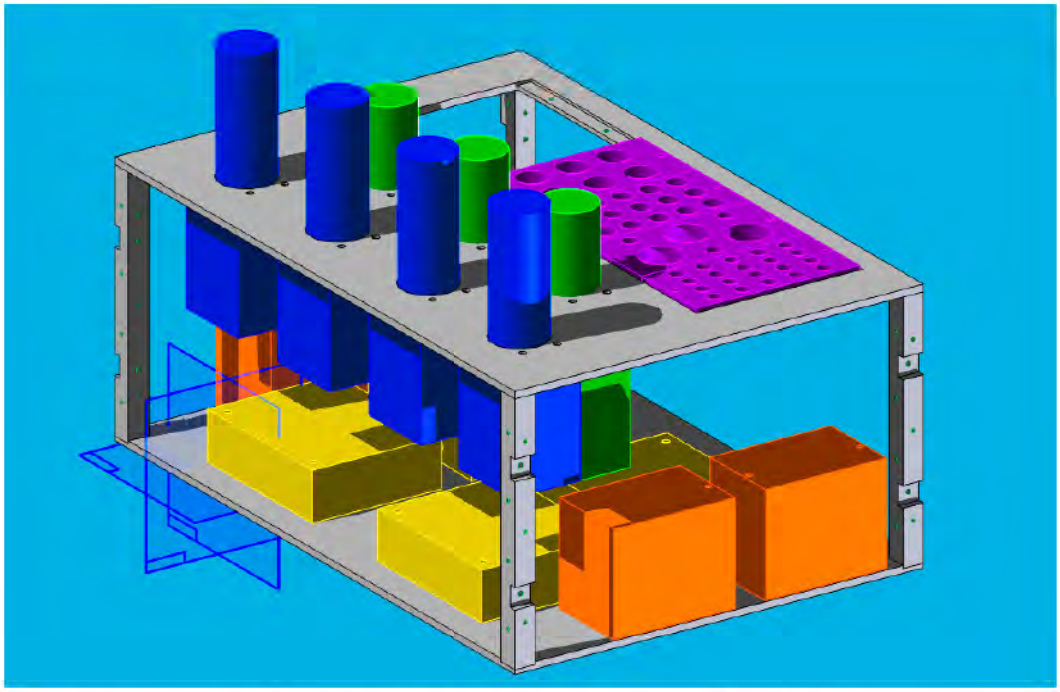

Figure 3.5
SolidEdge rendering of the fully assembled liquid handling platform.
Blue: Pumps
Orange: Pump controllers
Green: Selection valves
Yellow: Valve controllers
Purpule: Liquid vessel holders
Grey: Metal frame

I had been in contact with him previously during my master thesis and he really is extraordinary in manufacturing and building parts. Within a couple of weeks Rune produced all the parts and I finally had an organized, easy to use liquid handling system to work with. I was sad when I heard that he would retire in the beginning of 2012, he was a very valuable resource and is a nice person.

I was now at a point where I could finally run my first experiments with the pumps and it felt great. I, at last, had a liquid handling system that was capable of tightly controlling the flow rates of four pumps and was adjusted to my needs. It took some time and effort to get there, but it was a great feeling to see everything put together, working as expected and I think it was definitely worth the time.

Lab-in-a-box dream

Microfluidics has been a very promising technique for more than two decades and it has certainly lived up to some of the expectations in selected area, but it did not had the anticipated large impact on a wide variety of fields [3], [48]. It has not yet transitioned into a technique that is easily accessible to end-user researchers that want to use it rather than develop it. There are two

main problems for this transition. First, the large expertise needed to use many microfluidic chips and trouble shoot problems during operation. Second, the high investment cost into equipment to operate microfluidic systems, like pumps and microscopes. [48]

During my experiments a dream was born, I thought it would be great to build a whole lab-in-a-box, something that could be carried around and contained all parts to perform a variety of cell experiments. People had shown how much different functionality could be integrated into microfluidic chips, for example Christopher J. Easley et al. built a setup to purify and amplify DNA from whole blood automatically in a microfluidic platform [47] and Chun H. Chen et al. integrated a fully functional fluorescence-activated cell sorter (FACS) on a chip [49]. Other people had demonstrated different approach of portable, on-site microfluidic systems, but those were mainly focused on diagnostics, for example the work from George M. Whitesides laboratory on paper-based microfluidics [50], [51].

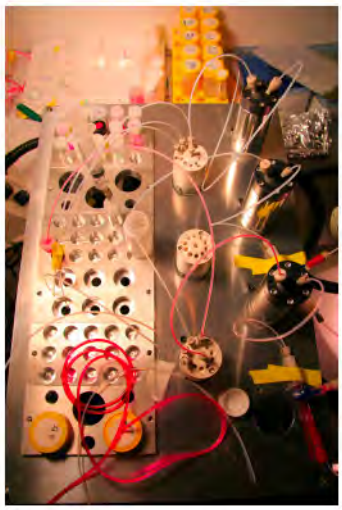

Figure 3.6
Assembeled liquid handling platform with connected tubes and liquid vessles.

My dream was more to build a system that could work with different kinds of microfluidic channels, integrated a powerful liquid handling system, had capabilities to analyze experiments and was suitable for cell culture. I thought that this might not only be interesting for research, but also for education. If it was possible to reduce the cost to a certain amount, such a system could be used in undergraduate education and maybe even in high schools. Yolanda Fintschenko described in her paper how microfluidics could be integrated into education [52] and my system might be able to facilitate this idea.

I felt a desire to develop a setup that could help to connect education with research. I did not go that road much further, besides a few small side projects, because I was aware of the fact that I needed to run research experiments and produce results that I could publish in order to get my PhD at some point, but I still have this dream left. Maybe, I will go back to the idea later on, maybe when I am finished with my PhD.

Figure 3.7
Microfluidic chip in home-build holder attached to x-y rail system with webcam microscope underneath and light source at the top

Simple image capabilities

I did know that if I wanted to have a lab-in-a-box capable of running microfluidic cell experiments, which could be even used in education and other areas not working with microfluidics yet, I would need to integrate some kind of analysis, most appropriately something to look at the cells. In a research environment, we often take for granted that we have access to the required key technology to run and analyzed our experiments and tend to forget that infrastructure might differ significantly between different

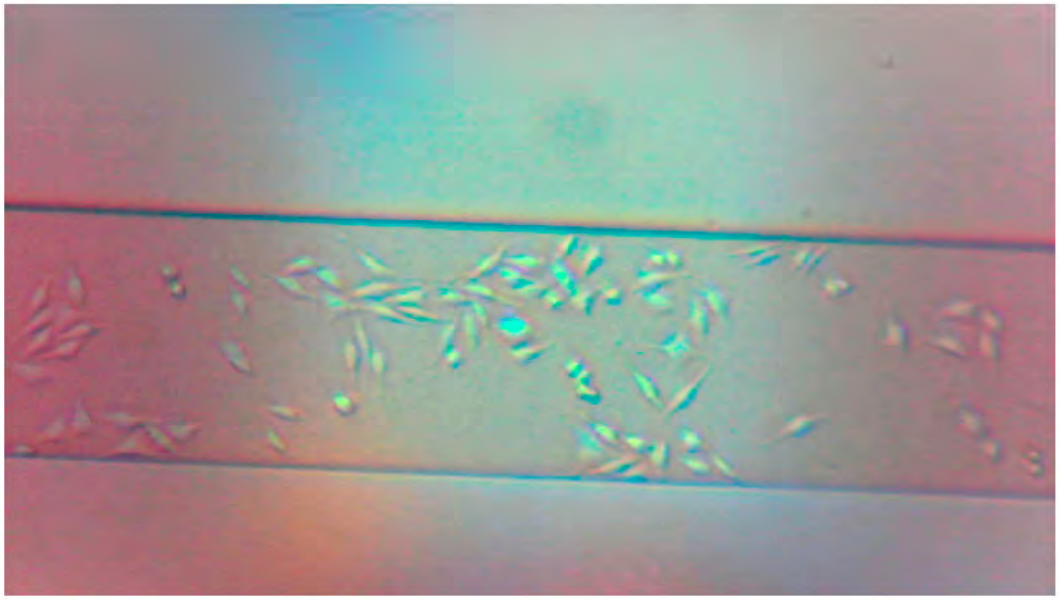

Figure 3.8
HeLa cells in microfluidic channel after 2 hours. Image taken with a home build microscope using a webcam image sensor.

places and equipment might be too expensive to purchase. Therefore, I played with some ideas to integrate at least some basic imaging capabilities based on mass produced parts and consumer electronics that are available at low costs.

My first approach was to use a USB microscope, those are available from as low as 800 SEK. The image quality was fine and it was possible to see microfluidic channels, but the problem was that the magnification was limited to 2.25 micrometer/pixel with 1280x1024 pixel. That was not really enough for me to see cells well and I wanted to increase the magnification, thus I started to play around with different types of lenses. I figured out that by using the eyepiece of an old microscope and an image sensor from a webcam, I could actually achieve fairly high magnifications (1 micrometer/pixel with 1280x720 pixel), when using transmitted light. The image quality was not great and illumination was unequal, but I could see cells during injection and how they adhere to the substrate, Figure 3.8. I thought it was actually quite good.

To improve the image quality and keep the cost under control, I tried to use a digital single-lens reflex (DSLR) system camera. The advantage of such a camera in comparison with other digital cameras is their large image sensor (25.1x16.7 mm for APS-C and 36x24 mm for full frame) and the ability to modify the lens. In order to get a magnified image my sample, I used combined two different principles. I, first, inverted the lens, I mounted it to the camera with the front element nearest to the sensor and the back facing the sample. Second, I put a bellow between the objec-

Figure 3.9
Objective attached in reverse to a DSLR camera and a microfluidic chip hold in position. The long working distance is illustrated with a finger.

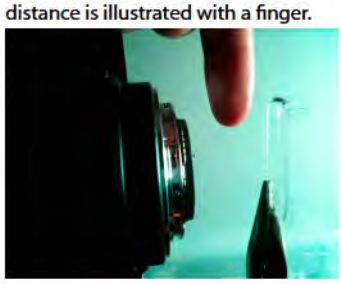

tive and the camera to adjust the distance to image plane. In this way, I was able to get magnifications of up to 0.65 micrometer/pixel on a 2304x3456 pixel image sensor. I thought this was great, because I could take images of things that I could not see by eye at home at my dining table with equipment that costs less than 8.000 SEK. I was fascinated by what you could do with everyday items and how far you could go by using your creativity. Sure, the microscopes that we have in the lab have better image quality, but they also cost way more.

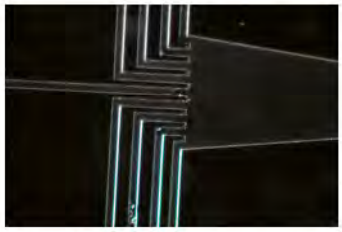

Figure 3.10
Microfluidic gradient network. Image taken with DSLR microscope setup and illuminated in transmission mode with a slight angle.

In general, I think both the USB microscope based approach and the DSLR camera approach offer some great opportunities and by using mass produced items, it is definitely possible to build microscope setups for small amounts of money. The advantage is, they will get even better over time, because new generations of cameras are introduced regularly, pushing the limits of low light imaging and noise reduction further and further. The total amount of research and development money spend in this area is huge due to the large market in comparison to specialized microscopy companies. All this could help to realize my dream of a lab-in-a-box.

The USB microscope setup had even some benefits for my own research experiments, although, I had access to much better microscopes, the webcam microscope was a handy system that could easily be used and placed wherever needed. I used it quite often at the beginning to monitor cell injection into microfluidic chips and for quick confirmation that cells did attach and spread.

Image based feedback control

I also investigated the idea to use a USB microscope for online image recognition. Erik Miller et al. had used a closed loop feedback control with a high speed camera for the production of micro-droplets with a microfluidic network [53]. My idea was that if I have different color dyes in my solutions and was continuously monitoring the flow behavior in the channel, I could use a real time control algorithm that adjusts the flow rates in response to the image data. You would tell the software you want a stripe in the center that covers 70 percent of the whole channel and the algorithm sets the pump rates to establish the desired conditions. This was motivated by the same wish mentioned before, the wish to make microfluidics more accessible and operation intuitive.

I started to program some simple control algorithm in LabView. The first step was some image recognition part to detect the channel boundaries using an edge detection algorithm [54]. The boundaries were used to define a region-of-interest (ROI) in which the fluid stream was detected. I tested different real-time

image processing methods to increase the contrast in the image and thus the robustness of the detection. Most promising was to run a color separation filter over the image data and isolate the color of the center stream. This might not be necessary and there are certainly other ways, but it was an easy way to improve the detection and commonly used in machine vision [55]. In the filtered image a second edge detector was used to identify the center fluid stream and its properties were measured. The two main values were the size of the center stream in percentage of the whole channel and the position of the center stream as deviation from the center of the channel in percentage.

I tested two different control algorithms, a standard proportional-integral-derivative controller (PID) and a fuzzy control system (see "BOX 3.6" on page 85). I pre-filtered the two input signals from the image recognition part with a fifth-order low pass to stabilize the control routine. For me it was more important to have a robust controller, than very fast response times. The advantage of fuzzy controllers is that they rely on a set of empirical rules instead of a mathematical model and that they are easier to implement. I fine-tuned the PID controller gain constants manually and it did work under certain conditions, but for an optimized PID controller it would be necessary to mathematically model the whole systems and derive the gain constants from that model [56], [57]. The fuzzy controller approach offered an easier and more flexible way by defining the rules given in Figure 3.11, I was able to program a controller that worked, it was far from optimal, but it worked. One of the major problems was that both the PID and the fuzzy controller had problems when the stream

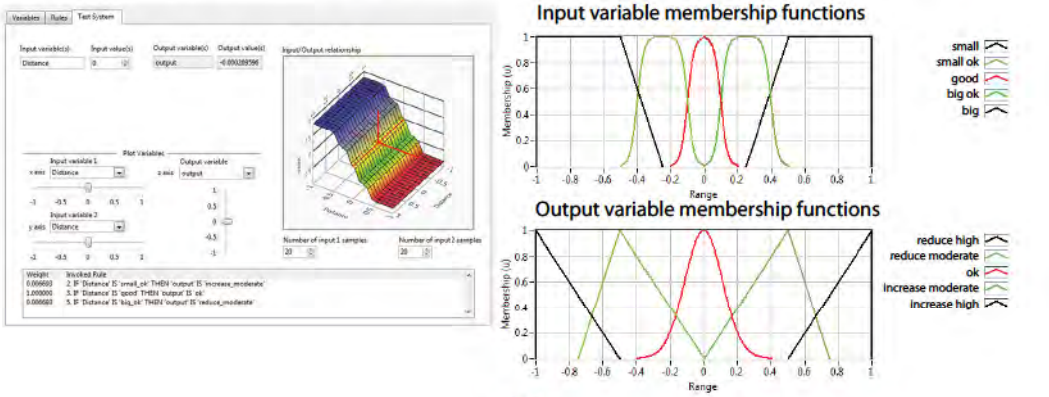

Figure 3.11
(Right) Screenshot of the fuzzy controller development environment with a graphical representation of the system. (Left) Definition of the Fuzzy controller with input variable membership functions, output variable membership functions and a set of rules.

properties were far off the desired ones. The algorithms were not able to approach the desired properties in a slow consistent way, but were often resulting in undefined states were one or several of the streams were completely stopped. The difficulty is that if the flow rate of one pump in relation to the other ones gets too high, the pressure in the whole channel network might be altered significantly and liquid flow is stopped in channels with a low flow rate. The whole system is easily destabilized, which is demanding for the controller [56], [58–60]. I tried to address this issue, by limiting the maximal change in flow rate per iteration and a restricted range in which the controller could change the flow rate. The challenging part was to find a balance here between limiting the algorithm, so it did not resulted in undefined states and a reasonable fast response time. Even though, it was not important to have a response times below a second, the stream should at least be adjusted within 10-20 seconds for the input parameter was changed.

Overall, I think it was an interesting approach and the developed feedback control system based on image recognition worked fine within given boundaries. One could argue that the system is not suitable for microfluidic cell culture approaches, because it is relying on a color dye to detect the different fluid streams. However, we are even today often using phenol red in cell culture media as a pH indicator, and it is probably possible to use some biological inert color dye for the purpose described here. Kevin R. King, for example, used food color dyes in his cell experiments without problems [61]. An image based automatic feedback mechanism might help to increase the number of people that feel comfortable using microfluidics, by simplifying the operation and user interaction; thus reaching out to people unfamiliar with microfluidics today.

Microfluidic valves

Already early on in my microfluidic experiments, I thought that it would be very helpful to open and close channels with valves. Microfluidic valves have been used in many different channel designs [2], [66] and the most common way to actuate those valves is by using a second PDMS layer, the control layer, that uses air pressure to trigger the desire valve, see "BOX 3.7" on page 87 for a detailed description of microfluidic valves. It is even possible to pump liquids by placing three valves behind each other to act as a peristaltic pump [66]. In this way, integrated liquid pumps that control and pump very small amounts of liquid can be realized.

Automatic process control

BOX 3.6

Automatic process control is the regulation of processes without or with only limited human involvement. Figure 3.13illustrates the general concept in control theory, which is at the base for automatic process control. The user defines the reference input signal, the desired state of the system he wants to achieve. This value is compared with the current state, the measured output from the sensor. The difference between the desired and actual value, the measured error, is used by the controller to calculate the system input value which will result in the desired system output. In a closed-loop control system as shown in the figure, the controller constantly compares the measured signal with the reference and regulates the system via the input parameter to hold the reference signal, even if the system is influenced from the outside. A very simple example is a thermostat, where the user sets the desired temperature; the controller regulates the power of the heating element (system) and measures the ambient temperature (Sensor). If the system is disturbed by opening a window, the controller will increase the power of the heating element to maintain the ambient temperature at the reference point set by the user. [62]

There are several different control strategies that can be used to regulate a system, two very interesting strategies are the widely used proportional-integral-derivative controller (PID controller) and the fuzzy logic controller system, which is part of the intelligent control strategies. Both strategies do not need a complete mathematical representation of the system by its transfer function, but can be tuned empirically. Even though, they are not as optimized for a given system as mathematical developed controllers, they are much easier to setup, especially for systems with multiple inputs and outputs (MIMOs), where it is difficult to derive the transfer function. [62]

PID controllers are the most commonly used closed-feedback controller and the underlying algorithm involves three separate parameters: Proportional (P), Integral (I) and Derivative (D).

$$u(t) = K_P \cdot e(t) + K_I \int_0^t e(\tau)d\tau + K_D \frac{d}{dt} \cdot e(t)$$

The controller output u(t) is defined by three terms: the first term with the proportional gain K_P describes the present error e(t), the second term with the integral gain K_I represents the accumulation of previous errors and the third term with the derivative gain Kd predicts future errors. A high K_P will result in a large proportional response of the system to the current value, a too high value might result in an instable oscillating system, on the other hand a small value will limit the response of the system to disturbances. The K_I constant can accelerate the controller by taken into account the accumulated error, for a high K_I this can result in a signal overshoot above the target value. In the last term, K_D limits the response by considering the error change over time and thereby limiting the overshoot and can improve overall stability, but differentiation of the signal will also amplify the noise and might under certain conditions result in destabilization. [56]

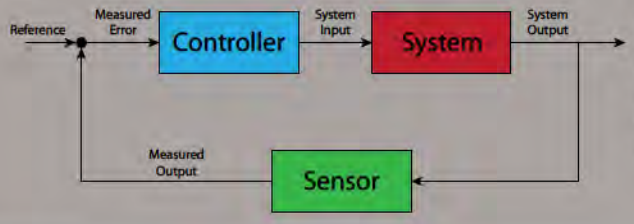

Figure 3.13
Schematic of the general concept in control theory. The system is controlled with a closed-feedback-loop which measures the current state with a sensor.

All three constants need to be adjusted depending on the system to tune the PID controller and get optimal results. This is a complex task due to some degree of non-linearity in the system and the need to have both fast response times and high stability. There are several ways to tune a PID controller, the simplest way is to change the parameters and observe system behavior, this approach does not require any deeper understanding of the system, but personal experience to tune controllers. Table 3.1 [56] shows some basic information about the effects from the different gain constants. All other approaches, like Ziegler-Nichols, Cohen-Coon and other proprietary methods are depended on some sort of mathematical representation of the system to find optimal gain constants. One way to generate a partial mathematical representation is by stimulating the system with a step function and monitor the output over time, but for certain systems it is very difficult to generate a step function.

Fuzzy controllers use a completely different approach based on probabilistic fuzzy logic to regulate systems. Instead of true (1) and false (0) as in digital logic a variable in fuzzy logic is represented by a value on a continuous scale from 0 to 1. For example whereas the room can be either warm or cold with digital logic, it can be a little bit warm and slightly cold at the same time with fuzzy logic. The advantage is that this is more closely related to how we think as a human and therefore it is easier to design powerful controllers based on fuzzy logic. The transfer from empirical human knowledge and experience is much easier transferred and represented by a fuzzy controller than in a PID controller. Furthermore, many systems are simply too represent them fully and take all input/output parameters into account, fuzzy controllers allow for approximation, interferences and incomplete data. In many process control tasks, it is not necessary to find the perfect solution, but rather that the result lies within a certain range. [63–65]

There are three basic operating stages in each fuzzy controller: Input, Processing and Output. In the first stage, input variables are mapped to a set of membership functions (fuzzification). Membership functions can have different forms, but are most commonly triangular or trapezoidal and each input value is mapped on several membership functions, e.g. 0.2 on "cold, 0.6 on "warm" and 0.1 on "hot". This is very important that each value is represented by several membership functions, usually 3 to 7 per input variable. In the second stage, all logic rules (IF-THEN) are evaluated and the ones applying are used to calculate value on the output membership functions. Rules can be formulated and combined in different ways, for example:

IF temperature is "warm" then turn heater "low"

IF temperature is "cold" and outside temperature is "high" then turn heater "medium"

…

In the third stage, the output membership functions are mapped back onto output variables (defuzzification) to generate an output that can be used by the system. The most common way of defuzzification is to calculate the center-of-mass (centroid) of the combined output member ship functions. [56–60]

	Rise time	Overshoot	Settling time	S-S Error
K_P	Decrease	Increase	No trend	Decrease
K_I	Decrease	Increase	Increase	Eliminate
K_D	No trend	Decrease	Decrease	No trend

Table 3.1 Effect of increasing each of the three parameters K_P K_I and K_D on the system dynamics.

Microfluidic valves

BOX 3.7

A valve is a basic element in all liquid handling systems independent of their size, by opening a valve fluid is allowed flow through the channel and by closing it fluid flow is stopped. For microfluidic systems different types of valves have been developed and certainly one of the most popular versions was published by people from Stephen R. Quakes laboratory at Stanford in 2000 [66]. They used a new multilayer soft lithography approach to stack two PDMS channel layers on top of each other and used one of the layers for fluid transport and the other one as a control layer pressurized with air. The basic principle that they proposed for monolithic microfluidic valves is shown in Figure 3.14. A control channel with air is placed either above or below a fluid channel filled with liquid and by increasing the pressure in the control channel the fluid layer is compressed, because only a thin flexible membrane is separating the two. For very complex systems with many valves, it is even possible to combine both push-down and push-up valves in a three layer platform. This can help to increase the density of valves per area. [2]

By using a rounded fluid channel and a rectangular pressure control channel, it is possible to achieve nearly full closure of the fluid channel upon actuation. The amount of leakage depends on the design, material used and pressure applied. It is very difficult to achieve full closure with a rectangular fluid channel, because there will always be some leakage at the channel walls. The pressure needed to close a valve is depending on the dimensions and in particular on the thickness of the flexible membrane. This membrane is commonly between 20 and 80 micrometer. [66] At this thickness the pressure need to close the valve is still manageable and the membrane is thick enough to withstand normal processing procedures like casting, bonding and liquid flow.

Besides actuating microfluidic valves with pressurized air, there are other ways to open and close them. Elizabeth Hulme et al. described a method to use screws or push-type solenoids to open and close valves [68] and others used braille modules for actuation [36], [67]. The principle is the same as described before, but the actuation is achieved in a different way.

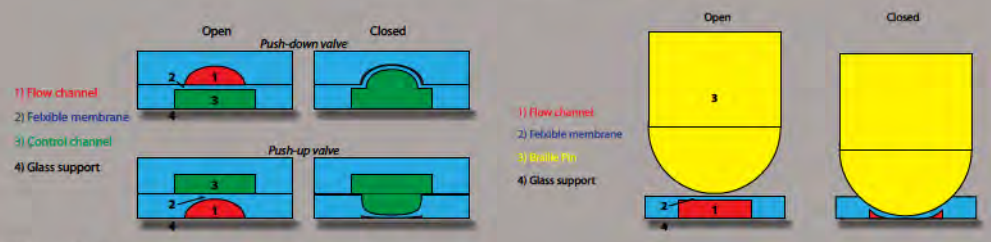

Figure 3.14
Schematic of monolithic microfluidic valves. Actuated by air pressure from a second PDMS layer either on top or beneath the fluid layer (on the left) or actuated by a braille pin (on the right).

Besides pressure actuated valves there is another very interesting approach to operate valves by using piezo-electric actors. Wei Gu et al. described in 2004 a system where they used braille modules to operate valves in microfluidic channels [67]. I thought that this was a brilliant idea, the braille modules could be controlled by a computer, there was no need for a second PDMS layer and connections could be limited to the essential fluid ports. It just seemed much simpler than using pressure channels to open and close valves. So, I decided to look into it and see if I could use a similar approach, I did not had a direct need for valves, but thought that it might be useful at some point in the future, as part of building a toolbox with microfluidic elements accessible for me.

It was more difficult than anticipated to find a supplier for those braille modules, companies were normally only selling the whole display that blind people could use to read. Those were quite expensive and I did not have any need to get a whole display. At the end, I decided to just send an email to the Dutch company Optelec, who produces braille displays, and asked were they got there modules from. I got in contact with Hans Vugts at the company and he, naturally, was very surprised by my question. I explained him my whole project and the idea to use braille modules to control flow in microfluidic channels. He thought it was very interesting and within less than a week he had send me over 15 braille modules for free to test my ideas. I am very grateful to Hans that he helped me in such an uncomplicated way, because he thought it was interesting and I think it also shows both how important personal relations are and that you need the courage to ask even if it is a very strange question.

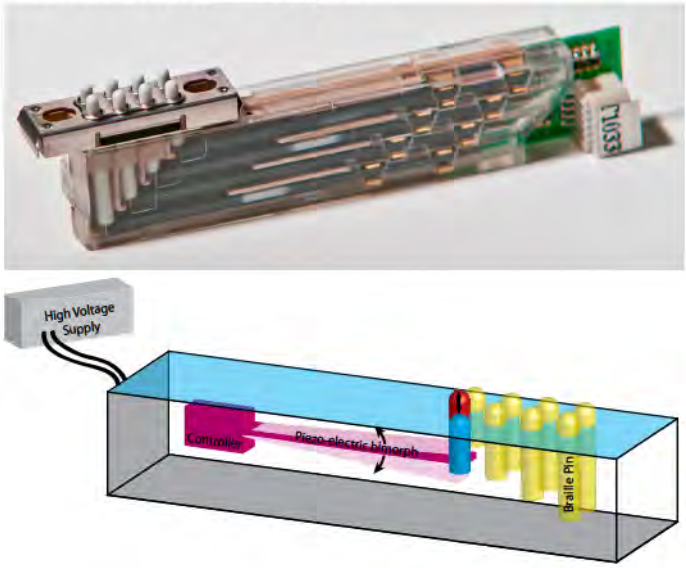

Figure 3.12
(TOP) Photograph of the braille module used in this study. (BOTTOM) schematic of the braille module showing how the piezoelectric element is moving a pin up and down. The modules that were used have 8 pins that can be controlled individually.

I decided to directly test the braille modules when I got them. I asked Rune to make me a holder for the module so I could clamp the microfluidic chip on top and that worked very well. I did not have any special designed channels, but I thought for a simple test it should be fine to use one of the channels I had. I used very little PDMS to just cover the master and get as thin PDMS films as possible, spin coating would have been another option and should be used in the future [66] to achieve more homogenous thin films. Figure 3.15 shows the opening and closing of the channel by actuation of the braille pins. It worked actually better than anticipated, the channels did not closed completely, but that is most likely due to the cross-section geometry and could easily addressed with specially designed channels. A channel with a rounded cross-section would be better [2], but all my channels had rectangular cross-sections. Another problem that I had at the beginning was to operate the modules at all. I could not find the connector counterpart on the module. Thus, I was forced to solder wires directly on the back part of the module, which is not the best way, but at least it worked and I am still looking to get the right connector. The fact that the piezo-electric bimorphs used in the modules need a driving voltage of 200 Volts did not really simplify the whole task.

I never continued on to build an electrical circuit with transistors to use my National Instruments digital input/output (I/O) interface to control the braille pins from a computer with a LabView program. This should be a very straight forward task, I think, but the whole project did not have a high priority and all the development was done on the side. The early results, however, look very promising and I still believe in the potential of this approach, especially in respect to my lab-in-a-box dream.

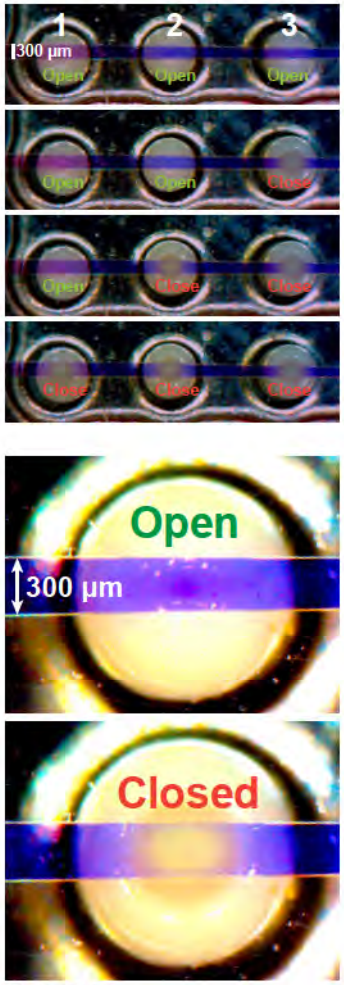

Figure 3.15
Micrographs of braille pin actuated microfluidic valves. (Top) Series with three braille pins closing one after another, using a defined sequence this could be used as a microfluidic pump. (Bottom) Close-up of a single pin with an open and closed channel filled with blue liquid.

LSPR sensing

My main aim was to use the liquid handling system and microfluidic channels for cell culture and rely mainly on microscopy techniques to analyze the results, which was one of the reasons why I wanted to integrate a cheap microscope into the setup. However, there are many other bio sensing schemes that can be combined with microfluidics [10], [11] and allow the characterization of cells in different ways. One interesting approach is to measure what cells are secreting and use this information to characterize them.

I worked together with Laurent Feuz (previously postdoctoral fellow at Biological Physics) during the fall 2010 and spring 2011 and we were investigating possibilities for real-time, on-chip,

Localized surface plasmon resonance

BOX 3.8

Bioanalytical sensing is essential to study cell responses and for example measure the concentration of cell secreted cytokines upon stimulation. There are many different biosensing systems available for example, fluorescence microscopy, QCM-D, or enzym-linked immunosorbent assays (ELISA), each with its own advantages and disadvantages. Localized surface plasmon resonance (LSPR) based systems can also be used for biosensing and one of their major advantage is that they are label-free, thus no fluorescence probe or something similar is needed to detec the molecule of interest.

LSPR systems are based on the principle that free electrons in metal nano sized objects can be excited to collectively oscillate by light. The resonance frequencies to excite these localized surface plasmons depend on the material, shape and size of the nano particles, but are normally in the visible spectrum. The resonance wavelength is directly related to the refractive index of the medium around the gold nano particle. Therefore, it is possible to use localized surface plasmon resonance for measuring changes of the refractive index. The refractive index near the gold nano particle changes for example, when a molecule binds to the gold surface, thus the binding can be detected as a shift of the resonance wavelength peak. If the refractive index at the surface increases the resonance peak is shifted towards higher wavelength (red-shift) and for a decrease of refractive index it is shifted to lower wavelengths (blue-shift).

The setup for a LSPR sensing device is fairly simple, the surface with the gold nano particles is illuminated with white light in transmission mode, the transmitted light is analyzed with a spectrophotometer and the peak position is measured continuously to monitor changes at the surface. To improve the signal, we use a LabVIEW program to track the center of mass of the peak (centroid) instead of relying only on the aboslute peak position.

One very important factor for bioanalytical sensing is that the nano plasmonic field is strongly localized at the nano particle and the decay length into the surrounding media is only in the range of tens of nanometers. This means that LSPR sensors are very sensitive at the surface interface, but not to the bulk properties of the surrounding media. In combination with a surface chemistry that allows specific binding of the molecule of interest and is inert to any other molecules, it is possible to use the highly localized LSPR field for high sensitivity sensing. The molecule specificity can be accomplished with antibodies for biomolecules like cytokines, whereas the passivation can be achieved with long polyethylene glycol (PEG) chains. Another advantage of using gold nano particles on silicon dioxide or glass is the material contrast and the ability to use different surface chemistries on both parts.

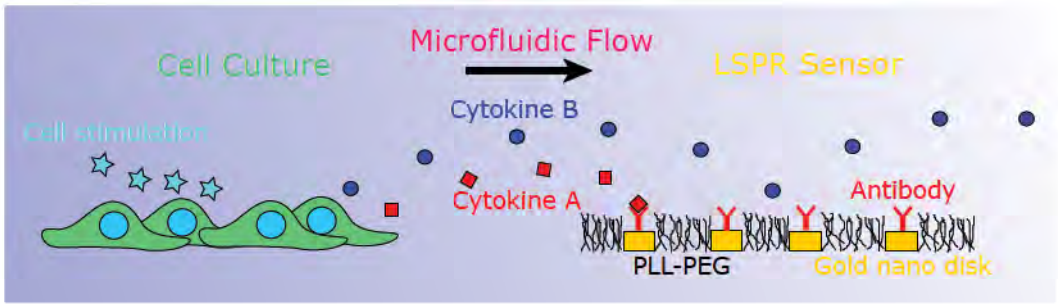

Figure 3.16
Schematic of a LSPR measurement setup integrated with an on-chip cell culture platform to measure cytokine production in response to a given stimulus in real-time.

label-free cytokine sensing. The idea was to characterize and classify cells growing in a microfluidic chip not only by their response amplitude to a certain stimulus, but gain additional information by measuring the temporal response properties. This idea had come up during the second meeting for the NanoII project in discussion with Nir Friedman from Weizman Institute, Fredrik, Julie and I. Instead of using ELISA (enzyme-linked immunosorbent assay) for detecting Interleukin-2 (IL-2) secretion from activated T-cells, we wanted to try to use localized surface plasmon resonance (LSPR, see "BOX 3.8" on page 90) and thought of a combined microfluidic system with upstream cell culture and downstream cytokine detection (Figure 3.16). The aim of the NanoII project (page 14) was to isolate and characterize a small subpopulation of regulatory T-cells and after expansion of the cells to reinject them as a therapy in autoimmune disorders and inflammatory diseases. We thought the temporal secretion pattern of cells might help to isolate a cell population that otherwise could not be identified and wanted to use IL-2 as a proof-of-principle cytokine to show that it was possible to measure secretion over time.

The first thing that needed to be done was to test if it was in general possible to detect cytokines with LSPR in microfluidic channels. Andreas B. Dahlin, previously at Biological Physics, had developed a LSPR setup that was capable of reading signals from an area as small as 10x50 micrometers by mounting a spectrophotometer on a light microscope [69] I was going to use this setup together with Laurent in combination with one of my microfluidic channels bonded to a glass substrate with nanoplasmonic features. We used gold nano discs that were 110 nanometers in diameter and 30 nanometer in height, which have a resonance peak around 780 nanometer. The microfluidic channel was a simple channel with 3/1 ports, we used one pump for the inlet and had three open outlets; the main channels was 300 micrometer wide 50 micrometer high. We characterized the sensitivity of the setup with glycerol steps of increasing concentration and calculated a sensitivity of 240 nanometer peak shift per refractive index unit, which is higher than for a bigger flow cell (160-170 nanometer).

In order to investigate the possibility to measure cytokines with LSPR, we decided to use recombinant Interleukin-2 from mouse (JES6-1A12, eBioscience, USA) in a first set of experiments, which is 17kDa in size. This allowed us to inject a known and high concentration of cytokines, and we did not need to rely on cell secretion. As an antibody, we used biotinylated anti-mouse Interleukin-2 (JES6-5H4, eBioscience, USA), which has been tested for binding to the Interleukin-2 we used. In the first approach, we used thiol-biotin chemistry to couple IL-2 antibodies via streptavidin to the nanoplasmonic gold discs and backfilled the area between the discs with PLL-PEG, as illustrated in Figure 3.17. The problem with this approach was that the distance between the gold nano disc and the antibody binding site was around 15-20 nanometer. For LSPR sensing this is a large distance and severely limits the signal strength, especially for a small, 17 kDa, Interleukin-2 molecule. It was basically not possible to detect any signal upon Interleukin-2 injection, even at high concentrations.

Laurent suggested using a different kind of binding chemistry to bring the antibody closer to the surface and we tried a Perfluoro-Phenyl-Azide (PFPA) adhesion promoter from SUSOS AG (Switzerland). PFPAs can be photo-activated by UV-light and the Perfluoro-Phenyl Nitrenes formed after activation can insert into any C-H or N-H bond of close-by molecules. We used a mixture of 5% disulfide-PFPA and 95% 6-mercapto-1-hexanol to functionalize the gold surface and backfilled the silicon dioxide substrate with PLL-PEG 2000. The adsorbed IL-2 antibodies were covalently coupled to the gold discs via the PFPA upon UV-activation and we tested the system with recombinant Interleukin-2, similar to the experiments we did before. It did not work either and after some discussions with Laurent and Fredrik we concluded that it probably was very difficult to get the system to work at all. One option might have been to use antibody fragments to decrease the distance even further [70], [71], but we never tried that approach. It was great working together with Laurent. He had a lot

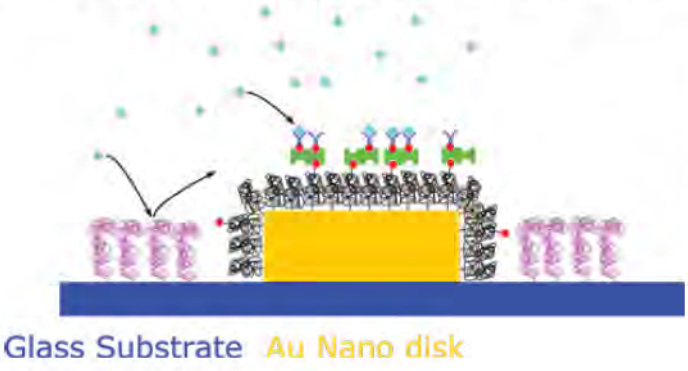

Figure 3.17
Schematic of the first surface functionalization approach with PLL-PEG and Biotin-Streptavidin.
Dark Blue: Glass substrate
Yellow: Gold nano disc
Pink: PLL-PEG passivation layer
Black: Thiol-PEG + Thiol-PEG-Biotin
Red: Biotin
Green: Streptavidin linker
Blue: Biotinylated antibody
Turquoise: Biomolecule of interest

of experience in surface chemistry and LSPR sensing. I learned a lot about different functionalization and passivation methods, so in contrast to my last encounter with surface chemistry during the experiments with lipid bilayers and gold nano dot surface (chapter 2), I worked closely together with someone with a lot of background knowledge and learnt very much during that process. [72]

Although, we failed with our original plan to detect cytokines with LSPR, we observed some very interesting phenomena during the experiments. As mentioned before, it was the first time I used the new liquid handling system for some real experiments. The first thing that we mentioned was some signal oscillation (Figure 3.18) when injecting solutions with different densities into the system like water, ethanol and glycerol. We could not explain this behavior at the beginning, but I analyzed the data and look at the power spectrum (Figure 3.18) of the measurements to check the frequency of the oscillation. The dominant frequency is around 4 and additional peaks are visible approximately 40 and 160; thus, all peaks are multiple of 4. I went back and looked at the descriptions and operation schemes for the pumps and everything fall into place. The problem was that the four, each 25 microliter large, liquid vessels in the pump which were not completely empty during operation and therefore mixing of the current and previous liquid solution appeared. The problem is much less pronounced when switching between liquids with the same density, but varying salt concentration, because those liquids mix much better and the residual liquid in the pump head gets exchanged faster. The reason we were able to measure those oscillations at all is the high refractive index sensitivity of the LSPR sensor.

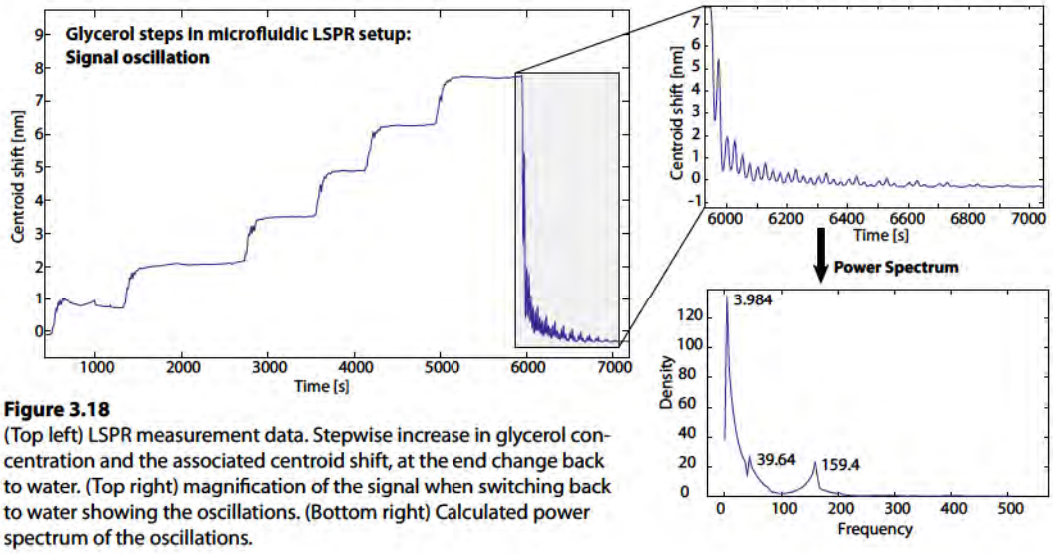

Figure 3.18
(Top left) LSPR measurement data. Stepwise increase in glycerol concentration and the associated centroid shift, at the end change back to water. (Top right) magnification of the signal when switching back to water showing the oscillations. (Bottom right) Calculated power spectrum of the oscillations.

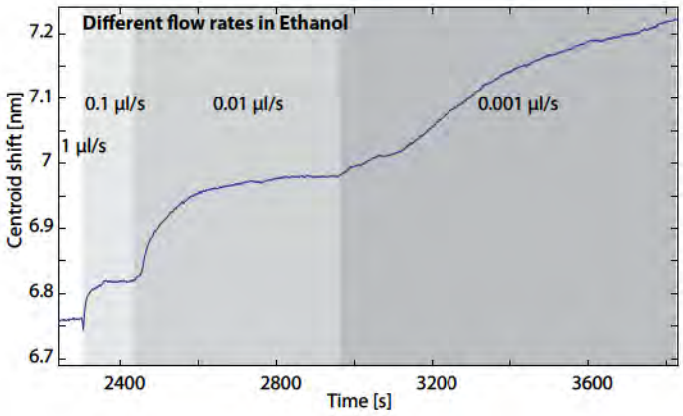

Figure 3.19
LSPR measurement data of ethanol in microfluidic channel at decreasing flow rates.

Another effect that we observed during our experiments was that the LSPR signal was changing, when the flow rate was altered Figure 3.19. The peak shift differed in height and response time, depending on the flow rate change. For slower flow rates, the shift was larger but the response time was slower than for changes at higher flow rates. This was very puzzling at the beginning and Laurent and I consider all different kinds of effects. I even thought that we might be on to something, taking into account that the LSPR sensing depth was limited to the surface, I thought that we maybe found a new way to study fluid flow phenomena at interfaces. I read some articles about Stern layers [73], [74] and talked to Jan-Erik Löfroth at Chalmers Surface Chemistry to get a better idea what might happen in our setup. He told me that it was unlikely that we measured changes in the Stern layer, but the signal was reproducible and especially with ethanol very clear. After some additional literature research, I found a paper talking about temperature dependence of refractive index shifts for ethanol [75]. LSPR measures changes in refractive index and because the measurement is based on illumination local heating will occur. I quickly tested this hypothesis by using a small hand fan to cool the microfluidic chip and I could clearly see a response signal. Thus, I came to the conclusion that there was not anything new or interesting happing within the samples, the simple fact was that a higher flow rate would cool down the sample and the LSPR signal would change in response. At higher flow rates the equilibrium temperature would be reached faster, thus the response time was slower than for low flow rates were it takes some time for the substrate to heat up.

I did not discover any new measuring system to study Stern layers, but I learned something else. I learned that you have to be very careful when running experiments, you might not even be aware of certain parameters that can greatly influence your results.

This story could have finished completely different if we would have injected only the Interleukin-2 at a lower flow rate to save material for example and measured a signal, we would have attributed it to the cytokine without knowing that the flow rate was actually playing an important role. My point here is that one should be aware of the fact that some things might be more important than they seem and that well designed controls are always needed to reduce the risk of false-positive results.

The idea for real-time detection of cell secreted cytokines still exists and we still think that it is a valuable approach in order to improve cell characterization. It might just be the case that LSPR is not the right technique for the task and that another type of sensor is needed. I am not actively pursuing this path at the moment, but it would be interesting to incorporate a none-microscope based sensor my microfluidic systems in the future.

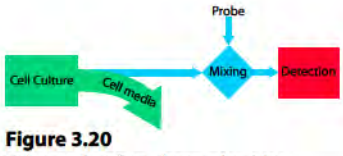

Figure 3.20
Schematic of an alternative idea to realize real-time sensing of cell secreted cytokines

[1] G. M. Whitesides, "The origins and the future of microfluidics.," Nature, vol. 442, no. 7101, pp. 368-73, Jul. 2006.

[2] J. Melin and S. R. Quake, "Microfluidic large-scale integration: the evolution of design rules for biological automation.," Annual review of biophysics and biomolecular structure, vol. 36, pp. 213-31, 2007.

[3] D. Mark, S. Haeberle, G. Roth, F. von Stetten, and R. Zengerle, "Microfluidic lab-on-a-chip platforms: requirements, characteristics and applications.," Chemical Society reviews, vol. 39, no. 3, pp. 1153-82, Mar. 2010.

[4] D. E. Hertzog, B. Ivorra, B. Mohammadi, O. Bakajin, and J. G. Santiago, "Optimization of a microfluidic mixer for studying protein folding kinetics.," Analytical chemistry, vol. 78, no. 13, pp. 4299-306, Jul. 2006.

[5] K. Sritharan, C. J. Strobl, M. F. Schneider, a. Wixforth, and Z. Guttenberg, "Acoustic mixing at low Reynold's numbers," Applied Physics Letters, vol. 88, no. 5, p. 054102, 2006.

[6] F. Lin, W. Saadi, S. W. Rhee, S.-J. Wang, S. Mittal, and N. L. Jeon, "Generation of dynamic temporal and spatial concentration gradients using microfluidic devices.," Lab on a chip, vol. 4, no. 3, pp. 164-7, Jun. 2004.

[7] N. P. Rodrigues, Y. Sakai, and T. Fujii, "Cell-based microfluidic biochip for the electrochemical real-time monitoring of glucose and oxygen," Sensors And Actuators, vol. 132, pp. 608-613, 2008.

[8] S. Joo, K. Hyun, H. Chan, and T. Dong, "Biosensors and Bioelectronics A portable microfluidic flow cytometer based on simultaneous detection of impedance and fluorescence," Biosensors and Bioelectronics, vol. 25, pp. 1509-1515, 2010.

[9] F. S. Ligler, "Perspective on optical biosensors and integrated sensor systems.," Analytical chemistry, vol. 81, no. 2, pp. 519-26, Jan. 2009.

[10] K. B. Mogensen, H. Klank, and J. P. Kutter, "Recent developments in detection for microfluidic systems.," Electrophoresis, vol. 25, no. 21–22, pp. 3498-512, Nov. 2004.

[11] P. J. Viskari and J. P. Landers, "Unconventional detection methods for microfluidic devices.," Electrophoresis, vol. 27, no. 9, pp. 1797-810, May 2006.

[12] C. Yi, Q. Zhang, C.-W. Li, J. Yang, J. Zhao, and M. Yang, "Optical and electrochemical detection techniques for cell-based microfluidic systems," Analytical and Bioanalytical Chemistry, vol. 384, no. 6, pp. 1259-1268, Feb. 2006.

[13] J. Putzeys, G. Reekmans, K. Verhaegen, L. Lagae, K. Verstreken, and G. Borghs, "Lable-free biosensor based on localized surface plasmon resonance in a multi-channel microfluidic chip," 2009 IEEE Sensors Applications Symposium, no. 016817, pp. 43-46, Feb. 2009.

[14] P. Jönsson, J. P. Beech, J. O. Tegenfeldt, and F. Höök, "Shear-driven motion of supported lipid bilayers in microfluidic channels.," Journal of the American Chemical Society, vol. 131, no. 14, pp. 5294-7, Apr. 2009.

[15] G. Ohlsson et al., "Solute transport on the sub 100 ms scale across the lipid bilayer membrane of individual proteoliposomes," Lab on a Chip, no. 207890, 2012.

[16] M. P. Jonsson, A. B. Dahlin, L. Feuz, S. Petronis, and F. Höök, "Locally functionalized short-range ordered nanoplasmonic pores for bioanalytical sensing.," Analytical chemistry, vol. 82, no. 5, pp. 2087-94, Mar. 2010.

[17] J. C. McDonald and G. M. Whitesides, "Poly(dimethylsiloxane) as a material for fabricating microfluidic devices.," Accounts of chemical research, vol. 35, no. 7, pp. 491-9, Jul. 2002.

[18] S. M. Kim, S. H. Lee, and K. Y. Suh, "Cell research with physically modified microfluidic channels: a review.," Lab on a chip, vol. 8, no. 7, pp. 1015-23, Jul. 2008.

[19] J. C. McDonald et al., "Fabrication of microfluidic systems in poly(dimethylsiloxane).," Electrophoresis, vol. 21, no. 1, pp. 27-40, Jan. 2000.

[20] E. Berthier, E. W. K. Young, and D. Beebe, "Engineers are from PDMS-land, Biologists are from Polystyrenia.," Lab on a chip, Feb. 2012.

[21] T. Squires and S. Quake, "Microfluidics: Fluid physics at the nanoliter scale," Reviews of Modern Physics, vol. 77, no. 3, pp. 977-1026, Oct. 2005.

[22] T. Bayraktar and S. B. Pidugu, "Characterization of liquid flows in microfluidic systems," International Journal of Heat and Mass Transfer, vol. 49, no. 5–6, pp. 815-824, Mar. 2006.

[23] K. B. Mogensen, F. Eriksson, O. Gustafsson, R. P. H. Nikolajsen, and J. P. Kutter, "Pure-silica optical waveguides, fiber couplers, and high-aspect ratio submicrometer channels for electrokinetic separation devices.," Electrophoresis, vol. 25, no. 21–22, pp. 3788-95, 2004.

[24] S. Kim, H. J. Kim, and N. L. Jeon, "Biological applications of microfluidic gradient devices.," Integrative biology : quantitative biosciences from nano to macro, vol. 2, no. 11–12, pp. 584-603, Nov. 2010.

[25] V. Vickerman, J. Blundo, S. Chung, and R. Kamm, "Design, fabrication and implementation of a novel multi-parameter control microfluidic platform for three-dimensional cell culture and real-time imaging.," Lab on a chip, vol. 8, no. 9, pp. 1468-77, 2008.

[26] T. Frisk, S. Rydholm, T. Liebmann, H. A. Svahn, G. Stemme, and H. Brismar, "A microfluidic device for parallel 3-D cell," Cell, pp. 4705-4712, 2007.

[27] J. H. Sung and M. L. Shuler, "Prevention of air bubble formation in a microfluidic perfusion cell culture system using a microscale bubble trap.," Biomedical microdevices, vol. 11, no. 4, pp. 731-8, Aug. 2009.

[28] N. L. Jeon, S. K. W. Dertinger, D. T. Chiu, I. S. Choi, A. D. Stroock, and G. M. Whitesides, "Generation of Solution and Surface Gradients Using Microfluidic Systems," Langmuir, vol. 16, no. 22, pp. 8311-8316, Oct. 2000.

[29] A. Shamloo, N. Ma, M.-M. Poo, L. L. Sohn, and S. C. Heilshorn, "Endothelial cell polarization and chemotaxis in a microfluidic device.," Lab on a chip, vol. 8, no. 8, pp. 1292-9, Aug. 2008.

[30] J. Atencia and D. J. Beebe, "Steady flow generation in microcirculatory systems.," Lab on a chip, vol. 6, no. 4, pp. 567-74, Apr. 2006.

[31] S. Pennathur, "Flow control in microfluidics: are the workhorse flows adequate?," Lab on a chip, vol. 8, no. 3, pp. 383-7, Mar. 2008.

[32] D. a Ateya, J. S. Erickson, P. B. Howell, L. R. Hilliard, J. P. Golden, and F. S. Ligler, "The good, the bad, and the tiny: a review of microflow cytometry.," Analytical and bioanalytical chemistry, vol. 391, no. 5, pp. 1485-98, Jul. 2008.

[33] P. Skafte-Pedersen, D. Sabourin, M. Dufva, and D. Snakenborg, "Multi-channel peristaltic pump for microfluidic applications featuring monolithic PDMS inlay.," Lab on a chip, vol. 9, no. 20, pp. 3003-6, Oct. 2009.

[34] L. Kim, Y.-C. Toh, J. Voldman, and H. Yu, "A practical guide to microfluidic perfusion culture of adherent mammalian cells.," Lab on a chip, vol. 7, no. 6, pp. 681-94, Jun. 2007.

[35] J. El-Ali, P. K. Sorger, and K. F. Jensen, "Cells on chips.," Nature, vol. 442, no. 7101, pp. 403-11, 2006.

[36] N. Futai, W. Gu, J. W. Song, and S. Takayama, "Handheld recirculation system and customized media for microfluidic cell culture.," Lab on a chip, vol. 6, no. 1, pp. 149-54, Jan. 2006.

[37] G. Marshall, "Zone fluidics in flow analysis: potentialities and applications," Analytica Chimica Acta, vol. 499, no. 1–2, pp. 29-40, Dec. 2003.

[38] J. Essick, Hands On Introduction to LabVIEW for Scientist and Engineers. New York: Oxford University Press, Inc., 2008.

[39] C. Elliott, V. Vijayakumar, W. Zink, and R. Hansen, "National Instruments LabVIEW: A Programming Environment for Laboratory Automation and Measurement," Journal of the Association for Laboratory Automation, vol. 12, no. 1, pp. 17-24, Feb. 2007.

[40] J. Jehander, "Graphical Object-Oriented Programming In LabVIEW," National Instruments White paper, no. 3390, pp. 1-9, 2006.

[41] NI, "Handling Errors in NI LabVIEW," 2012. [Online]. Available: http://www.ni.com/gettingstarted/labviewbasics/handlingerrors.htm. [Accessed: 08-Aug-2012].

[42] NI, "Application Design Patterns : State Machines," no. 3024, 2011.

[43] R. Bitter, M. Taqi, and N. Matt, "State Machines," in LabVIEW Advanced Programming Techniques, Boca Raton: CRC Press LLC, 2001.

[44] H.-petter Halvorsen, Introduction to State-based Applications in LabVIEW. Porsgrunn: Telemark University College, 2011.

[45] D. Erickson, "Integrated microfluidic devices," Analytica Chimica Acta, vol. 507, no. 1, pp. 11-26, 2004.

[46] R. F. Ismagilov, "Integrated microfluidic systems.," Angewandte Chemie (International ed. in English), vol. 42, no. 35, pp. 4130-2, Sep. 2003.

[47] C. J. Easley et al., "A fully integrated microfluidic genetic analysis system with sample-in–answer-out capability," Image (Rochester, N.Y.), vol. 103, no. 51, pp. 1-6, Dec. 2006.

[48] D. Mark, F. von Stetten, and R. Zengerle, "Microfluidic Apps for off-the-shelf instruments," Lab on a Chip, 2012.

[49] C. H. Chen, S. H. Cho, and F. Tsai, "Microfluidic cell sorter with integrated piezoelectric actuator," Biomedical Microdevices, pp. 1223-1231, 2009.

[50] E. Carrilho, A. W. Martinez, and G. M. Whitesides, "Understanding Wax Printing : A Simple Micropatterning Process for Paper-Based Microfluidics," Analysis, vol. 81, no. 16, pp. 7091-7095, 2009.

[51] A. W. Martinez, S. T. Phillips, G. M. Whitesides, and E. Carrilho, "Diagnostics for the developing world: microfluidic paper-based analytical devices.," Analytical chemistry, vol. 82, no. 1, pp. 3-10, Jan. 2010.

[52] Y. Fintschenko, "Education: A modular approach to microfluidics in the teaching laboratory," Lab on a Chip, 2011.

[53] E. Miller, M. Rotea, and J. P. Rothstein, "Microfluidic device incorporating closed loop feedback control for uniform and tunable production of micro-droplets.," Lab on a chip, vol. 10, no. 10, pp. 1293-301, May 2010.

[54] T. Lindeberg, "Edge detection and ridge detection with automatic scale selection," in Proceedings CVPR IEEE Computer Society Conference on Computer Vision and Pattern Recognition, 1998, pp. 465-470.

[55] M. Sonka, V. Hlavac, and R. Boyle, Image Processing, Analysis, and Machine Vision, 3rd ed. Toronto: Thomas, 2008.

[56] G. C. Y. Chong, "PID control system analysis and design," IEEE Control Systems Magazine, vol. 26, no. 1, pp. 32-41, Feb. 2006.

[57] J. Zhong, "PID Controller Tuning : A Short Tutorial," 2006.

[58] Y. Stepanenko, "Adaptive control of a class of nonlinear systems with fuzzy logic," Proceedings of 1994 IEEE 3rd International Fuzzy Systems Conference, vol. 2, no. 4, pp. 779-785, 1994.

[59] J. Carvajal, "Fuzzy PID controller: Design, performance evaluation, and stability analysis," Information Sciences, vol. 123, no. 3–4, pp. 249-270, Apr. 2000.

[60] H. O. Wang, K. Tanaka, and M. F. Griffin, "An approach to fuzzy control of nonlinear systems: stability and design issues," IEEE Transactions on Fuzzy Systems, vol. 4, no. 1, pp. 14-23, 1996.

[61] K. R. King, S. Wang, A. Jayaraman, M. L. Yarmush, and M. Toner, "Microfluidic flow-encoded switching for parallel control of dynamic cellular microenvironments.," Lab on a chip, vol. 8, no. 1, pp. 107-16, Jan. 2008.

[62] G. F. Franklin, J. D. Powell, and A. Emami-Naeini, Feedback Control of Dynamic Systems, 6th ed. New Jersey: Pearson Prentice Hall, 2008, p. 840.

[63] K. Tanaka and M. Sugeno, "Stability analysis and design of fuzzy control systems," Fuzzy Sets and Systems, vol. 45, no. 2, pp. 135-156, Jan. 1992.

[64] C. C. Lee, "Fuzzy logic in control systems: fuzzy logic controller. I," IEEE Transactions on Systems, Man, and Cybernetics, vol. 20, no. 2, pp. 404-418, 1990.

[65] L. A. Zadeh, "Fuzzy logic, neural networks, and soft computing," Communications of the ACM, vol. 37, no. 3, pp. 77-84, Mar. 1994.

[66] M. a. Unger, "Monolithic Microfabricated Valves and Pumps by Multilayer Soft Lithography," Science, vol. 288, no. 5463, pp. 113-116, Apr. 2000.

[67] W. Gu, X. Zhu, N. Futai, B. S. Cho, and S. Takayama, "Computerized microfluidic cell culture using elastomeric channels and Braille displays.," Proceedings of the National Academy of Sciences of the United States of America, vol. 101, no. 45, pp. 15861-6, Nov. 2004.

[68] S. E. Hulme, S. S. Shevkoplyas, and G. M. Whitesides, "Incorporation of prefabricated screw, pneumatic, and solenoid valves into microfluidic devices.," Lab on a chip, vol. 9, no. 1, pp. 79-86, Jan. 2009.

[69] A. B. Dahlin, S. Chen, M. P. Jonsson, L. Gunnarsson, M. Käll, and F. Höök, "High-resolution microspectroscopy of plasmonic nanostructures for miniaturized biosensing.," Analytical chemistry, vol. 81, no. 16, pp. 6572-80, Aug. 2009.

[70] J. E. Dover, G. M. Hwang, E. H. Mullen, B. C. Prorok, and S.-J. Suh, "Recent advances in peptide probe-based biosensors for detection of infectious agents.," Journal of microbiological methods, vol. 78, no. 1, pp. 10-9, Jul. 2009.

[71] N. Backmann et al., "A label-free immunosensor array using single-chain antibody fragments.," Proceedings of the National Academy of Sciences of the United States of America, vol. 102, no. 41, pp. 14587-92, Oct. 2005.

[72] L. Feuz, M. P. Jonsson, and F. Höök, "Material-selective surface chemistry for nanoplasmonic sensors: optimizing sensitivity and controlling binding to local hot spots.," Nano letters, vol. 12, no. 2, pp. 873-9, Feb. 2012.

[73] B. J. Kirby and E. F. Hasselbrink, "Zeta potential of microfluidic substrates: 1. Theory, experimental techniques, and effects on separations.," Electrophoresis, vol. 25, no. 2, pp. 187-202, Jan. 2004.

[74] H. Zhang, A. a Hassanali, Y. K. Shin, C. Knight, and S. J. Singer, "The water-amorphous silica interface: analysis of the Stern layer and surface conduction.," The Journal of chemical physics, vol. 134, no. 2, p. 024705, Jan. 2011.

[75] R. J. Riobóo, M. Philipp, M. a Ramos, and J. K. Krüger, "Concentration and temperature dependence of the refractive index of ethanol-water mixtures: influence of intermolecular interactions.," The European physical journal. E, Soft matter, vol. 30, no. 1, pp. 19-26, Sep. 2009.

Chapter 4

Multi-parametric microenvironments

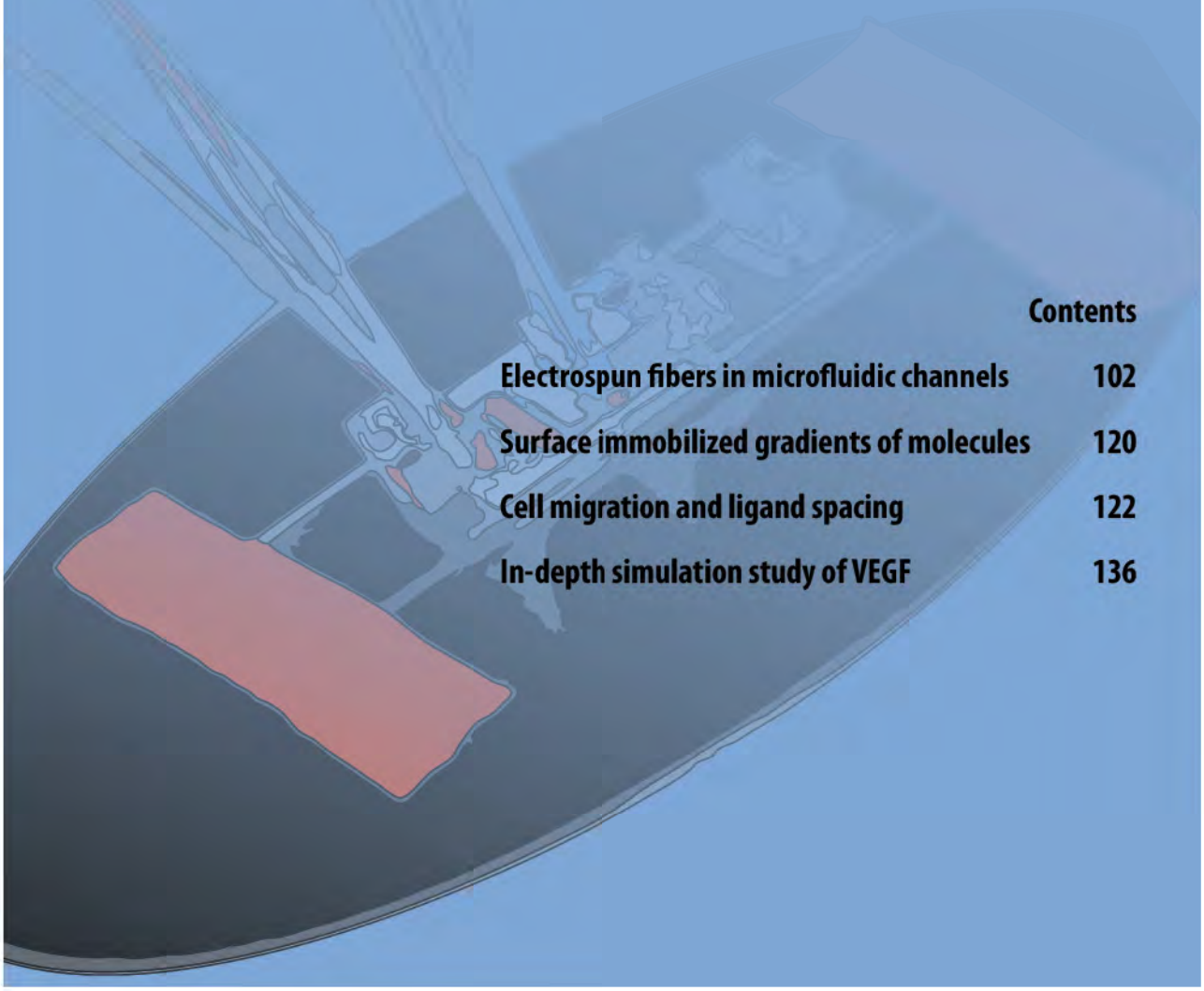

Contents

I had worked with microfluidics for a while and I was very happy about the liquid handling system that I had designed and build ("Liquid handling" on page 71). Now, it was time to apply the equipment and expertise to actually create cell microenvironments *in vitro* with the help of microfluidics. I wanted to explore the abilities microfluidics offered to influence cells in different ways and do things that I could not do with standard cell culture in a petri dish. One particular area that I found extremely fascinating were chemical gradients.

As I mentioned in the introduction most signals a cell is receiving in the body are not coming in an on/off manner, but are rather continuous shifts of concentration, stiffness, density, distance and other properties of the cell microenvironment. Therefore, it is important to have *in vitro* model systems that can mimic these condition and form gradients of different types to stimulate cells. Technologies to create such gradients with standard cell culture techniques exist and the first device was developed by Stephen Boyden in 1962 [1]. The principle is still used today in Boyden chambers, other techniques to study cell responses to chemical gradients include the Zigmond chamber [2] and the Dunn chamber [3], but they are all fairly limited in their capabilities due to large static liquid volumes [4–7]. The same holds true for the under agarose cell migration assay [8] or the agarose spot assay [9], and all offer limited control over the gradient shape, steepness and other properties.

Over the last two decades microfluidic systems have been established to fill this gap and provided new approaches capable of tightly controlling the formation of chemo-attractant gradients [6], [10–17]. Since mixing is limited to diffusion in microfluidic channels, due to the low Reynolds number, liquid flows can be controlled much better in those channels than in standard cell culture dishes [18]. I was very interested in microfluidic gradient generators, because it felt like it was something special and it was something that was not easily done without microfluidics. I thought it was great that microfluidics could be used to solve a specific problem by using its intrinsic properties and the physical phenomena occurring on these small length scales – and that was the beginning of a series of very interesting designs, challenges and experiments.

Electrospun fibers in microfluidic channels

The money that was paying my salary did not entirely come from the two European projects mentioned before, but there was a third, much smaller, project that Julie and I were involved in. This Vinnova funded project was about stem cell differentiation,

in particular neural stem cell differentiation into neurons, and the effects of electrospun fibers on this process (see page 14 for more details). Originally, our group was supposed to work on different surface modifications and characterize surface properties of electrospun fibers, but it was not very clear and our part in the project was not that big.

The idea to produce multifactorial microenvironments to steer cellular fate processes had interested me for a long time. I thought that if you are able to mimic most of the parameters a cell is experiencing *in vivo* then it should be possible to get the same response as in the body. Like I mentioned in the introduction (page 4), if you use the right cells they have all the potential needed. The difficult part is to put them into the right context and give them the right cues to do what you want them to do.

I thought it would be much more interesting to work on complex microenvironments instead of functionalizing the electrospun fibers. My idea was to integrate electrospun fibers into a microfluidic platform to gain control both of the liquid composition around the cells and the substrate underneath. I presented this idea way back in February 2010 with a single image (Figure 4.1) during one of the project meetings. Everybody thought that it was a very interesting idea and worth pursuing. So, I started to work on it in more detail.

Although, my main focus during that time was still on lipid bilayers and how to use them as cell culture substrates (chapter 2), I really liked this project. It enabled me to work more in the direction that I thought was very interesting; towards the combination of different factors to form complex microenvironments. I was, however, limited in the amount of time I could spend on this

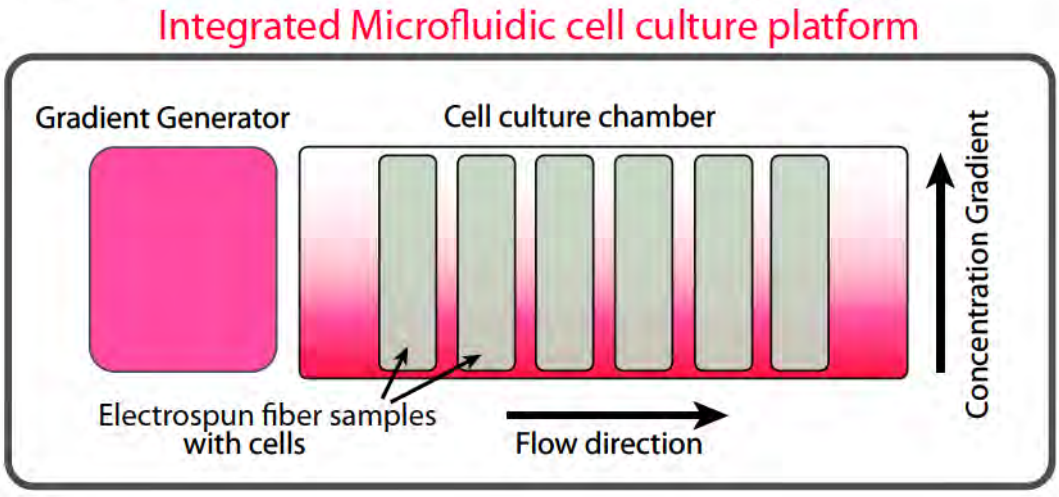

Figure 4.1
Schematic of a microfluidic platform that allows the integration of electrospun fiber pads with a microfluidic gradient generator.

project at the beginning and before I could start I needed to have a suitable liquid handling system, as described in chapter 3.

During the following month, the idea of how to use a microfluidic platform with integrated electrospun fibers developed more and more, and a scientific question became clearer. In the developing brain neural stem cells are migrating along radial glial cells to their target destination [19–22]; this process can be mimicked with electrospun fibers [23–25]. Contact guidance alone is, however, not enough for cell migration and axon outgrowth *in vivo* different neurotrophins are stimulating the process further [26], [27]. One cytokine that promotes neural stem cell migration is stromal cell-derived factor 1 alpha (SDF-1a) [28]. SDF-1a is secreted at pathological sides in the brain and forms a gradient in the surrounding tissue that cells migrate along.

The question that we wanted to investigate was how cells respond to different cues (topographical vs. chemical), if they are acting in the same direction or perpendicular to each other. In particular, we were interested in axon outgrowth of neurons and migration of neuronal stem cells out from neurospheres. The question was what would happen if electrospun fibers were aligned in the same direction as the gradient or perpendicular to it; would the cells response more strongly to the fibers or the chemical cue; would the response be stronger if both were acting in the same direction. In order to answer any of those questions, we first needed to design a microfluidic network to produce gradients and develop a method to integrate electrospun fibers with microfluidics. The results of this project are presented in paper 1 (page 152).

Microfluidic flow based gradient generator

I was eager to start working on my new project and the first thing that I needed to do was to design a microfluidic network that could generate a gradient. I decided to work on a flow based gradient generator design, similar to the one presented by Noo Li Jeon in 2000 [29], for more information on flow based gradient generators see "BOX 4.1" on page 105. I do not really remember why I chose that type of design, but I think it was mainly for its flexibility and capacity to produce different kinds of gradients by adjusting the inflow parameters. This was the first time I designed a complex microfluidic network on my own and even though the basic design principles were already published, I was excited about this work. I designed the network in AutoCAD (Autodesk, UK) and performed computational fluid dynamics simulations in Comsol (Comsol, Sweden, "BOX 4.2" on page 106) throughout the whole design process to optimize the design and study its properties.

Flow based gradient generators

BOX 4.1

Various designs to generate gradients have been proposed in the literature, aiming at different applications and having specific advantages and disadvantages. In general, gradient generators can be divided in flow-based and free-diffusion-based systems (see "BOX 4.3" on page 123) [6].

One of the most common designs to create flow-based gradients was developed by Jeon et al. [29]. It relies on repetitive splitting and recombining fluid streams with different concentrations. A fluid stream with high concentration is combined with one of lower concentration and both are mixed in a serpentine channel resulting in an intermediate concentration which is again divided in half. At the end of the premixing network all fluid streams are combined to form a concentration gradient in a wide probing channel. This principle allows the formation of linear and parabolic gradients, as well as dynamic manipulation of the gradient by controlling the flow rate in each inlet individual.

Dertinger et al. [30] developed this principle further and showed that it is possible to create complex gradients by combining several premixing networks in one wide channel. Campbell et al. [31] and Amarie et al. [10] optimized the use of premixing networks and were able to create gradients with compact channel networks. Another alteration of the basic principle was proposed by Lin et al. [13], they used an additional premixing stage to create complex gradients that could be adjusted dynamically by changing the relative flow rates. One approach that slightly differs from the previously described principle was proposed by Irimia et al. they suggested to use parallel dividers in the direction of flow to generate nonlinear chemical gradients [11].

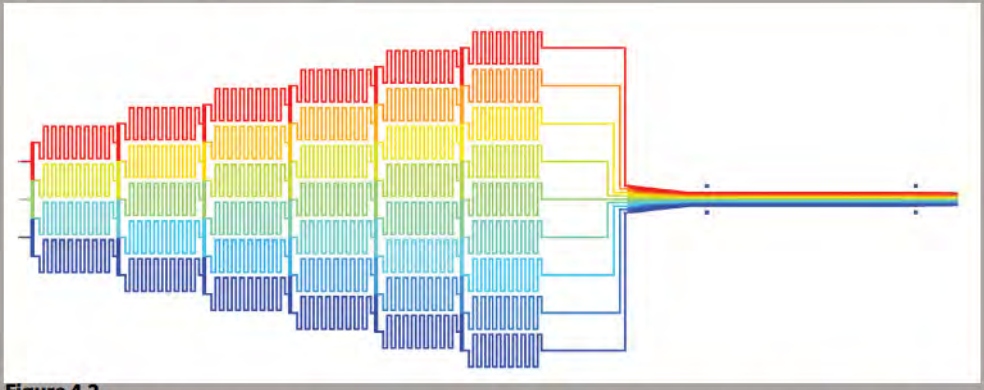

Figure 4.2
Simulation data of a typical flow based gradient generator with 3 inlets, 6 mixing stages and 9 outlets. Red: high concentration Blue: low concentration

Comsol multiphysics

BOX 4.2

Comsol multiphysics is a simulation software environment to model complex problems involving one or more physical phenomena. It uses the finite element method (FEM) to find approximated solutions for the modeled problem. FEM is a numerical method to solve algebraic equations, ordinary differential equations and partial differential equations that describe the model system to predict its behavior under given conditions. To achieve this complex problems are divided into small elements and the equations for each element are solved in relation to its neighbor elements. The division of the model into small elements is done with a mesh, for two-dimensional problems triangular mesh elements are commonly used and for three-dimensional problems tetrahedrons are often used for the mesh. Other shapes might be used particular problems and it is important to consider the nature of the problem and choose an appropriate mesh strategy with a suitable mesh element and size. The solution of the whole model should be independent from the mesh size and type to ensure that the results are adequate; this condition is referred to as mesh-independency. [32–34]

The Comsol multiphysics software environment integrates the whole process of setting up a model, defining the boundary conditions, meshing the model, solving the equations and visualizing the results in a single package. The model geometry can be either build up directly in Comsol or it can be imported from various computer-aided design (CAD) programs, including AutoCAD. The big advantage of Comsol over other FEM software packages is the ability to couple different physical phenomena together and thereby model more complex problems. For example, instead of only calculating the flow field for a given geometry, Comsol allows you to couple the results from the flow field equations to another physical phenomenon like the transport of molecule within the channel or heat dissipation. The software incorporates modules with predefined equations for electrical, mechanical, fluid dynamical and chemical problems, and own equations can be integrate either directly or via a MATLAB (Mathworks, USA) link. This ensures a fast setup time for a new model, but at the same time offering full flexibility to build a precise model representation of the problem at hand. [34]

I did not have a lot of experience with finite element method (FEM) based simulation, but I had been working with ANSYS (ANSYS, USA) a long time ago when I worked as a student research assistant in Germany. The good think about Comsol was that it is fairly straight forward to use and I was able to quickly make progress despite the lack of experience. Multiphysics FEM simulations are a very powerful tool for microfluidics, because they allow the evaluation and characterization of a channel network prior to its production. Thus, it is possible to test, fine-tune and optimize different parameter of the microfluidic channel geometry to generate the indented conditions. This would be very time consuming and expensive to do with several hardware revisions. Furthermore, simulations can provide additional data that is very difficult to access otherwise, for example the shear stress at the cell-liquid interface.

My first Comsol model used the laminar flow module to model the fluid velocity field within the microfluidic network and the transport of diluted species module to model the concentration gradient. To couple both together, the velocity field was used as convective transport for the molecule. I varied the number of mixing stages in the gradient generator network and investigated different probing channel geometries to find conditions that formed linear gradients over the whole length of the probing channel. I also used the model to test different inflow velocities to define a range that would be useful for later experiments. It worked very well and it was a very useful for later. I even extended the model later to look more specifically at the effects at the interface of electrospun fibers with the liquid (page 114).

The final design based on the simulation results is shown in Figure 4.3. The network has three inlets (left), a gradient generator, a cell culture chamber and one outlet (right). I wanted to have a more universal design that is capable of not only forming linear

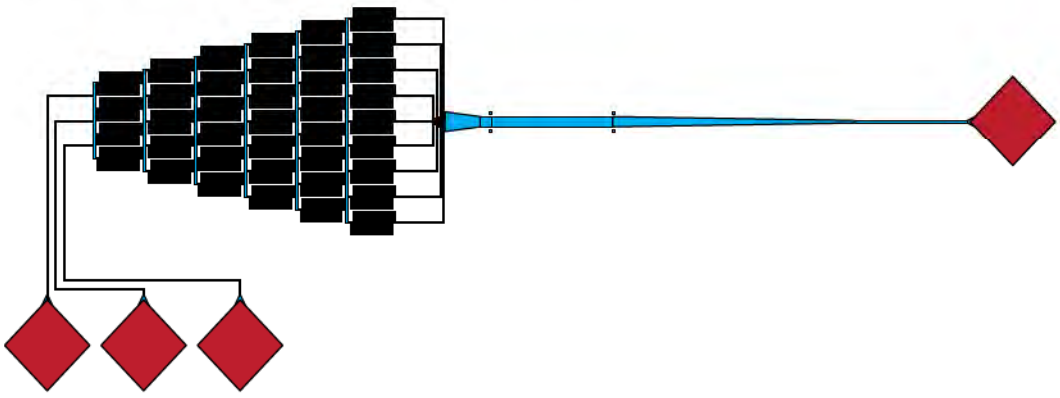

Figure 4.3
Final design of the flow based gradient generator used in Paper I, showing the 3 inlets on the bottom left, the gradient network on the left, the probing channel in the center and the outlet to the right.

gradients (Figure 4.4 top), but also more complex ones with for example parabolic shapes (Figure 4.4 bottom). Therefore, I choose to have three inlets instead of two, which would have been sufficient to produce controlled linear gradients [30]. I do not know if that was a wise decision, I gained flexibility for the future, but I have never used anything other than linear gradients until now. Additionally, three inlets are more error-prone and three pumps are always needed to operate the system. One could argue for and against both routes, and Stephan Dertinger et al. showed clearly that a similar design has great potential to produce very advanced gradient shapes [30] and maybe I will use the channel to its full potential in the future.

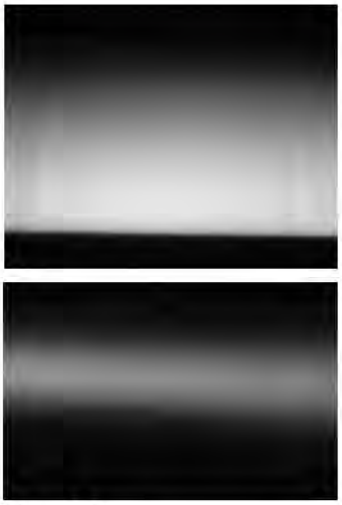

Figure 4.4
(TOP) Linear gradient formed by using 100%, 50% and 0% of fluorescence solution in inlet 1 to 3. (Bottom) Parabolic gradient formed by using 0%, 100% and 0% in inlet 1 to 3.

After the final design was finished, I sent the AutoCAD file to Zonghe Lai at MC2, who produced a dark field chrome mask by electro-beam lithography; a detailed description of the fabrication route from the design to microfluidic chips is given in "BOX 3.2" on page 67. There were some problems at the beginning and a little bit confusion about what design elements one could use in AutoCAD to get a successful conversion into the format of the electron-beam lithography machine, but it worked out eventually. Hossein Agheli used the mask to produce a SU-8 master in the MC2 cleanroom for me. I am very grateful to all the people and especially Hossein for helping me with the production. My focus is definitely more on cells and biology and thus, it was great to work together with people how know so much about microfabrication and could help me on that part.

Experimental characterization of gradients

When I finally had the first microfluidic chip in my hands, I was so curious to know if it would work that I did a little experiment right away. I carefully placed three droplets, red, transparent and blue, on the three inlets and used a syringe at the outlet to suck them in. I immediately saw a gradient forming in the main chamber – it was fascinating that by the means of three droplets and a syringe, a gradient could be formed by just using the right channel geometry. I think this was a very important moment for me for several reasons; it was my first complex microfluidic design and it worked, I realized that with the right channel design you could do all kinds of things and behavior was predictable from simulations, and it was simply beautiful. After all the work, I had a microfluidic channel that could produce gradient. Sure, other people had been doing this for years and showed all kinds of fancy alterations and applications, but for me personally, it was the first time and the excitement and fascination was as if I had been the first one. Maybe, you should not be so attached to your research projects, but that is the way I felt.

Figure 4.5
First gradient image taken with the webcam microscope setup. The gradient was formed by placing three droplets on the inlets and sucking them in from the outlet with a syringe

After this initial test and assurance that the network was actually working, the next task was to more thoroughly characterize the gradient and study, effects of different flow parameters and see if the data was correlating with the simulations. Although, the red and blue color solutions were great for visualization and very easy to see, they were not suitable for quantitative characterization of the gradients, because the contrast is too low and color cameras are normally not suitable for such a task. Therefore, sodium fluorescein, a green fluorescence marker, was used to measure gradient properties with a fluorescence microscope and an attached CCD (Charged-coupled device) black and white camera. A CCD image sensor has a higher dynamic range and more uniform response in comparison with a CMOS (complementary metal-oxide-semiconductor) image sensor found in most cheaper cameras [35–37], like the one used for the color images presented here.

I used a 10 mM sodium fluorescein PBS solution in inlet 1, 5 mM in inlet 2 and pure PBS in inlet 3 to produce linear gradients ranging from 10 to 0 mM and took images at two different positions along the main channel; the whole experimental setup is shown in Figure 4.6.

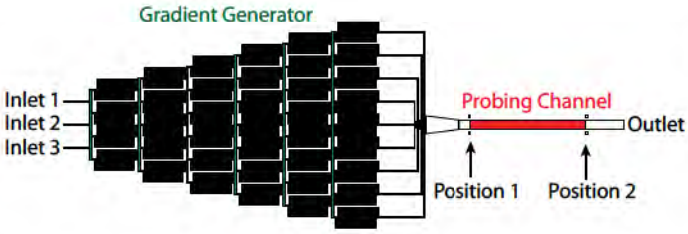

Figure 4.6
Schematic of the experimental setup for the characterization of the flow based gradient generator

Figure 4.7 shows line profiles of fluorescence intensity for different flow velocities at position 1 in the probing channel of the microfluidic gradient chip. The gradient has a large linear portion at the center of the channel and differs closer to edges. This is most likely an effect of the walls of the microfluidic channel and the fact that fluid velocity fields are parabolic under laminar flow conditions. Thus, the flow velocity near the wall is much lower than in the center of the channel, since the influence of diffusion increases. The importance of diffusion is also obvious from the difference between different inflow velocities. For slow inflow velocities the gradient does not span the whole range from 100-0%, because the random movement of molecules by diffusion blurs the gradient. Due to the slow flow molecules traveling slower in the x-direction and therefore have more time to diffuse in y-direction. For very fast flows the gradient has small steps, this is due to the design of the gradient generator. The gradient generator does not produce a continuous concentration gradient, but divides the inlet concentration in nine separate concentrations, ranging from

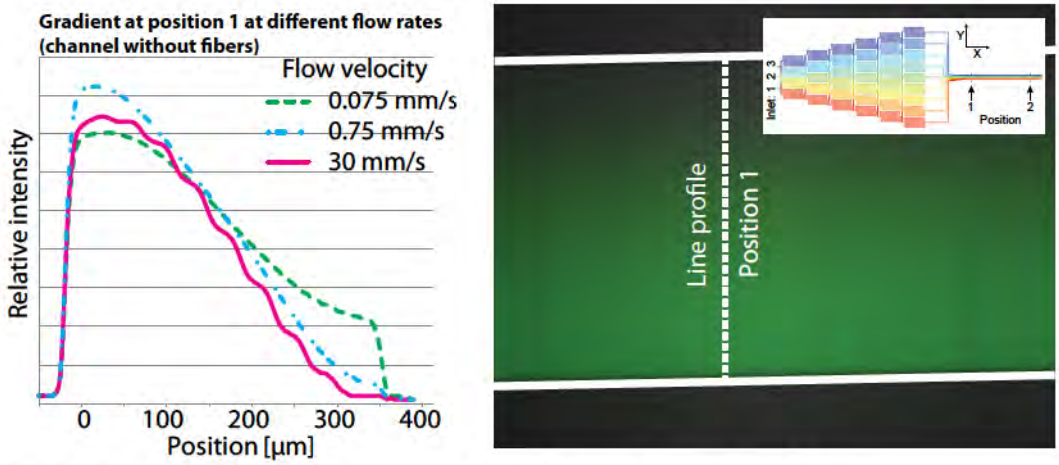

Figure 4.7
(RIGHT) Fluorescence micrograph of the probing channel taken at position 1 with the line indicating the position for the line profiles. (LEFT) Line profiles from position 1 for three different flow velocities showing the relative intensity across the channel.

100-0% in our configuration. These steps are normally blurred out by diffusion and a linear gradient is formed, but if the fluid velocity is too high diffusion is limited and discrete steps can be seen. The best results, a steep linear gradient with the slowest flow, were achieved at an inflow velocity of 0.75 millimeter/seconds which corresponds to a flow rate of 5 nanoliter/second for each of the three inlets.

The gradient networked worked and both the experimental results and CFD simulations were in good accordance to each other. I had found parameters that I could use for my experiments and was happy with the microfluidic design. There are, however, three things that I would definitely change in the design, looking back now with more experience in designing different microfluidic channels, simulating them and using them for cell studies:

1) I would place the inlets differently and ensure that they all have the same channel length from the inlet to the first stage of the gradient generator. In this way, the pressure drop from all inlets would be the same and the gradient would be even more predictable. The current configuration has not caused any problems, and both simulations, as well as experimental measurements, did not show any negative effects, but it would be easy to adjust and rule out uncertainties with a modified design.

2) The channel connecting the cell culture chamber with the outlet should be straight and not narrow down from 400 micrometer to 100 micrometer. There is basically no good reason to have a design like it is at the moment and there is a risk is that the increase in pressure towards the outlet will cause problems. Normally, microfluidic should be designed in a way that the pressure drop is in the direction of the outlet [18], [38].

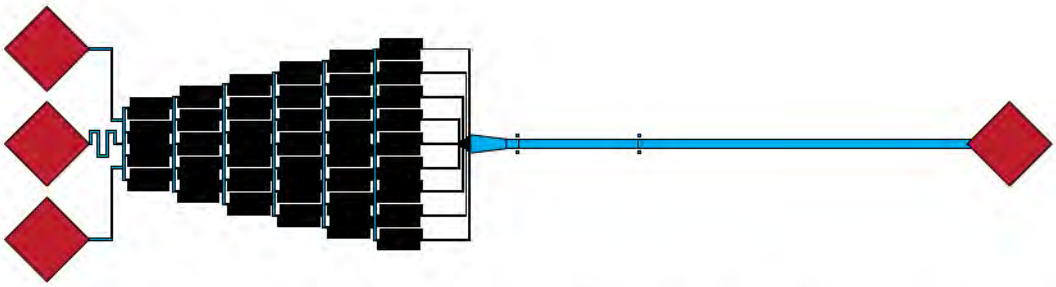

Figure 4.8
Improved design of the flow based gradient generator with better inlet and outlet placement.

3) I would change the overall dimensions of the network, increasing both the height of the channels from 50 to around 150-200 micrometer and the channel width by the factor of 3 or 4. The larger dimensions will help a lot in cell culture and overall handling. I designed the original network without any experience of culturing mammalian cells in microfluidic channels, and from the experiments I performed since then I would say that larger channels definitely simplify long term cell culture and improve overall cell survival. Furthermore, a larger cell culture area would mean that more cells are present in the channel and can be analyzed to get statistical more solid data. Drawbacks of increasing the size would be a higher consumption of media and a more difficult production process of the SU-8 master (see page 127).

Bonding PDMS channels above fibers

The next important step was to find a way to integrate electrospun polyurethane fibers with the microfluidic network. On this part, I worked very closely together with Carl Zandén and Björn Carlberg from Johan Liu's group at MC2 who were also involved in the Vinnova project. They had developed a fabrication technique to pattern electrospun fiber pads on the micrometer length scale with photolithography and were able to not only produce random orientated fibers, but also aligned fiber. They provided me with all the substrates that I used. Figure 4.9shows a schematic of the production process and a detailed description of the technique can be found in the paper published by Björn Carlberg et al. in 2010 [39]. We used two different fiber patterns in our experiments, 250x200 micrometer rectangular pads with a 200 micrometer pitch or a single 250x4000 micrometer pad. The fibers were either aligned or randomly orientated and for the smaller pads we had samples with alternating fiber orientation, as suggested in the production scheme.

The design was chosen in a way that the fiber pads, 250 micrometer wide, were slightly smaller than the part of the microfluidic network, 400 micrometer wide that was placed over them to simplify the alignment and restrict the fibers to the area within

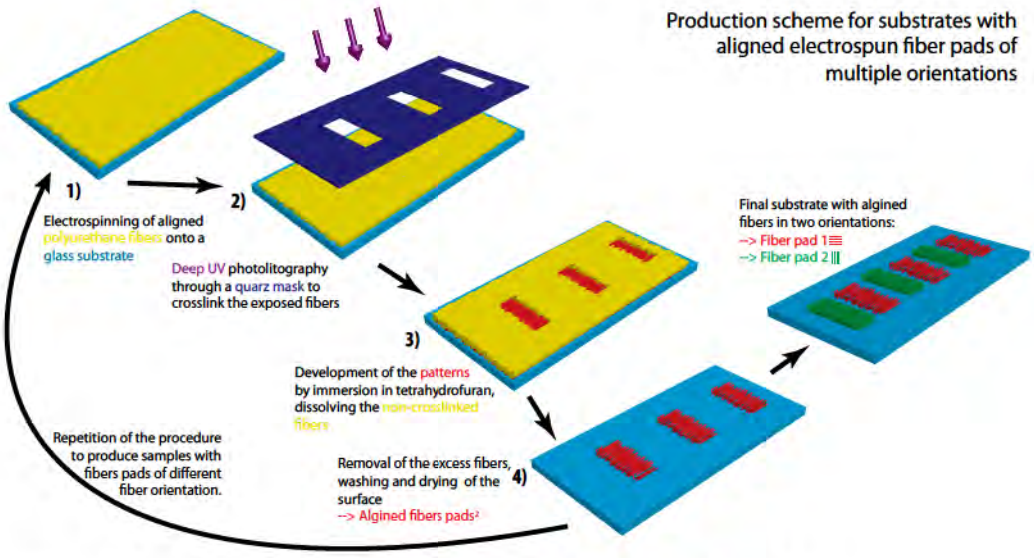

Figure 4.9
Schematic of the production process to pattern aligned electrospun fibers on a glass substrate for the integration with microfluidic networks.

the channel. Previous approaches of using electrospun fibers in combination with microfluidics were using fiber mats covering the whole substrate and relying on press fitting to seal the channels [40–42]. Press fitting can generate tight seals, but the hydraulic pressure that the system can withstand is limited and there is a high risk of liquid slowly creeping into small voids outside the microfluidic network. Because those previous systems were mainly used for biosensing, using the fibers mainly to increase the surface area and operating for a couple of hours, the limitations of press fitting were not restricting these systems. But we wanted to culture cells for several days, maybe even weeks, in our system, which would probably be problematic with a seal relying on press fitting. The risk of accumulation of molecules and infectious agents in the small voids, or in the worst case, complete failure of the seal, was just too large and therefore we decided to limit the fibers to the inside of the microfluidic channel.

The alignment of the substrate with the fibers and the microfluidic network proved to be fairly difficult at the beginning. Already during the design of the patterns and channels, we discussed possibilities to incorporate special features to assist in this process and the photolithography mask for the fibers patterns had special marks to ensure that the fibers would sit at the right position. I, also, designed a special two part assembly device, one part that was used as a mold and placed on the SU-8 master during PDMS casting, and a second part that could hold the glass substrates with the fibers. Once the PDMS was cured both parts could be put together and two guiding rails were ensuring the right position and alignment of both parts – at least that was the theory.

I have to admit that it did not really work, the PDMS was too flexible and the precision of the whole device was not suitable for the task. In addition, we changed from thin cover slide glass substrates to thicker ones and the dimensions differed, thus all the alignment marks were basically useless. At least, the two Teflon parts of the assembly device are very useful supports when placing SU-8 masters with PDMS in the oven for curing.

After this failure, I considered solvent assisted alignment, where a small amount of ethanol is applied at the interface between PDMS and substrate; this inhibits direct bonding and allows for movement. As soon as the right alignment is achieved the chip is placed in the oven to evaporate the ethanol through the PDMS and a stable bond is formed [43]. I never tried this method, but I think for more complex alignment tasks it is definitely a good option. For me the easiest way in the end was to align the fibers with the channels by hand, working under a stereomicroscope. After some experience and with a steady hand, I was actually able to get very good, reproducible alignments within the margins. Sometimes, you just need to appreciate the simple solutions. Figure 4.10 shows the alignment of fiber pads along the main channel in the microfluidic network. The importance of patterning is further illustrated by the image (B), which shows a cross-section of a misaligned channel.

For Johan Liu's group, this was also a very nice way to show the potential of the patterning technique they developed and there were other potential benefits of this approach. In general, it would

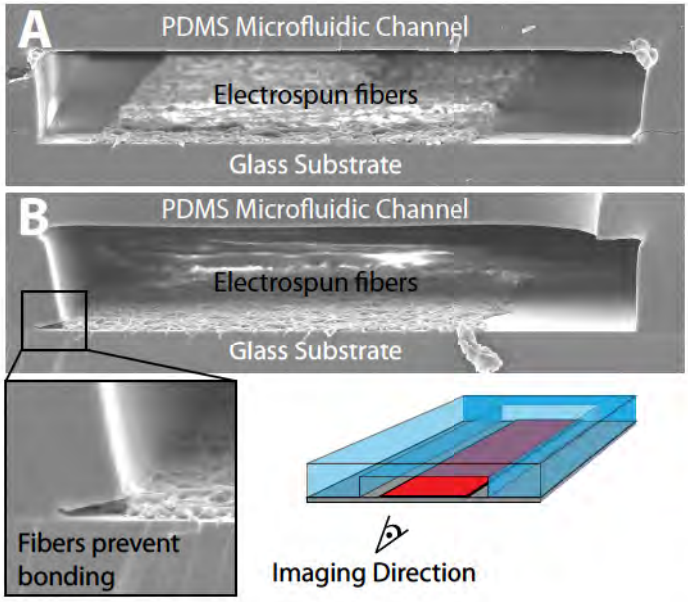

Figure 4.10
Scanning electron micrographs of diced microfluidic chips with electrospun fibers. (A) Microfluidic channel aligned over the fibers. (B) Microfluidic channel misaligned over the fibers, resulting in an incomplete bonding of the PDMS to the glass.

be possible to have much higher fiber pads than the 5 micrometer ones we use at that time, and thereby creating three dimensional scaffolds for cells to interact with. We never tested this idea and there are certainly limitations. It is for example questionable, how well controlled fluid flow can be achieved when half of the channel diameter is covered with fibers. I did some very simple simulations that show that the gradient above the fibers gets less and less steep, when increasing the fiber pad height (Figure 4.11). There are, however, other ways to control the liquid composition in a three dimensional fiber scaffold. A microfluidic channel that is relying on diffusion to form a gradient, like the one we developed later (page 127), would be more suitable for this approach. The three dimensional aspect and the possibilities it offers are definitely interesting, but at the beginning we were more interested in getting the system to work at all and study the effects of fiber alignment in respect to the gradient direction.

Figure 4.11
Simulation data of the main cell culture chamber. (TOP) 5µm thin fiber mat. (BOTTOM) 40µm thick fiber mat.

The important part about the method that we developed to combine electrospun fibers with microfluidic networks is its flexibility. Both parts, the definition of electrospun fiber pads and the design of the microfluidic channels, are relying on photo lithography techniques. Thus, it is possible to produce nearly any arbitrary pattern with very high spatial resolution and use it with the described methods. The freedom in microfluidic design is not limited and all structural microfluidic elements can be integrated.

Gradients over electrospun fibers

As mentioned above the gradient steepness decreases for increasing fiber pad thickness, but one thing I was wondering was how much the fiber pad we used (3-5 micrometer high) would influence gradient formation in the microfluidic channels. I was pretty optimistic that the influence would be limited and that it was possible to form soluble gradients similar to the ones in channels without the fibers; this feeling was supported by the preliminary simulations that I did, which showed successful gradient formation even with the fibers. Although, I was optimistic the first experiment is always a bit special, I was again very excited. All the parts were finally falling in place, I had a microfluidic network that could produce gradients, I had promising simulation data and I had a chip with electrospun fibers carefully aligned to the main microfluidic channel. I switched on the pumps and within less than a minute of stabilization I saw a fluorescein gradient; I could change the flow rates in the three inlets and observe how the fluid stream was changing. Everything worked as it was supposed to - I was very happy and relieved. I used the same characterization procedure that I had been using for the channel without fibers and the data is shown in Figure 4.12.

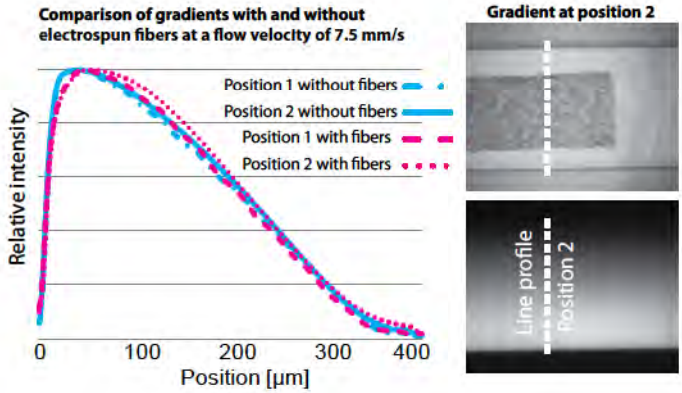

Figure 4.12
(RIGHT TOP) Brightfield image of the channel with the fibes. (RIGHT BOTTOM) Fluorescence micrograph of the probing channel taken at position 2 with the line indicating the position for the line profiles. (LEFT) Line profiles for position 1 and 2 for channels with and without fibers, all showing similar intensity profiles across the channel.

The line profiles for channels with and without fibers were very similar and no systematic difference was observed. The small differences on the left side were most likely due to variations in the microfluidic channels due to minor deformations during bonding. Overall the fibers seemed not to influence the gradient in the channel.

The experimental results looked very good and I was quite satisfied, but there was one problem. It was basically impossible to study fluid behavior only at the interface of the fibers. I was measuring the fluorescence intensity throughout the whole liquid volume and that gives a good indication, but there was the possibility that directly above the fibers the situation would be different and that were exactly the place where the cells would sit. Because it is very difficult to experimentally investigate the interfacial flow, I modeled the interface in Comsol (flow velocity 7.5 mm/s). The two most interesting properties I looked at were the shear stress directly on the surface and the formation of vortices.

The vorticity magnitude is a measure of the rotation in a fluid and is calculated as the curl of the fluid velocity vector [18]. Figure 4.13 shows the simulation data. A small eddy is formed at the edge of the fiber pad, but it is locally restricted (within 10 micrometers) and should not influence the cells dramatically. Another importatnt parameter is the shear stress at the fiber interface shown in Figure 4.14. The shear stress is highest at the front edge (5 dynes/cm2) and below 2.3 dynes/cm2 on the rest of the fiber pad. Cells react very different to shear stress, but the values from the simulation can be regarded as low and should not have any significant effect on cells. [44], [45]

The shear stress tensor (τ) which can be approximated as the sum of the derivative of the flow velocity u with respect to position z and the derivative of the flow velocity w with respect to position x, multipled by the dynamic viscosity μ.

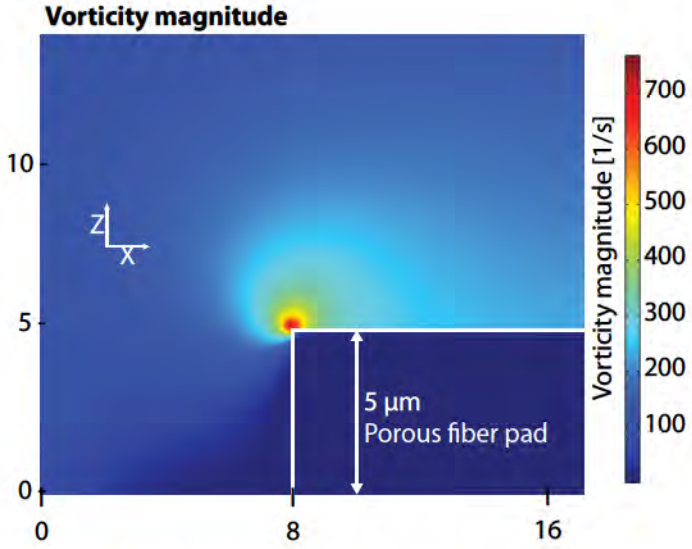

Figure 4.13
Simulation data showing the vorticity magnitude at the modeled edge of the fiber pad in a microfluidic channel.

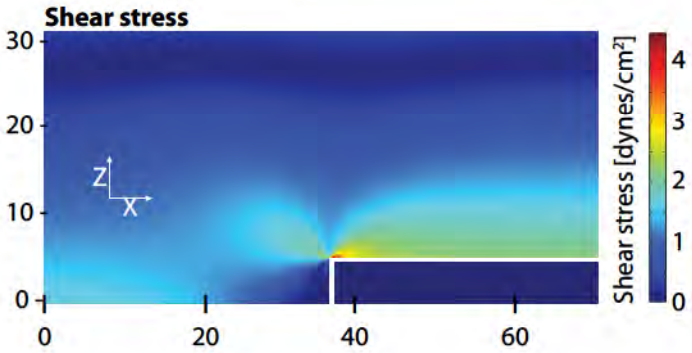

Figure 4.14
Simulation data showing the shear stress at the interface between the fluid and the fibers.

Cells on fibers in channels

The development of a method to integrate electrospun fibers with microfluidic networks took some time, but once the platform was characterized and simulations had helped to understand the effects at the fiber interface, it was finally time to run some cell experiments. After all, the main aim of the whole platform was to culture cells in defined microenvironments and study their behavior in response to different stimuli. Before I started the cell experiments Carl, Björn, Johan, Julie and I discussed how we would like to present the whole study and what we would like to include in a publication. We agreed to focus the first publication on the method development and characterization and only include some basic cell results to show the general suitability of the platform for cell culture, under protest from Julie, who thought it was necessary to include more cell results in the paper. The plan was to run a second study afterwards that was focused on a cell biology question,

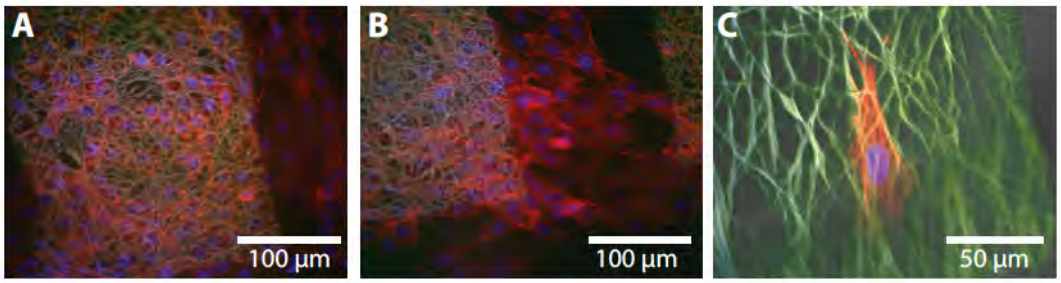

Figure 4.15
Fluorescence micrographs of 3T3 cells cultured in microfluidic channels with electrospun fibers for 24 hours. Cells are stained with phalloidin coupled rhodamine (red: actin filaments) and DAPI (blue: cell nucleus), the fibers are autofluorescent. (A/B) 20x magnification showing the cells on the fibers, as well as in between the fiber pads on the glass.. Cells were seeded at a high density (C) 40x magnification showing a single cell on a fiber pad. Cells were seeded at a low density.

where the platform would be used to its full potential. Looking back, this was not a good decision and Julie was right, but I will come back to that in a little while.

I did run the first cell experiments with 3T3 fibroblast cells and the aim was mainly to see if it was possible to culture the cells in the microfluidic chip and if the cells were attaching to the electrospun fibers. I did know from previous experiments that it was possible to culture cells in microfluidic channels and had even tested this particular microfluidic chip before, but without the fibers. During those experiments, I had optimized the cell seeding procedure and learned that sucking the cells in from the outlet port was the best way to avoid cell clogging in the small channels of the gradient network. Once the cells were inside the channels, the flow should be switched off to allow cells to attach for 1-2 hours, before the flow was switch on again to form a gradient. This procedure worked very well and cells were attaching to the electrospun fibers without problems. Figure 4.15 shows 3T3 fibroblast cells in the main probing channel on electrospun fibers after 24 hours; the cells are attaching to the fibers and spread.

Within some boundaries, it was, also, possible to control the cell density by having different numbers of cells per milliliter, and thereby varying what kind of cell behavior could be studied. Two different cell densities are shown in Figure 4.15. At low densities it is much easier to study single cells and get detailed information about the cell morphology. This also limits the effect of cell-cell communication and cell crosstalk, because it is possible to isolate cells from each other. This comes, however, at a price, the limited number of cells makes it necessary to run a lot of samples to get statistical significant numbers and the isolation might affect cells. It is not a natural condition for a cell to be isolated and without cell-cell contacts. The ability to fine tune the cell density allows taking both facts into account and design a study with an optimal cell density for the question at hand.

At this point, we had all the information and data that we wanted to include in the manuscript. It was the first time that I was writ-

ing a manuscript for submission myself, I had been working with Nina T. on a manuscript before, but this time I was responsible for writing everything up. I got some input from Carl and Björn on the parts about electrospun fibers and Julie was commenting, correcting, editing and improving the text and in the end of August 2011 we finally submitted the manuscript to Lab-on-a-chip. It was a very good feeling to have the paper submitted, the writing process took some time and things got changed over and over again, but in the end it was very nice to press the submit button. It took around a month before we got the comments from the reviewers and editor. I was in California at the Lab-on-a-chip world congress to present the work [46], when I got the email. The comments were mainly positive, but both reviewers were missing more extensive cell results. They wanted to see data where the gradient generator was used to stimulate the cells some way. Therefore, the editor rejected the manuscript in the submitted form.

"The potential of these electrospun fibers for biology is obviously very exciting, and integrating it with micro-fluidics is of potential interest too, even if an in depth characterization of the effect of fibers on cells would be first needed. The main achievement here is to show that the integration is feasible and would not perturb the fluidics."

(Reviewer 2)

I got similar comments during the conference and my visit at Stanford talking to people from Sarah Heilshorns group and Bianxiao Cui; everybody thought that it was a very interesting platform that we had developed, but also asking for more cell results.

All of us knew that this could happen, but we still felt that we wanted this manuscript to be focused on the method of combining electrospun fibers with microfluidic networks in a general way and not to focus on a specific cell study. Julie was again the only one who said that we needed more cell results to make our point. But instead of listening, we decided to rewrite some parts of the manuscript to strengthen the focus on method development and resubmit it to Biomicrofluidics four days before Christmas 2011. The reviewer comments, we got in the middle of February 2012, were very similar to the once we got for the Lab-on-a-chip submission before; both reviewers were requesting more cell results again. This time, however, the editor was more positive and after some discussing suggested that we should add some proof-of-principle cell data to demonstrate the usefulness of the platform and how the gradient could be used, but not run a complete cell study.

We agreed with the suggestion from the editor and decided to run some cell experiments that could show how the platform could be used. We discussed different options and also talked to Nina Erkenstam and Georg Kuhn from the Center for Brain Repair and Rehabilitation in Gothenburg. They were also involved in the Vinnova projects and we have discussed the whole platform with them before and were running some other experiments together at the time. In those experiments, we used primary rat neural

stem cells isolated from Wistar rats (hippocampus and subventricular zone) and we thought that these cells would be very interesting to use with the electrospun microfluidic gradient platform.

In order to be able to inject the cells, it was necessary to disassociate the neurospheres they are forming in culture to get a single cell solution. With this cell solution, the same seeding procedure as for the 3T3 cells could be used, but it was necessary to coat the surface with laminin using a poly-L-ornithine pre-coating. As cell stimuli, we used stromal cell-derived factor 1 alpha (SDF-1a) and substrates with aligned electrospun fibers, which both should stimulate the cells to form outgrowths along their direction. There were three different conditions that we tested to demonstrate the potential of our platform: fibers aligned parallel to the chemotractant gradient, fibers perpendicular to the gradient, and no fibers at all. Nina E. had previously shown that these cells would align along electrospun fibers and use them as contact guidance, thus we did not include that condition in our experiments.

Figure 4.16 shows the results from the different conditions, the cells are stained with rhodamine-phalloidin to visualize the actin skeleton (red) and DAPI to show the cell nucleus (blue). In the first condition with no fibers, the cells responded to the chemical gradient and directional outgrowth along the gradient is seen. For the second condition both stimuli were working in the same direction and again directional outgrowth of the cells is observed. The interesting part was condition three, where we wanted to test if the contact guidance by the fibers or the chemical SDF-1a gradient is influencing the cells more strongly. Under this condition, the cell outgrowth was along the clearly along the SDF-1a gradient and the cells were not influenced by the fibers. This data is very interesting and illustrates the potential have the developed platform, the ability to study cells in defined complex microenvironments and study the influences of multiple cues in a systematic manner. A more thorough study with more cell experiments is clearly needed to make any conclusions about the response of

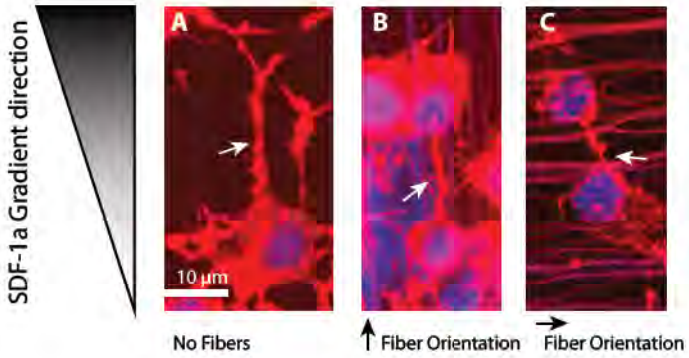

Figure 4.16
Fluorescence micrographs of neural stem cells cultured in microfluidic channels with electrospun fibers for 24 hours with a SDF-1a gradient as indicated. Cells are stained with phalloidin coupled rhodamine (red: actin filaments) and DAPI (blue: cell nucleus). (A) Condition 1 without fibers. (B) Condition 2 fibers aligned in the same direction as the gradient. (C) Condition 3 fibers aligned perpendicular to the gradient.

neural stem cells to electrospun fibers in combination with SDF-1a gradients, but the our aim was a proof-of-principle cell study.

I took a while to get the system to work, run all the cell experiments, analyze the data and rewrite the manuscript, but everything worked out. I resubmitted the manuscript, including the new cell results and some additional simulation data on the 1st of June 2012, it got accepted the same day and published online the 19th of June 2012. I was so happy. Nearly a year after our initial submission to Lab-on-a-chip the manuscript was finally published – in Biomicrofluidics. I learned a lot during the whole process of writing, submitting, rewriting, arguing and resubmitting and I think it was a very valuable lesson. It was probably not the most efficient way, but the experience that I gained from all the mistakes that I did was definitely worth the time. Sure, it would have been very nice to get everything right from the beginning and it might have gone faster if Julie had insisted more strongly to include cell results from the beginning, but I would not have learned nearly as much during the process. I experienced all the difficulties of writing a paper with several different authors, how complicate it is to keep the focus through all revisions and rewritings and how important it is to have a clear message and data supporting your arguments. Looking back, the cell results were definitely needed to make a whole story, it was incomplete without them. If we wanted to focus the paper entirely on the method development part, we would have needed to show the combination of several different microfluidic networks with varying fiber patterns and write the paper in a more general way.

Surface immobilized gradients of molecules

In the beginning of March 2011, I got some information about a small start-up company called ClineTechnologies at that time, now called ClineScientific AB. It was based on research from Hans Elwings group at Gothenburg University and focused around a method to produce substrate bound gradients. They used the electrostatic interaction between gold nano particles and were able to vary the short-range interparticle distance by changing the ionic strength of the solution. By using a special setup, the ionic strength could be varied in a gradient of varying spacing could be formed. The gold nano particles were immobilized on a gold surfaces via a dithiol linker.[47]

I thought that those surfaces were very interesting, especially if used in combination with microfluidic networks. My idea was to combine surface bound gradients with soluble gradients. I was supervising a group of students in the tissue engineering course at that time, they were exploring some ideas in that direction.

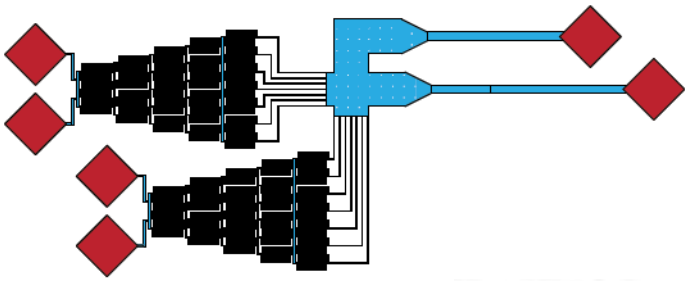

Figure 4.17
Design of a double gradient channel that allows the formation of gradients in two different orientations (perpendicular to each other) in a sequential manner.

They used a double gradient generator (Figure 4.17) to first immobilize a laminin gradient by physisorbtion, and afterwards a soluble gradient could be applied perpendicular to the immobilized one using the second gradient generator. Stephan Dertinger et al. had previously shown that it was possible to form surface bound laminin gradients; in their experiments, they detached the microfluidic network from the glass afterwards and used the glass substrates with standard cell culture techniques [48].

I also did some tests on my own using a similar immobilization approach with my microfluidic chips, but keeping the network attached and using substrates with patterned fibers. Figure 4.18 shows a fluorescence micrograph of antibody stained laminin and line profiles in front of the fiber pad and over the fibers. It worked quite well in the areas without the fibers; it was not perfect, but I got a laminin gradient immobilized on the surface. In the areas with fibers, however, there was basically no gradient; the laminin was adsorbing to the fibers, but instead of a gradient I got a more or less homogenous coating with laminin. This was most likely due to the approach that was used to immobilize the gradient. The process relies solely on physical adsorption and in order to form a gradient a second molecule that adsorbs in competition to the first one is needed. In my case, I used laminin as the molecule of interest and bovine serum albumin (BSA) as a counter molecule. On one side, I had 100% laminin and 0% BSA, and on the other side 0% laminin and 100% BSA. The problem is that there is no flow within the fiber pad, as my simulations had shown, and transport within was exclusively governed by diffusion. Even though, a gradient was present directly above the fibers where cells would be sitting there was no gradient within the fiber mesh, and since the laminin and BSA were freely diffusing within the mesh adsorption was random.

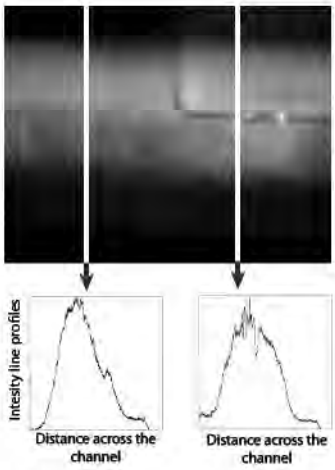

Figure 4.18
(TOP) Fluorescence micrograph of laminin visualized with a primary/secondary antibody staining in a microfluidic gradient channel with electrospun fibers. (BOTTOM) Intensity line profiels across the channel before the fibers and over the fibers.

Combining surface immobilized gradients with soluble gradients was an interesting approach and I wanted to continue to work on it. The problem was that relying on physisorbtion did not really work and I felt that another approach was needed. In general, I do not think that physisorption is a very good way to form immobilized gradients on surfaces. There are quite a few potential

problems, like stability, especially over longer time periods, and the fact that a counter molecule is needed, which should be inert, but have similar adsorption characteristics to the molecule that is studied. Therefore, I was very interested when I heard about the surfaces that Cline could produce.

Cell migration and ligand spacing

I sat down and started to think about a project and more importantly a clear scientific question that I wanted to investigate with a platform that could provide immobilized gradients and soluble gradients, where both gradients could be either in the same direction or perpendicular to each other. One particular area that I thought was interesting to look at was cell migration stimulated by a soluble chemotractant gradient. I was wondering if cell migration speed was influence by the density of cell attachment ligands on a surface. My plan was to have a system in which the spacing between attachment ligands would change gradually on the nanometer scale over a distance of several millimeters. At the same time, a soluble gradient of a chemotractant would be applied perpendicular and would stimulate cell migration. Ideally, all cells would start at one side of the channel and migrate to the other side over time, by comparing how far the cells had migrated at the different spacings, it would be possible to draw some conclusions about the interplay between cell attachment and migration speed.

My hypothesis was that there was an optimal ligand density for cell migration, a density at which cell migration was fastest. If the density was too low, it would be difficult for cells to form new attachment points and migration would be slowed down. If the density was too high, cells might attach very firmly and form many attachment points, thus migration would be slowed down, as well. I thought it was a great idea and I was very curious to find out if there was such a relation. It was also at the intersection of the two things I had been working on so far, because it combined microfluidics and surface modifications. I was intrigued by the possibilities such multi-combinatorial gradients would offer not only for cell migration studies, but for defined cell microenvironments in general.

I was excited that I might had developed my first own scientific question. Such a relationship of cell migration speed and ligand density would not only be interesting from a basic cell biological point of view, but could also be useful for tailor-made tissue engineering scaffolds in the long run, where some areas would increase cell migration and others could limit cell migration. First however, I need to see if there was such a relation at all.

Cell migration and angiogenesis

BOX 4.3

Directed cell migration along chemo-attractant gradients plays an important role in many *in vivo* processes and is responsible for example for inflammatory cell invasion to sites of infection and is essential during wound healing [49]. One particular process of directed cell migration is angiogenesis [50], in which new blood capillaries are formed to reestablish or improve the blood circulation in a certain part of the body in response to e.g. low oxygen levels. Furthermore, it plays an important role in cancer biology where neovascularization facilitates cancer growth and progression, and will eventually lead to metastase formation [51], [52]. The process of endothelial cell migration is tightly controlled by many different factors including a varity of growth factors, integrins binding to specific substrates, matrix metalloproteinases, heparin sulfate proteoglycans and cell-surface receptor tyrosine kinases [21], [53], [54].

One particular powerful stimulant for endothelial cell migration is vascular endothelial growth factor (VEGF). Under normal conditions *in vivo*, VEGF is secreted by cells in response to low oxygen levels , leading to a series of actions. First, VEGF will diffuse out from the originating area in the tissue and thus create a concentration gradient of VEGF. Second, endothelial cells will migrate along the VEGF gradient and new blood vessels are formed. Third, the oxygen levels will normalize in the tissue area and VEGF secretion stops.

VEGF describes a family of structural related dimeric glycoprotein growth factors of approximately 40kDa and include VEGF-A, VEGF-B, VEGF-C, VEGF-D, VEGF-E and placental growth factor (PIGF) [Olsson 2006]. The different VEGF forms have overlapping but varying binding kinetics to the three tyrosine kinase receptors VEGFR-1, VEGFR-2 and VEGFR-3. Additionally, the binding properties are further modified by neuropilins (NRP1 and NRP2) co-receptors that enhance and modulate the binding affinities of the different VEGF forms to the corresponding tyrosine kinase receptors [50], [55].

The most potent stimuli for endothelial cell migration is through binding of VEGF-A to VEGFR-2, despite the fact that VEGF-A is binding to VEGFR-1 with a ten-fold higher affinity than to VEGFR-2 the cell internal signal through tyrosine phosphorylation is much stronger for VEGFR-2 binding. It was therefore suggested that VEGFR-1 might act like a sink for VEGF-A and thus modulate the amount which can bind to VEGFR-2 and eventually modify cell migration speed [56].

VEGF-B on the other hand is considered to play a crucial role predominantly in myocardiac development and coronary vascularization by binding both to VEGFR-1 and NRP1 co-receptor. Therefore, it might offer a potential candidate in growth factor therapy to stimulate neovascularization of the myocardium to minimize the effects of atherosclerosis. Besides its important function in the myocardium, VEGF-B can form heterodimers with VEGF-A and in this way change the availability of free VEGF-A, thus influence mitogenic activity [57].

During cell migration, a cell has a very high turnover rate of cell contacts with the underlying substrate, and forms mainly nascent adhesions and focal complexes, but not focal adhesion (see "BOX 1.3" on page 6 for details). Protrusions are formed by the cells via dynamic polymerization of actin fibers at the leading edge of the cell. A migrating cell has three different forms of actin organization: at the very front filopodia are probing

the surface, they are moved and stabilized by parallel actin bundles. Directly behind the filopodia is the sheet like lamellipodia with a dense and branched actin network. Spanning the rest of the cell from the front to the back are stress fibers, anti-parallel actin bundles with incorporated myosin II. The myosin II allows the cell to contract stress fibers and thereby move the back of the cell. During movement new focal complexes are formed at the leading edge and old focal complexes at the back get internalized by endocytosis and moved to the front for recycling. [21], [53], [54], [58–60]

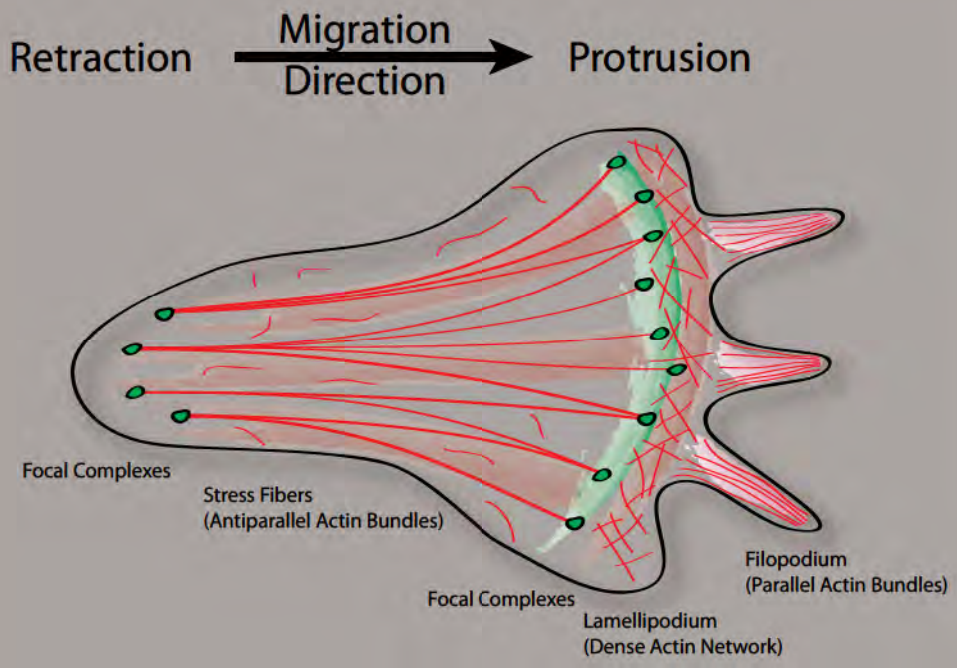

Figure 4.19
Schematic of a migrating cell showing the different cytoskeletal organizations and how a cell is able to move forward.

A master thesis project

I thought that this would be a perfect master thesis project; it was well defined with a clear hypothesis and a limited amount of work. The last part about the amount of work proved to be not entirely correct later. I discussed my idea with Julie and we put together a description for a Master thesis project that should start after the summer of 2011. The announcement went out at the beginning of June 2011, which was a little bit late since all the students were already on vacation. The single application that I got was from Elin Bernson, one of the students I had been supervising in the tissue engineering course during spring. I was very happy that she applied, I thought she was a great student and confident that she was a very good candidate for the project. Elin started after the summer in the beginning of September 2011 and we were both very excited and motivated, that the project finally started.

The aim of the master thesis project was to design a microfluidic gradient generator and characterize it both with fluid dynamics simulations, as well as with experiments. Furthermore, the integration of the gradient network with a suitable surface capable of presenting cells with a defined spacing of ligands in a gradient manner. The integration should be tested and the necessary surface functionalization steps tested and characterized. Depending on the time, initial cell experiment in the microfluidic chip should be carried out. It was a very ambiguous plan, but Elin was exactly the right person for the project.

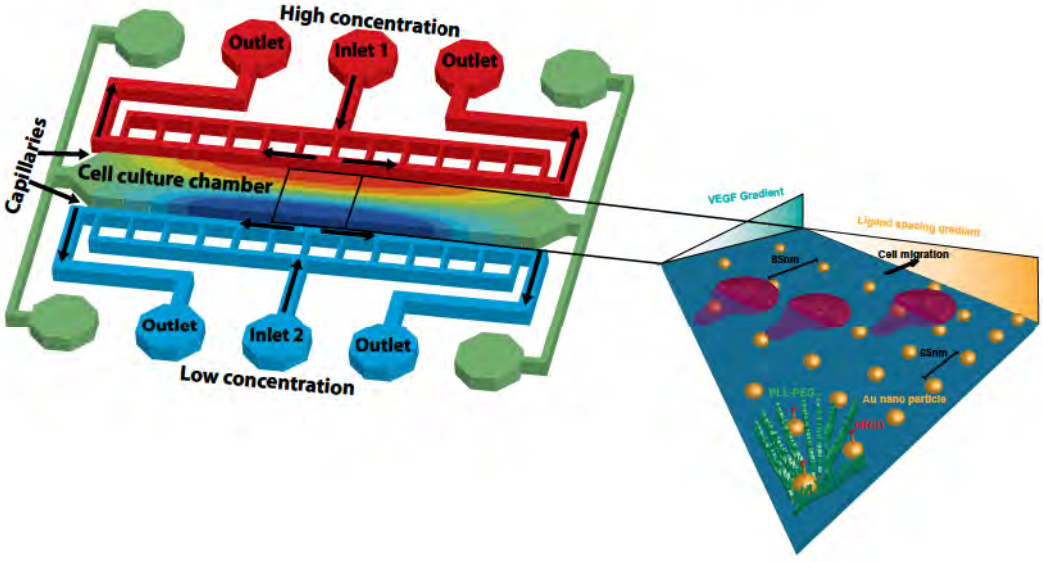

Figure 4.20
Schematic illustrating the idea for Elins master thesis project to look at cell migration speed dependance on ligand sapcing.

Diffusion based gradient generators

BOX 4.4

Diffusion based gradient generators use a different approach to from gradients than flow based gradient generators. They are solely based on diffusion and an equilibrium forming between two reservoirs. There is one reservoir with a high concentration of the molecules of interest, the soruce channel, and one reservoir without the molecule of interest filled with media. Both reservoirs are connected to a probing channel, where the gradient is formed. If the reservoirs are static a gradient would form, but it would not stabilize and eventually the entire system would equilibrate at a concentration of 50% from the original source concentration. In order to from stable gradients, the liquid in the source and sink channel needs to be exchanged continuously, as a consequence the source and sink concentration are stable and the equilibrium state is in the form of a gradient.[6]

There are different ways to connect the source and sink channels to the main probing channel to achieve stable conditions. One important fact that all of them have in common is that they ensure that the sink and source channel are hydrodynamically decoupled from the probing channel. This means that there is no convective flow from the source and sink channel into the main probing channel, and the gradient is formed by diffusion only. To fulfill this boundary condition, one can use for example very small channels for the connections [16], [17], [63]. A large difference in channel diameter will present a large hydrodynamic resistance and thus limit the fluid flow within the source and sink channel. Another approach is to use membranes or hydrogels as barriers to separate the compartments from each other [64–66]. In that case, it is important that the membrane or gel is permeable for the molecule of interest and calculations need to be carried out to estimate the time delay for the molecule to diffuse through the barrier.

The overall advantage of the diffusion based gradient generators is the ability to design systems which do not require constant liquid flow above the cells. In this way, it is possible to recreate chemo-attractant gradients that mimic conditions found *in vivo* and study their effect on cell migration without having any interrelated factors, such as shear stress attributed to flow above cells. Furthermore, it is in general possible to build more robust systems, because the entire liquid volume in the main chamber acts as a buffer. Even if there is a short disturbance of the liquid flow in the sink or source channel, it will not directly affect the gradient provided that the main chamber is sufficiently decoupled from the flow. Diffusion based gradient generators can also realized smaller than flow based gradient generators, because they do not require a large channel network to repetitively split and combine fluid streams. This allows integrating more gradient chambers on a single microfluidic chip and improves multiplexing approaches.

The disadvantage of this approach compared to flow based solutions are that the shape and steepness of gradients cannot easily be modified and are mainly intrinsic properties of the network design. Additionally, the gradient takes longer time to form and reach steady state, depending on the geometry and liquid volumes this can take up to a couple of hours. These factors are limiting diffusion based systems for studies of stable gradients over longer periods of time and where no fast temporal alteration of gradient properties is needed.

New gradient generator design

I knew that we would need a new microfluidic design to create a chemotractant gradient to stimulate cell migration, because the one that I had been working with before was not suitable for this project. There were a lot of reason for a new design, but most importantly the aim was to have a diffusion based gradient generator rather than the flow based one used in my previous study. The advantage of a diffusion based gradient generator (detailed description in "BOX 4.4" on page 126) is that there is no active flow within the main chamber where the cells are sitting. This is particular important for the culture of endothelial cells, because they are very shear stress sensitive [61] and even low flow speeds can stimulate them. Other researchers have actually been using various microfluidic designs to stimulate endothelial cells with fluid shear and showed that it is possible to enhance angiogenesis and microvessel formation with shear stress [62]. In our case, however, we wanted to investigate cell migration in response to a chemotractant gradient on a substrate with defined ligand spacing and therefore it was important to exclude any confounding factors like shear stress. Sarah Heilshorns group at Stanford had published a paper on endothelial cell migration in 2008, where they used a diffusion based gradient generator [17] and others had published different designs of diffusion based gradient generators for various applications [63–66].

We based our design on what Sarahs group had published previously, but changed it in some aspects. Elin and I had a lot of discussions at the beginning, and Figure 4.21 shows the boundary conditions that we came up with at the end. We felt that it was important to have a sufficiently large cell culture area, where cells could migrate over a distance of up to 2 millimeters and that was wide enough to cover the whole spacing gradient on the substrate (6-8 mm). Another important aspect that should be facilitated by the design was the ability to seed cells exclusively on one side of the channel and the ability to easily flush the main cell culture

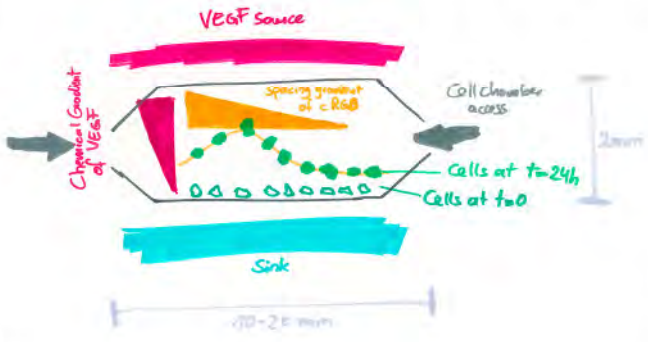

Figure 4.21
Scanned hand drawn sketch from the beginning of the project, describing the aim and boundary conditions for the microfluidic chip design

chamber, for example during fixation and staining procedures at the end of an experiment. I tried to integrate as much of the knowledge that I had gained from my first microfluidic design and microfluidic cell culture experiments, as possible, and Elin did a fantastic job of putting all those information together and designing the chip.

She tested a lot of different designs and systematically changed parameters like, inlet/outlet configuration and shape, channel height, channel length and capillary dimensions in a Comsol multiphysics model. The different designs were evaluated based on their ability to form soluble gradients at low flow rates (1-10 nl/s) and the steepness and linear portion of the gradient were measured at different positions along the channel. Based on the results from those simulations, we decided on the final design shown in Figure 4.22. Additional simulations were carried out to further characterize the system, a wide range of flow rates was tested, the time to reach a stable gradient and shear stress profiles were calculated, and the clearance of molecules of different size from the cell culture chamber were simulated. A detailed description of all simulation data is available in Elins Master Thesis [67].

In summary, the gradient shape depends on the flow rate and for slower flow rates it is more linear, but less steep than for higher flow rates. An optimum for our application is around 5 nl/s, for this flow rate the gradient is linear nearly through the whole cell culture chamber and still is spanning the whole concentration range from 0-100%. For this flow rate, it takes approximately 7.5

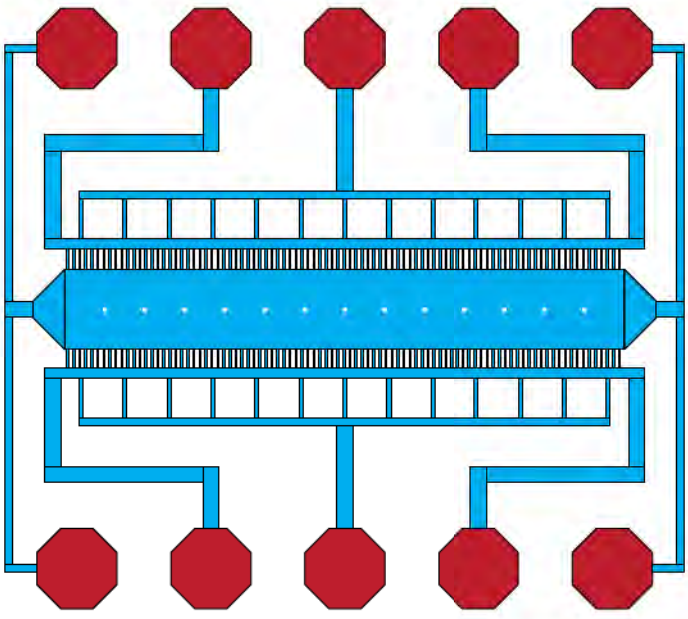

Figure 4.22
Final design for the diffusion based gradient generator with a large cell culture chamber in the center.

hours to reach a stable gradient, which is not considered a problem in our experimental setup, but needs to be considered when planning experiments. The clearance of molecules from the culture chamber is depending on their size and diffusion coefficient: Glucose (Mw=180 Da) 2.3 hours, Insulin (5.8 kDa) 3 hours, and Hyaluronan (3 MDa) 5 hours. As expected from the design, the shear stress in the main cell culture chamber was minimal, 3*10-7 dyne/cm2, and way below levels that have been shown to effect cells (3 dyne/cm2) [62].

After all the simulations, Elin and I thought that we had come up with a good design and were very curious to see if it would work in reality. By now, I had quite some experience in ordering masks from MC2 and everything worked without problems. We decided to place three exactly similar designs on one mask, so we would later have a master to produce three networks at the same time. Not being able to make several networks at once had been a bottleneck for me before and I was looking forward to improve this fact. The design of the new microfluidic network was different from the ones I had been using before, because it had two layers of different height. Thus, we needed two masks, but that was not a problem – the problems began during the fabrication of the SU-8 master.

Francesco Mazzotta (PhD student at Biological Physics) helped us with the fabrication of the SU-8 master in the clean room. The master for this microfluidic network did not only have two layers, but the second layer needed to be quite thick (150 micrometer). I specially ordered a different kind of SU-8 photo resist (SU-8 2150, MicroChem, USA) that could be spun directly in a single step to reach that thickness, but it was very difficult to work with, Francesco told me. There were air bubbles in the spin-coated layer all the time and it was nearly impossible to remove them. Therefore, we changed strategy and Francesco used the normal SU-8 (SU-8 2035, MicroChem, USA) and spun in total three layers, a first layer with the capillaries and a second and third layer for the sink, source and main channel. The final thickness of the capillaries was 50 micrometer and 200 micrometer for the other channels. Francesco put a lot of effort into producing those masters and there were quite a few problems at the beginning, but in the end it worked and I highly appreciate Francescos help.

Once the master was ready, Elin and I produced the first microfluidic chips in PDMS and bonded them on normal glass slides for evaluation. We used a different approach for connecting tubes to the inlets of the system than we had previously done. Instead of gluing small tubes on each inlet and outlet, we bonded a second thicker piece of PDMS directly over the part of the chip were the

inlets were located. After punching holes through both PDMS layers, we were able to attach the Teflon tubes from the pumps directly. This approach was much more practical and less time consuming than the previous way.

I was as excited as before, when I tested the flow based gradient system for the first time, and Elin was also curious to know if the system would work. This time, it was not an option to use a syringe for a quick test, due to the principle of the gradient generator, and we connected the chip directly to the pump setup. The difference with a diffusion based gradient generator compared to a flow based system is that it takes some time before the gradient is actually formed, so Elin and I were sitting in the lab and hoping that it would work. After a while, we begun to saw a gradient forming in the main channel, since the main chamber was quite big (2x14 millimeter), it was easy to see the gradient by eye. It looked great. In order to be able to image the gradient, we used a stereomicroscop at low magnification and attached a digital camera to it. It was clear that we would need a better setup that was capable of taking fluorescence images for later characterization, but at least we could take some first images. In the meantime, I got in contact with Zeiss and we got two different lenses, 2.5x and 5x magnification, to test if they were suitable for our purpose – we got both at the end. They were not only very useful for the characterization of gradient properties, but also proved valuable to take overview images of cells both in microfluidic channels, as well as petri dishes. Those images were an important step towards more quantitative cell experiments for us.

For the gradient characterization Elin used FITC-CM-Dextran (Sigma-Aldrich, USA) with a molecular weight of 40 kDa, which is similar to the size of VEGF (38.2 kDa) and thus as a similar diffusion coefficient. Figure 4.23 shows a fluorescence image that is stitched together from six individual micrographs. The line plots shown in Figure 4.23 demonstrate the linearity of the gradient and also a good correlation between the experimental and simulation data. The small differences between experiments and simulation could be due to small variations in the geometry of the PDMS, because the gradient shape is heavily relying on the geometry even minor deviations can cause a different shape. This could easily happen in the course of the production of the master, the PDMS molding or even during operation. PDMS is an elastic material and the main cell culture chamber is fairly large, which means that the roof could be deformed under the applied liquid pressure. This would explain the more ball shaped curves for the experimental data compared to the S-shaped curves from the simulation, because the deformation would be largest in the center and thus the intensity would increase in that area. Even though,

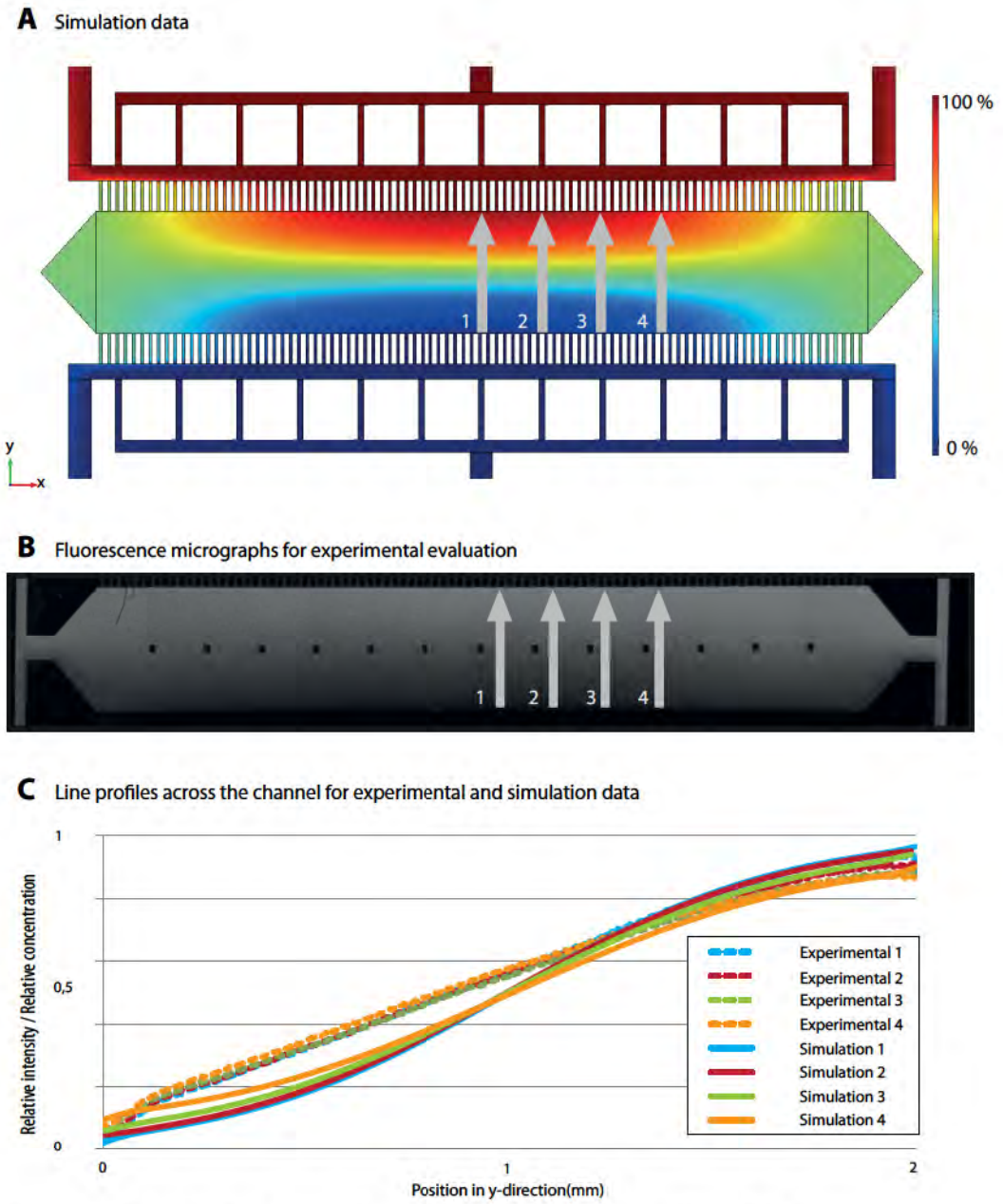

there was a slight variation, Elin and I were very happy with the results. A linear gradient was forming in the channel, and it was definitely possible to predict gradient properties from the simulations. After successful characterization, we were ready to move on.

Figure 4.23
Diffusion based gradient chip characeterization. (A) Simulation data showing the color coded concentration. (B) Fluorescence micrographs stitched together showing a FITC-dextran gradient. (C) Line profiles across the channel comparing simulation and experimental data.

Surface chemistry and cell experiments

With the microfluidic part covered, we needed a suitable substrate to provide the second gradient immobilized to the surface and perpendicular to the soluble one. The surfaces that ClineTechnologies could produce for us did not really work for our application, thus we needed to find something else. After some literature research I found a paper published in 2008 by Marco Arnold et al. from Joachim Spatzs group [68], where they described a modification of their standard technique (see "BOX 2.2" on page 26) to form nanoparticle spacing gradients instead of substrates with single spacings. This was great, because Joachim and we were still working on the same European projects and to study HUVEC cell migration on those substrates would be a very nice contribution to NanoCARD (page 14). I got in contact with Joachim and he told me that Vera Hirschfeld-Warneken was working with those gradient substrates and that she could provide us some without problems. So, we had great substrates to work with and everything turned out even better than anticipated during the first planning phase.

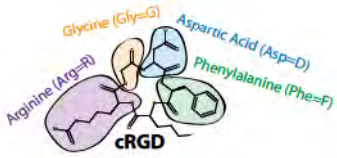

In order to be able to study cell migration speed dependence on ligand spacing, we also needed to have suitable surface chemistry. The gold nano dot spacing gradients provided a good material contrast, gold and glass, and Joachim's group had developed different surface functionalization protocols for this surfaces. The idea was to couple a cRGD peptide to the gold nano dots and then passivate the surrounding glass with PLL-PEG. It is necessary to passivate the glass, because otherwise proteins will adsorb on it and cells will be able to attach to the surface in between the gold nano dots. This needed to be avoided to be able to study the effect of the spacing gradients. Furthermore, it was important that the cRGD peptide was accessible for the cells; therefore, it was necessary to have a spacer sequence so the peptide would stick out from the PLL-PEG passivation layer. At the end, we used a cRGD peptide coupled to a thiol linker via a spacer with 15 polyethylene glycol (PEG) units which we got from Joachim's group. To prepare the surfaces, they were incubated with peptide solution (cRGD T3, 25 µg/ml) for 2 hours, repetitively rinsed with sterile milliQ water and kept in milliQ overnight. Afterwards, the remaining surface was passivated with PLL-PEG (10 µg/ml, PLL(20)-[3,5]-PEG(2), SuSoS, Switzerland) for 1 hour and washed with PBS. Elin and I got a lot of help regarding the protocol from the people in Stuttgart and it was very interesting to learn all the details about different spacer lengths and passivation procedures.

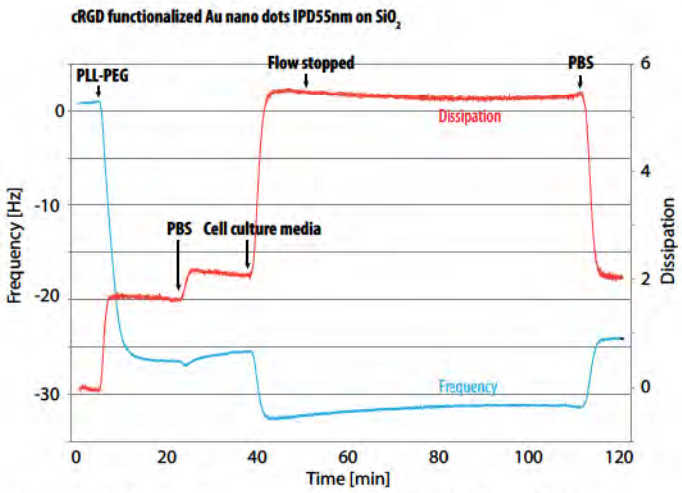

Figure 4.24
QCM-D data showing the passivation of a cRGD functionalized gold nano substrate with PLL-PEG and subsequent testing with complete cell culture media.

Once we had a working protocol, Elin tested the surface chemistry both with QCM-D (see "BOX 2.3" on page 29) and cell attachment studies. The QCM-D measurements shown in Figure 4.24 proved that all the different functionalization steps worked and that the resulting surface was inert to protein adsorption. The frequency and dissipation shift after injecting cell media is transient and there is no permanent deposition as the signals return to their original values after rinsing. For the cell attachment study, cells were seeded on the prepared surfaces and cultured for 24 hours before being fixed and stained. We used skeletal muscle progenitor cells (C2C12) for this study, because we did not have endothelial cells in culture at that time. Even thought, we wanted to work with endothelial cells later, it should be ok to test the surface functionalization with a different cell type - not optimal but sufficient, because initial cell attachment is similar between most cell types and nearly all cells have receptors for the cRGD sequence [49]. Figure 4.25 shows the analyzed cell count data. Cells are able to attach to gold nano dot substrates functionalized with cRGD and passivated with PLL-PEG slightly better than to

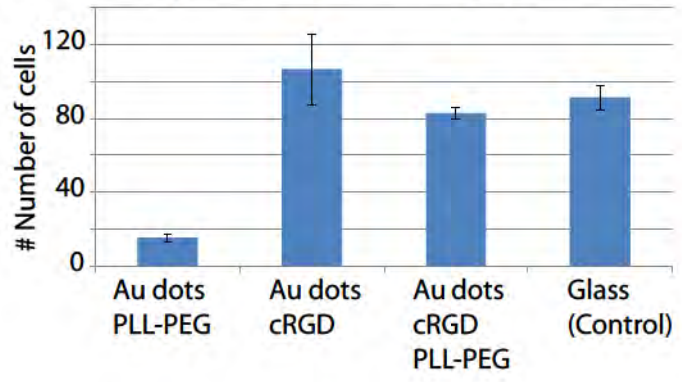

Figure 4.25
Number of cells for the different surface modifications and a glass control sample. Much less cells adhere to Au nano dots only coated with PLL-PEG as expected.

glass control surfaces. Taking away the PLL-PEG passivation does little for cell attachment, but it can be assumed that these cells are not experiencing the same defined ligand spacing as without the passivation. Without the cRGD peptide on the other hand, cell attachment was inhibited and the number of adherent cells is significantly lower. When Elin showed me the results, I was very happy; it looked like everything was working and that we could use this functionalization protocol for our experiments.

Now that all the parts were ready, Elin and I were both eager to see if everything worked together, to run the real cell migration experiments and test my hypothesis. In the meantime, Elin had developed a way to seed cells selectively on one side of the main microfluidic chamber, as shown in Figure 4.26. This was achieved by injecting the cells with the pumps and use hydrodynamic focusing to push them to one side; the principle is depicted in Figure 4.26.This was a great advantage over the way Sarah Heilshorns group had seeded and analyzed their samples. Instead of seeing a relative increase of cells at the higher concentration of the gradient, we were now able to exclusively have cells where the concentration was lower and directly follow cells migrating from there. This would make analysis much easier and more robust later on, because the starting conditions were better defined.

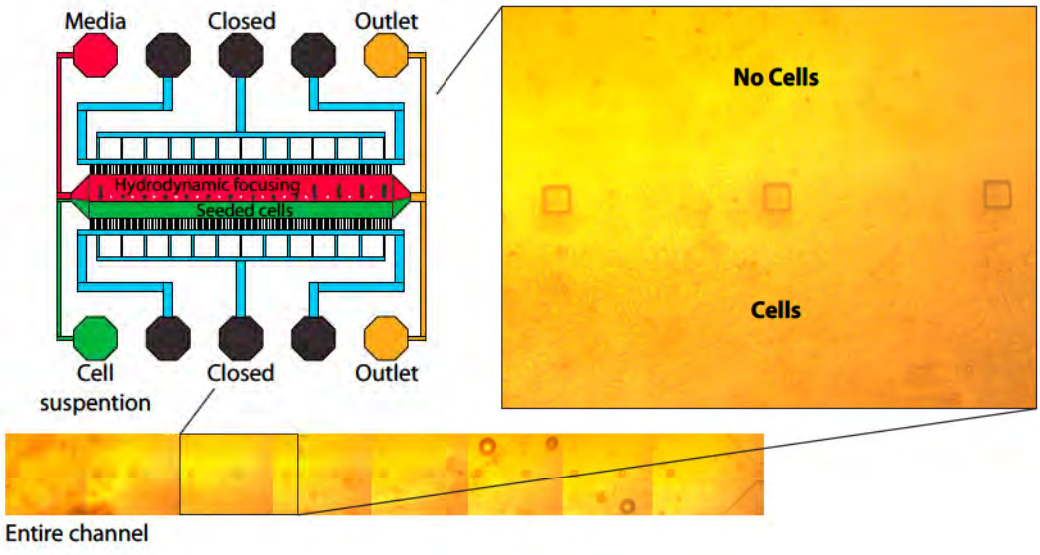

Figure 4.26
(TOP LEFT) Schematic of the process to selectively seed cells on one side of the channel by hydrodynamical focusing the cell suspension. (TOP RIGHT) Micrograph of attched cells after 24 hours in the channel, cells are nearly exclusively present in the lower half of the channel. (BOTTOM) Overview of the entire channel.

When we did the first cell experiments there was however a problem, we just did not see any cell migration. We used similar gradient conditions as other before, but there was no response of the cells to the VEGF gradient. Elin did run experiments both on the functionalized gold nano dot samples, as well as on plain glass substrates coated with collagen; the results were the same. The cells were surviving in the channels and we were able to maintain than for up to 96 hours, but we could not observe any migration even for those extended periods of time. We started to look into possible reasons for this problem from the cells over the VEGF to the gradient. The cells that we use are human umbilical vein endothelial cells (HUVEC) from Cell Applications Inc. and they are pre-screened to have VEGF-A receptors. Thus, we did not suspect the cells to be the problem, but Elin defrosted new cells to see if that would make a difference, without any success. She even repeated some of the gradient characterization measurements, but the results were similar to the ones before. There should be a stable VEGF gradient forming that is similar to the ones others had used. The only thing left is the VEGF itself, we have not tested this yet, but we are going to order a new vial of VEGF. It could be that the VEGF got inactivated, destroyed or for other reasons does not function any longer as it is supposed to do. I really hope we will be able to solve this problem soon, since everything else is ready and I want to know if there is a relation between ligand spacing and migration speed.

In-depth simulation study of VEGF

During the time Elin was focusing on the cell experiments and optimizing the surface functionalization procedure, I was working on a new simulation model of the diffusion based gradient generator. I thought it would be interesting to extend the model that we had used so far and simulate both the gradient formation in the microfluidic network and the binding of molecules to their cell receptors. I was wondering if the chemical gradient that we simulated was really what the cells was experiencing, how they would interact with the gradient and if the binding of VEGF to cells would influence the gradient shape. When we started to see the problems with the cell experiments and were unable to observe cell migration, I thought that this new model might even help to explore these problems and to find the reason why our cells were not migrating.

The model that I developed is described in detail in Paper II (page 171). The idea was to add a surface reaction and thereby modeling VEGF binding to its receptor. This reaction was limited to an entity in the channel representing a cell. I wanted to maintain the ability to simulate the liquid composition and flow behavior in the entire microfluidic network and just add an additional layer. Fortunately, this is one of the advantages of Comsol Multiphysics simulation environment and it is possible to add modules with different physical phenomena to existing models. So, I added a surface reaction model and coupled it to the VEGF concentration via the binding and dissociation rate given in:

$$r_{on} = k_{on} \cdot c_{VEGF} \cdot VEGFR_{free} \cdot VEGFR_{density}$$
$$r_{off} = k_{off} \cdot VEGFR_{bound} \cdot VEGFR_{density}$$

The effects of VEGF on endothelial cell stimulation and its binding kinetics have been intensively studied both experimentally and theoretically, thus it was possible to get suitable model parameters from literature (Table 4.1). In theoretical approaches, the binding of VEGF to its receptors had mainly been modeled in Monte-Carlo simulations [50], [55], with a focus on the competitive binding of different VEGF isoforms to different receptors. I was not so much interested in the details of the binding kinetics in complex systems with many receptors, but rather wanted to know if a cell in our channel would sense a significant difference in concentration from its front to its back. In order for a cell to be able to response to a gradient, it needs to sense it, and therefore it is essential that there is a difference in concentration over the cell surface. With my model I was able to simulate the entire system, from how the gradient is formed to how it is sensed by the cell.

Parameter	Value	Unit	Description
c_{VEGF}	calculated	mol/m^3	VEGF concentration in solution
$c_{VEGF\ t=0}$	0	mol/m^3	VEGF concentration in the network at t=0
$c_{VEGF\ inlet\ 1}$	$1.25 \cdot 10^{-5}$ – $1.25 \cdot 10^{-8}$	mol/m^3	VEGF concentration at inlet 1 (parametric sweep)
cs_{VEGF}	calculated	mol/m^2	VEGF concentation bound to the surface
$cs_{VEGF\ t=0}$	0	mol/m^2	VEGF concentation bound to the surface at t=0
$VEGFR_{density}$	$3.4 \cdot 10^{-9}$	mol/m^2	VEGF receptor density [50]
$VEGFR_{free}$	calculated	Ratio 0-1	Ratio of free VEGF receptors
$VEGFR_{bound}$	calculated	Ratio 0-1	Ratio of bound VEGF receptors
u_{inlets}	$6.25 \cdot 10^{-5}$	m/s	Flow velocity at inlet 1 & 2
D_{VEGF}	$2 \cdot 10^{-6}$	cm^2/s	VEGF diffusion constant [50]
k_{on}	$3.6 \cdot 10^{6}$	L/mol·s	Association rate constant VEGF-VEGFR [50]
k_{off}	$2 \cdot 10^{-6}$	1/s	Dissociation rate constant VEGF-VEGFR [50]
$Cell_{position-y}$	-800 -400 0 400 800	µm (from the center of the channel)	Cell position in y-direction (parametric sweep in study)

Table 4.1
Summary of all parameters used for the simulation of VEGF binding to its cell receptor.

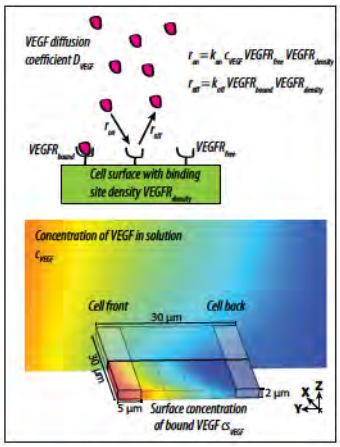

Figure 4.27
Schematic of the simulation model showing the surface reaction (TOP) and the cell geometry (BOTTOM).

This is not very common, because either people look at the gradient formation or at the cell interactions.

In brief, the results clearly show that there is a large difference between a soluble gradient simulated without cells and how a gradient is sensed by cells. It is not possible to assume how a cell will perceive the gradient from simple simulations only including the gradient formation; the gradient is not directly imprinted onto the cell. The cell is rather acting as a local sink for VEGF and changes the gradient in solution in its close proximity. The size of this local depletion is depending on the inlet concentration, for low concentrations (10^{-8} mol/m3) it is extending nearly 100 micrometer in all directions. Local depletion is also affecting the difference in VEGF bound receptors between the front and the back of a cell. There are two different effects to consider here: saturation of the receptors for high concentrations and depletion for low concentrations. If the receptors get saturated at high concentrations, there is no big difference between the front and the back of the cell, because all receptors are occupied. If the concentration is very low, there are too few molecules and the local depletion will disturb the gradient so much that it will disappear

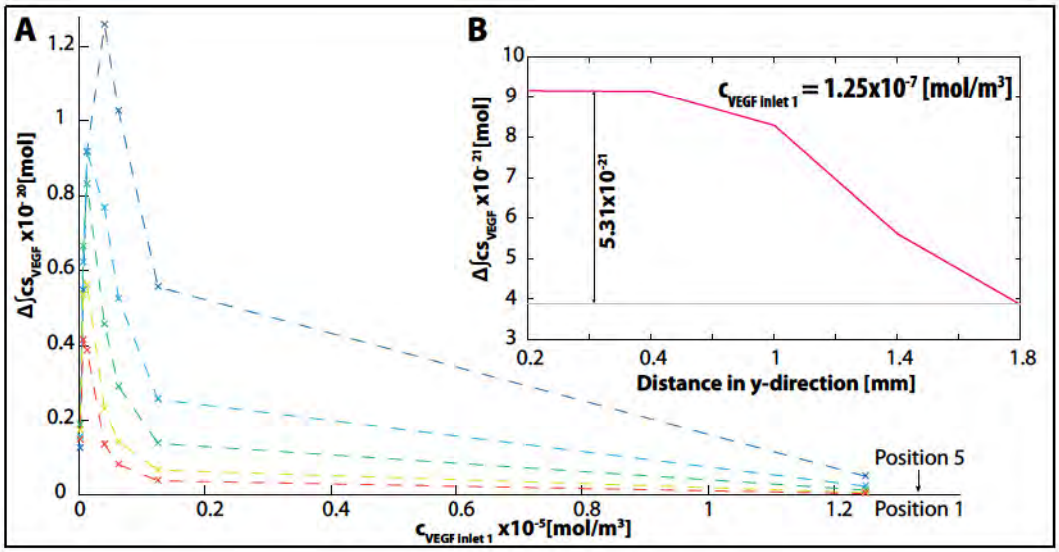

Figure 4.28
Simulation data showing the difference between the front and the back of a cell in relation to the inlet concentration. The inlet shows the delta against the position across the channel (0mm = at the sink channel)

directly above the cell and thus there is no gradient over the cell surface. This is shown in Figure 4.28 where inlet concentration is plotted against the difference between the front and the back of a cell at different positions (position 1: near to the source channel and position 5: near to the sink channel). These leads to the conclusion that there is an optimal inlet concentration for which the difference between the front and the back of a cell is maximal, for my simulation conditions this is the case for an inlet concentration of $2x10^{-7}$. This concentration is around one magnitude lower than the one that we used for experiments so far.

Furthermore, the concentration at different positions along the channel varies, as intended by the gradient formed in the cell culture chamber, but his means that the difference between front and back is not equal for all positions. It varies with position. This was something that we had not expected before. We were assuming that a linear gradient would result in a constant delta over the cell and that each cell would be stimulated similar independent of its position. This is clearly not the case and the new simulation model allows us to explore the different implications of receptor saturation and local depletion in great detail.

It is, however, important to note that the model is not taking all aspects of the VEGF signaling system into consideration. It does not incorporate other receptors or isoforms binding to each other and other possible local sinks of VEGF. Therefore, it is not possible to directly predict if a lower concentration will work better, but at least it gives some idea about the way a cell is sensing the gradient and how the different parameters will change the perception.

[1] S. Boyden, "The chemotactic effect of mixtures of antibody and antigen on polymorphonuclear leucocytes.," The Journal of experimental medicine, vol. 115, pp. 453-66, Mar. 1962.

[2] S. H. Zigmond, "Orientation chamber in chemotaxis.," Methods in enzymology, vol. 162, pp. 65-72, Jan. 1988.

[3] D. Zicha, G. A. Dunn, and A. F. Brown, "A new direct-viewing chemotaxis chamber.," Journal of cell science, vol. 99 (Pt 4), pp. 769-75, Aug. 1991.

[4] J. Li and F. Lin, "Microfluidic devices for studying chemotaxis and electrotaxis.," Trends in cell biology, vol. 21, no. 8, pp. 489-497, Jun. 2011.

[5] I. Meyvantsson and D. J. Beebe, "Cell Culture Models in Microfluidic Systems," Annual Review of Analytical Chemistry (2008), vol. 1, no. 1, pp. 423-449, Jul. 2008.

[6] S. Kim, H. J. Kim, and N. L. Jeon, "Biological applications of microfluidic gradient devices.," Integrative biology : quantitative biosciences from nano to macro, vol. 2, no. 11–12, pp. 584-603, Nov. 2010.

[7] T. M. Keenan and A. Folch, "Biomolecular gradients in cell culture systems.," Lab on a chip, vol. 8, no. 1, pp. 34-57, Jan. 2008.

[8] B. Heit and P. Kubes, "Measuring chemotaxis and chemokinesis: the under-agarose cell migration assay.," Science's STKE : signal transduction knowledge environment, vol. 2003, no. 170, p. PL5, Feb. 2003.

[9] H. Wiggins and J. Rappoport, "An agarose spot assay for chemotactic invasion.," BioTechniques, vol. 48, no. 2, pp. 121-4, Feb. 2010.

[10] D. Amarie, J. a Glazier, and S. C. Jacobson, "Compact microfluidic structures for generating spatial and temporal gradients.," Analytical chemistry, vol. 79, no. 24, pp. 9471-7, Dec. 2007.

[11] D. Irimia, D. a Geba, and M. Toner, "Universal microfluidic gradient generator.," Analytical chemistry, vol. 78, no. 10, pp. 3472-7, May 2006.

[12] T. Kang, J. Han, and K. S. Lee, "Concentration gradient generator using a convective-diffusive balance.," Lab on a chip, vol. 8, no. 7, pp. 1220-2, 2008.

[13] F. Lin, W. Saadi, S. W. Rhee, S.-J. Wang, S. Mittal, and N. L. Jeon, "Generation of dynamic temporal and spatial concentration gradients using microfluidic devices.," Lab on a chip, vol. 4, no. 3, pp. 164-7, Jun. 2004.

[14] A. Tirella, M. Marano, F. Vozzi, and A. Ahluwalia, "A microfluidic gradient maker for toxicity testing of bupivacaine and lidocaine.," Toxicology in vitro : an international journal published in association with BIBRA, vol. 22, no. 8, pp. 1957-64, Dec. 2008.

[15] X. Jiang, Q. Xu, S. K. W. Dertinger, A. D. Stroock, T.-M. Fu, and G. M. Whitesides, "A general method for patterning gradients of biomolecules on surfaces using microfluidic networks.," Analytical chemistry, vol. 77, no. 8, pp. 2338-47, Apr. 2005.

[16] E. Cimetta et al., "Microfluidic device generating stable concentration gradients for long term cell culture: application to Wnt3a regulation of catenin signaling.," Lab on a chip, vol. 10, no.

23, pp. 3277-83, Dec. 2010.

[17] A. Shamloo, N. Ma, M.-M. Poo, L. L. Sohn, and S. C. Heilshorn, "Endothelial cell polarization and chemotaxis in a microfluidic device.," Lab on a chip, vol. 8, no. 8, pp. 1292-9, Aug. 2008.

[18] T. Squires and S. Quake, "Microfluidics: Fluid physics at the nanoliter scale," Reviews of Modern Physics, vol. 77, no. 3, pp. 977-1026, Oct. 2005.

[19] O. Marín, M. Valiente, X. Ge, and L.-H. Tsai, "Guiding neuronal cell migrations.," Cold Spring Harbor perspectives in biology, vol. 2, no. 2, p. a001834, Feb. 2010.

[20] M. Valiente and O. Marín, "Neuronal migration mechanisms in development and disease.," Current opinion in neurobiology, vol. 20, no. 1, pp. 68-78, Feb. 2010.

[21] R. J. Petrie, A. D. Doyle, and K. M. Yamada, "Random versus directionally persistent cell migration.," Nature reviews. Molecular cell biology, vol. 10, no. 8, pp. 538-49, Aug. 2009.

[22] M. E. Hatten, "Riding the glial monorail: A common mechanism for glialguided neuronal migration in different regions of the developing mammalian brain," Trends in Neurosciences, vol. 13, no. 5, pp. 179-184, May 1990.

[23] E. Schnell et al., "Guidance of glial cell migration and axonal growth on electrospun nanofibers of poly-epsilon-caprolactone and a collagen/poly-epsilon-caprolactone blend.," Biomaterials, vol. 28, no. 19, pp. 3012-25, Jul. 2007.

[24] J. Xie, M. R. MacEwan, A. G. Schwartz, and Y. Xia, "Electrospun nanofibers for neural tissue engineering.," Nanoscale, vol. 2, no. 1, pp. 35-44, Jan. 2010.

[25] S. H. Lim, X. Y. Liu, H. Song, K. J. Yarema, and H.-Q. Mao, "The effect of nanofiber-guided cell alignment on the preferential differentiation of neural stem cells.," Biomaterials, pp. 1-9, Aug. 2010.

[26] J. L. Goldberg, "How does an axon grow?," Genes & development, vol. 17, no. 8, pp. 941-58, Apr. 2003.

[27] D. J. Solecki, "Sticky situations: recent advances in control of cell adhesion during neuronal migration.," Current opinion in neurobiology, pp. 1-8, May 2012.

[28] J. Imitola et al., "Directed migration of neural stem cells to sites of CNS injury by the stromal cell-derived factor 1alpha/CXC chemokine receptor 4 pathway.," Proceedings of the National Academy of Sciences of the United States of America, vol. 101, no. 52, pp. 18117-22, Dec. 2004.

[29] N. L. Jeon, S. K. W. Dertinger, D. T. Chiu, I. S. Choi, A. D. Stroock, and G. M. Whitesides, "Generation of Solution and Surface Gradients Using Microfluidic Systems," Langmuir, vol. 16, no. 22, pp. 8311-8316, Oct. 2000.

[30] S. K. W. Dertinger, D. T. Chiu, N. L. Jeon, and G. M. Whitesides, "Generation of Gradients Having Complex Shapes Using Microfluidic Networks," Analytical Chemistry, vol. 73, no. 6, pp. 1240-1246, Mar. 2001.

[31] K. Campbell and A. Groisman, "Generation of complex concentration profiles in microchannels in a logarithmically small number of steps.," Lab on a chip, vol. 7, no. 2, pp. 264-72, Feb.

2007.

[32] K.-J. Bathe, Finite Element Method. Wiley Encyclopedia of Computer Science and Engineering, 2008.

[33] R. Söderlund, "Finite Element Methods for Multiscale / Multiphysics Problems," Umeå University, 2011.

[34] W. B. J. Zimmerman, Multiphysics Modeling With Finite Element Methods. London: World Scientific, 2006, p. 432.

[35] F. S. Ligler, "Perspective on optical biosensors and integrated sensor systems.," Analytical chemistry, vol. 81, no. 2, pp. 519-26, Jan. 2009.

[36] J. P. Golden and F. S. Ligler, "A comparison of imaging methods for use in an array biosensor.," Biosensors & bioelectronics, vol. 17, no. 9, pp. 719-25, Sep. 2002.

[37] D. Litwilller, "CCD vs . CMOS : Facts and Ficition," 2001.

[38] J. Melin and S. R. Quake, "Microfluidic large-scale integration: the evolution of design rules for biological automation.," Annual review of biophysics and biomolecular structure, vol. 36, pp. 213-31, 2007.

[39] B. Carlberg, T. Wang, and J. Liu, "Direct photolithographic patterning of electrospun films for defined nanofibrillar microarchitectures.," Langmuir, vol. 26, no. 4, pp. 2235-9, Feb. 2010.

[40] E. Jo, M.-C. Lim, H.-N. Kim, H.-J. Paik, Y.-R. Kim, and U. Jeong, "Microfluidic channels fabricated on mesoporous electrospun fiber mats: A facile route to microfluidic chips," Journal of Polymer Science Part B: Polymer Physics, vol. 49, no. 2, pp. 89-95, Jan. 2011.

[41] Y. Liu, D. Yang, T. Yu, and X. Jiang, "Incorporation of electrospun nanofibrous PVDF membranes into a microfluidic chip assembled by PDMS and scotch tape for immunoassays.," Electrophoresis, vol. 30, no. 18, pp. 3269-75, Sep. 2009.

[42] D. Yang et al., "Electrospun Nanofibrous Membranes: A Novel Solid Substrate for Microfluidic Immunoassays for HIV," Advanced Materials, vol. 20, no. 24, pp. 4770-4775, Dec. 2008.

[43] J. C. McDonald and G. M. Whitesides, "Poly(dimethylsiloxane) as a material for fabricating microfluidic devices.," Accounts of chemical research, vol. 35, no. 7, pp. 491-9, Jul. 2002.

[44] C. Christophis, M. Grunze, and A. Rosenhahn, "Quantification of the adhesion strength of fibroblast cells on ethylene glycol terminated self-assembled monolayers by a microfluidic shear force assay.," Physical chemistry chemical physics : PCCP, vol. 12, no. 17, pp. 4498-504, May 2010.

[45] H. Lu, L. Y. Koo, W. M. Wang, D. a Lauffenburger, L. G. Griffith, and K. F. Jensen, "Microfluidic shear devices for quantitative analysis of cell adhesion.," Analytical chemistry, vol. 76, no. 18, pp. 5257-64, Sep. 2004.

[46] P. Wallin, C. Zandén, B. Carlberg, J. Liu, and J. Gold, "Patterned electrospun microfibers integrated in a microfluidics system to study cells in complex microenvironments," in Lab on a chip Worldcongress, 2011.

[47] A. O. Lundgren, F. Björefors, L. G. M. Olofsson, and H. Elwing, "Self-arrangement

among charge-stabilized gold nanoparticles on a dithiothreitol reactivated octanedithiol monolayer.," Nano letters, vol. 8, no. 11, pp. 3989-92, Nov. 2008.

[48] S. K. W. Dertinger, X. Jiang, Z. Li, V. N. Murthy, and G. M. Whitesides, "Gradients of substrate-bound laminin orient axonal specification of neurons.," Proceedings of the National Academy of Sciences of the United States of America, vol. 99, no. 20, pp. 12542-7, Oct. 2002.

[49] B. Alberts, A. Johnson, J. Lewis, M. Raff, K. Roberts, and P. Walter, Molecular Biology of the Cell, 5th ed. New York: Garland Science, 2007.

[50] F. Mac Gabhann and A. S. Popel, "Interactions of VEGF isoforms with VEGFR-1, VEGFR-2, and neuropilin in vivo: a computational model of human skeletal muscle.," American journal of physiology. Heart and circulatory physiology, vol. 292, no. 1, pp. H459-74, Jan. 2007.

[51] T. Bogenrieder and M. Herlyn, "Axis of evil: molecular mechanisms of cancer metastasis.," Oncogene, vol. 22, no. 42, pp. 6524-36, Sep. 2003.

[52] R. Leite de Oliveira, A. Hamm, and M. Mazzone, "Growing tumor vessels: More than one way to skin a cat - Implications for angiogenesis targeted cancer therapies.," Molecular aspects of medicine, vol. 32, no. 2, pp. 71-87, Apr. 2011.

[53] S. Kanda, Y. Miyata, and H. Kanetake, "Role of focal adhesion formation in migration and morphogenesis of endothelial cells.," Cellular signalling, vol. 16, no. 11, pp. 1273-81, Nov. 2004.

[54] D. a Lauffenburger and a F. Horwitz, "Cell migration: a physically integrated molecular process.," Cell, vol. 84, no. 3, pp. 359-69, Feb. 1996.

[55] F. Mac Gabhann, M. T. Yang, and A. S. Popel, "Monte Carlo simulations of VEGF binding to cell surface receptors in vitro.," Biochimica et biophysica acta, vol. 1746, no. 2, pp. 95-107, Dec. 2005.

[56] J. C. Chappell, S. M. Taylor, N. Ferrara, and V. L. Bautch, "Local guidance of emerging vessel sprouts requires soluble Flt-1.," Developmental cell, vol. 17, no. 3, pp. 377-86, Sep. 2009.

[57] D. Bellomo et al., "Mice Lacking the Vascular Endothelial Growth Factor-B Gene (Vegfb) Have Smaller Hearts, Dysfunctional Coronary Vasculature, and Impaired Recovery From Cardiac Ischemia," Circulation Research, vol. 86, no. 2, p. e29-e35, Feb. 2000.

[58] C. M. Consortium, "Cell Migration Gateway," EISSN: 1747-7883, 2012. [Online]. Available: http://www.cellmigration.org/. [Accessed: 10-Aug-2012].

[59] A. J. Ridley et al., "Cell migration: integrating signals from front to back.," Science (New York, N.Y.), vol. 302, no. 5651, pp. 1704-9, Dec. 2003.

[60] D. Vignjevic and G. Montagnac, "Reorganisation of the dendritic actin network during cancer cell migration and invasion.," Seminars in cancer biology, vol. 18, no. 1, pp. 12-22, Feb. 2008.

[61] O. Traub and B. C. Berk, "Laminar Shear Stress : Mechanisms by Which Endothelial Cells Transduce an Atheroprotective Force," Arteriosclerosis, Thrombosis, and Vascular Biology, vol. 18, no. 5, pp. 677-685, May 1998.

[62] A. Ueda, M. Koga, M. Ikeda, S. Kudo, and K. Tanishita, "Effect of shear stress on microves-

sel network formation of endothelial cells with in vitro three-dimensional model.," American journal of physiology. Heart and circulatory physiology, vol. 287, no. 3, pp. H994-1002, Sep. 2004.

[63] J. Atencia, G. a Cooksey, and L. E. Locascio, "A robust diffusion-based gradient generator for dynamic cell assays.," Lab on a chip, no. i, Nov. 2011.

[64] D. Kim, M. a Lokuta, A. Huttenlocher, and D. J. Beebe, "Selective and tunable gradient device for cell culture and chemotaxis study.," Lab on a chip, vol. 9, no. 12, pp. 1797-800, Jun. 2009.

[65] U. Haessler, Y. Kalinin, M. a Swartz, and M. Wu, "An agarose-based microfluidic platform with a gradient buffer for 3D chemotaxis studies.," Biomedical microdevices, vol. 11, no. 4, pp. 827-35, Aug. 2009.

[66] V. V. Abhyankar, M. a Lokuta, A. Huttenlocher, and D. J. Beebe, "Characterization of a membrane-based gradient generator for use in cell-signaling studies.," Lab on a chip, vol. 6, no. 3, pp. 389-93, Mar. 2006.

[67] E. Bernson, "Development of a Microfluidic Platform for Cell migration Studies along Gradients," Chalmers University of Technology, 2012.

[68] M. Arnold et al., "Induction of cell polarization and migration by a gradient of nanoscale variations in adhesive ligand spacing.," Nano letters, vol. 8, no. 7, pp. 2063-9, Jul. 2008.

Chapter 5

Improvements for the future

Contents

145 Chapter: 5 Improvements for the future

Many things have happened during the first half of my PhD studies and I explored a lot of different direction during the first two and a half years. Some experiments worked better than others and some approaches were published. All directions, from lipid tubes and cell culture on lipid bilayers over liquid handling and software programming to using microfluidics to create cell microenvironments and the simulation of those systems, have potential for continuation, but for me the most important part in the second half of my PhD education is to focus. I feel that I need to bundle my energy and effort more towards one direction, still allowing a little bit of flexibility. The most interesting part has been and still is the application of microfluidic networks and its combination with various scaffold materials to mimic cell microenvironments and control cell-liquid and cell-matrix interactions. This is what I want to focus on in the coming two and a half years.

I spent a lot of time on the development of a liquid handling system that is adjusted to my needs and I learned many things about cell culture in microfluidic systems. Now, I want to use and apply this expertise. There are, however, two development parts that I still want to finish. First, I want to rewrite the control application for the liquid handling system and use a state machine architecture to put it on a solid base for future users ("Liquid handling" on page 74). Second, I would like to finish the work on microfluidic valves actuated by braille pins ("Microfluidic valves" on page 87). The ability to integrate actuated valves into my microfluidic designs would be of high value and open new possibilities, I think. The development part will be done eventually, but the first thing that I am going to focus on straightaway are the experiments on cell migration dependence on ligand spacing.

Cell migration experiments

The cell migration experiments that Elin and I have been worked on for some time were a little delayed; we all had hoped to already have some results right now. The problem is that we are not 100% sure why we do not see cell migration at the moment. Elin has reevaluted the gradient generator and everything seems to be the way it should be. Experiments are currently ongoing to investigate if there is a problem with the VEGF molecule itself or with the cells that we have.

The aim of this study is still to study if there is a relation between cell attachment ligand density and migration speed. We want to use peptide functionalized gold nano dot substrates both with single spacings and with a gradient of different spacings to answer this question. Furthermore, it would be even interesting to look at different homogenous surface coating like collagen, fibronectin

and laminin, and compare if there is a difference in cell migration speed for these molecules. Thus, we would be able to show similar biological effects both for an artifical, well characterized substrates and on bilogical relevant surface modifications. Depending on the progress and the initial data, we also want to include experiments to look at the formation of cell focal adhesions for the different conditions in more detail. In this way, we would be able to gain a better inside of the underlying cell molecular mechanisms that govern cell migration.

Neurospheres in chemical gradients

I also want to use the diffusion based gradient generator (page 126) to investigate other biological questions. Together with Georg Kuhn and Nina Erkenstam, we have already started to look at the response of neurospheres to stromal cell-derived factor 1 alpha (SDF-1a) cytokine gradients. This is in some sense the continuation of the work presented in paper 1, but the focus will be on the chemical signaling without the combination of electrospun fibers. The advantages of the new diffusion based gradient generator are the larger dimensions and that there is no flow in the main culture chamber. The larger dimensions (200 micrometer high channels) allow the injection of whole neurospheres (150-300 micrometer in diameter) and thus we can study cells migrating out from a sphere in response to different stimuli. So far, Nina and I have been optimizing culture protocols and focused on the getting spheres into the channel, attaching and growing. This seems to work nicely now; Figure 5.1 shows neurospheres after 24 hours inside the main chamber of the diffusion based gradient chip. The cells are stained with a neural marker BETA-III tubulin in green and an astrocyte marker glial fibrillary acidic protein (GFAP) in red. The neurospheres are attached to the bottom of the microflu-

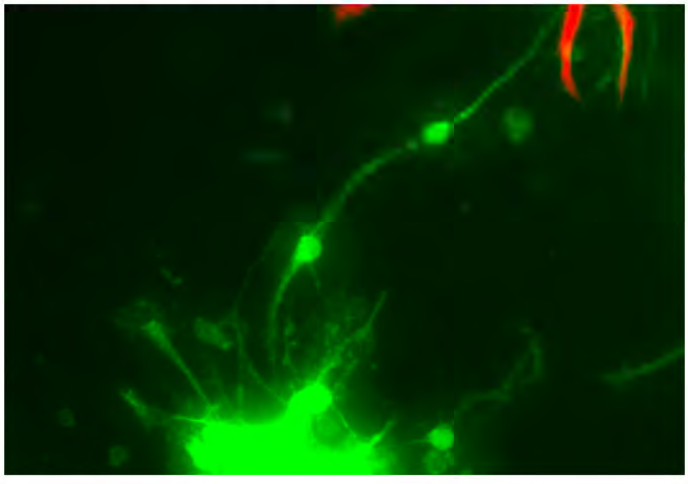

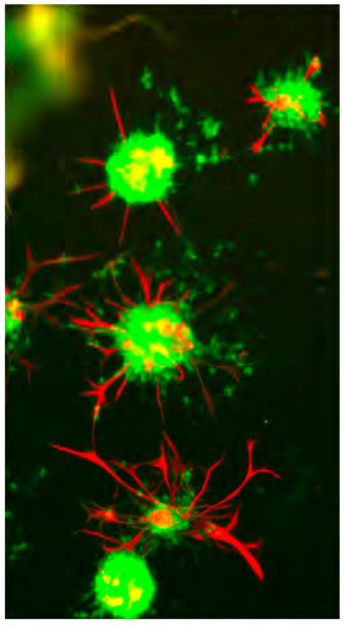

Figure 5.1
Fluorescence micrographs of neurospheres in microfluidic channels. Neurospheres were stained green for BETA-III Tubulin and red for GFAP. BETA-III Tubulin is a early neural marker and the image to the left shows two neurons that migrated out from the sphere. GFAP is a astrocyte marker. Cells were cultured for 24 hours in the diffusion gradient chip.

idic channel and look viable. It can be seen that some neurons are growing out from the spheres, as well as large astrocyte structures forming at the surface. This proves at least that neurospheres can be cultured within the microfluidic network, they are able to attach to the substrate, individual cells can migrate out from the sphere and overall cells survive in the system.

The current idea is to look at the effect of SDF-1a on the neurospheres, but there is also the possibility to use other neurotrophins like nerve growth factor (NGF) or brain-derived neurotrophic factor (BDNF). These could be either given separately or simultaneously, with gradients in the same or opposite directions. I am really looking forward to continue the collaboration with Georg and Nina, and hope that we are able to do some really interesting experiments together in the future.

Improving cell screening with gradients

Another interesting area would be to use microfluidic gradient generators for screening purposes. We have started to do some work together with Cellectris stem cells (formerly Cellartis) to investigate possibilities in that area. Again, the main focus until now has been to develop protocols to maintain the cells in the microfluidic network. I have been working with their DEF-CS™ cells, human pluripotent stem cells that grow as monolayers on a special coating. After some optimization, it was possible to reliably culture those cells in a microfluidic chip, but we have not yet looked into any chemical factors provided to the cells in a gradient manner. Figure 5.2 shows the cells cultured in the main chamber of the diffusion based gradient generator. Besides the DEF-CS™ cells, we recently started to look at human embryonic stem cell derived cardiomyocytes (hES-CMC™) from Cellectris stem cells, but we are still at an very early stage with those cells.

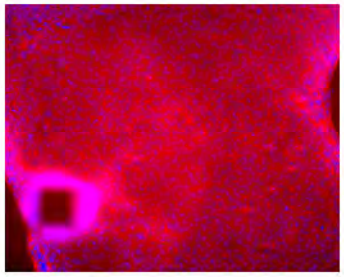

Figure 5.2
DEF-CS™ cells cultured in the main chamber of the diffusion gradient chip after 4 days. The cells are stained with phalloidin coupled rhomdaine (red: actin filaments) and DAPI (blue: cell nucleus). The cells have reached 100% confluency and are starting to detach from the substrate.

Microfluidic platform

In my opinion both directions, mimicking cell microenvironments and cell screening, are very interesting and microfluidics offer unique possibilities for them. Regarding microfluidic network design, I think that the diffusion based gradient generator that Elin and I are using at the moment is very suitable for both application areas and there is no immediate need to change the design. This is good, because it will allow me to build upon the simulation and characterization data that we have generated for this design. It might, however, become necessary or desirable to modify the design at some point before I am finished with my PhD. It could for example be interesting to incorporate automated valves at some point to add the ability to close channels during

seeding or to manipulate fluid flow over time. It might also be necessary to adapt the design for specific applications, like capturing neurospheres in some kind of trap to position them more precisely within the microfluidic cell culture chamber.

Two new master thesis projects

In addition to the ideas mentioned above on what I want to do in the future, there are two additional projects that I would like to run as master thesis projects.

The first project is a continuation of some experiments that students in the tissue engineering course 2012 did under Elins and my supervision. The focus is on combining microfluidics with surface topology to study muscle cell differentiation (see "Master thesis project 1" on page 150). It connects back somewhat to the experiments with the electrospun fibers, but instead of fibers microfabricated groves are used. I have used those groove substrates a long time ago (tissue engineering course 2008) during my master education to look at muscle cell alignment and differentiation, but not integrated with microfluidics.

The second project is directed towards the development of a wound healing model. The aim is to combine the same diffusion based gradient generator with starch microspheres to study endothelial cell migration in relevant three dimensional environments (see "Master thesis project 2" on page 151). The starch microspheres are very interesting, because they already used in hemostatic applications (Arista, Magle AB, Sweden) and Magle AB is interested in exploring their suitability for wound healing applications.

The ability to study cell migration through three dimensional scaffolds with microspheres and a second gel phase is very interesting, since it allows detail investigation of microsphere parameters and can help to get a better understanding of underlying principles on the cellular scale. It also extends the scope of the work I have been doing so far, from two-dimensional systems to three-dimensional systems, which is a very important step in mimicking the native cell environment. Early trials in this direction were successful and I was able to inject starch microspheres into microfluidic channels.

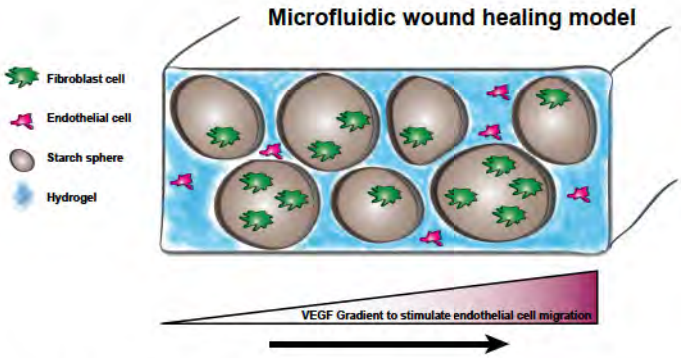

Figure 5.3
Schematic of the integration of starch microspheres into a microfluidic gradient system for the development of a new wound healing model

Over all there are many exciting experiments that I want to perform, but I am also aware that time will maybe be constricting. From the experiences I gained during the first half of my PhD education and what I have learned throughout the different projects, I think I am much better prepared to handle this today than I was when I started.

Master thesis project 1

In vitro muscle cell culture, both of skeletal myocytes as well as cardio myocytes, has many potential application areas, ranging from tissue engineered constructs for medical purposes, over *in vitro* drug testing models, all the way to cultured meat for nutrition. Therefore, it is important to understand the underlying effects of cell differentiation, function and contractibility and to be able to control the necessary factors during cell culture to achieve optimal results.

One known important factor is cell contact guidance and it has been shown by us and others that micro-structured surfaces are capable of achieving a high degree of cell alignment. It is, also, known that many different bio-active substances, in solution or bound to the surface, play in an important role during the differentiation process. During the last two years, we have been starting to work with different microfluidic setups to tightly control the liquid composition on the cellular length scale and even to combine such liquid handling capabilities with different surface properties to recreate closer mimics of cell microenvironments. These systems could also be used to investigate different factors in a defined cell culture media composition and optimize their concentration individually to achieve optimal results. Defined media compositions have many benefits over the cell culture compositions that we normally use today. Instead of using animal derived serum to supply cells with growth factors and hormones, these substances are produced by recombined expression in bacteria and added to the media at known concentrations. Thus, media composition is always the same, does not use any animal products and can be fine-tuned to cellular needs more easily.

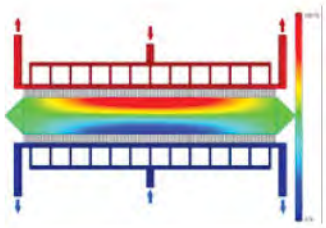

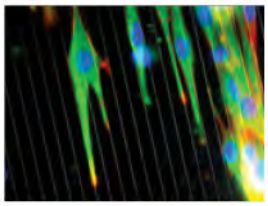

Master thesis project 2

Wound healing is a process by which the body is able to heal itself and partially restore tissue function. It is a complex process involving many different cell types and events happening both within minutes, but some taking up to years. One major aim for wound healing products is to reduce scar tissue formation and support biological processes leading to an increase of functional tissue formed after injury. One promising product in this respect is starch microspheres.

Although a lot of research has been performed in the area of wound healing, microspheres are a very recent development. It is therefore important to study the effect of microspheres on cells and processes ongoing during wound healing. The ability to study cellular fate processes on functionalized microspheres and the development of a relevant *in vitro* model for wound healing applications will be greatly enhanced and facilitated by the use of microfluidic networks. This will allow the application of gradients in chemical signaling molecules, gas concentration or extracellular matrix molecules, similar to the ones found *in vivo*, and thus will be a closer and more relevant model system for detailed studies of cellular behavior in a wound like situation.